Geologic repository of high-level nuclear waste

-Constitutive modeling and boundary value problems-

Ho CHO, Nagoya Institute of Technology

国立大学法人
名古屋工業大学

Taiwan-Japan joint Workshop, May 22-23, 2016, Taiwan

Background

Disposal of high-level radioactive waste (HLRW) becomes one of the largest environmental issues in 21st century

Nuclear waste contains radioactive substances that are dangerous to human being

Radioactivity usually decays with long time

Moreover

During the decaying, it can generate huge amount of heat

How to deal with HLRW, safely, certainly and permanently without care of human being ?

Background

Technological barrier & engineered barrier

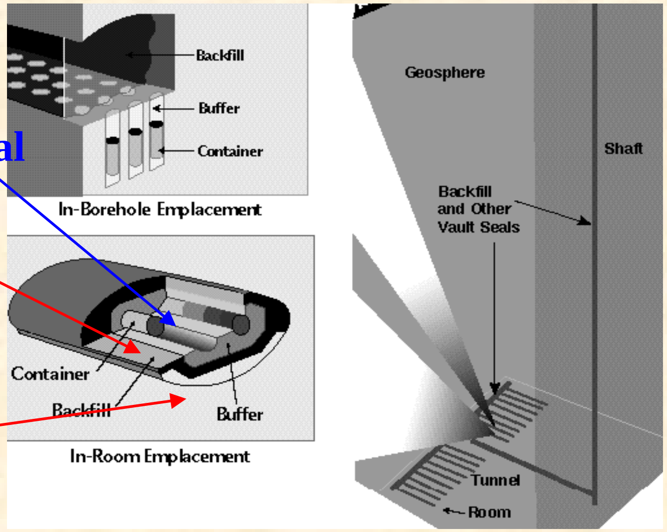

Natural barrier

Multiple barrier

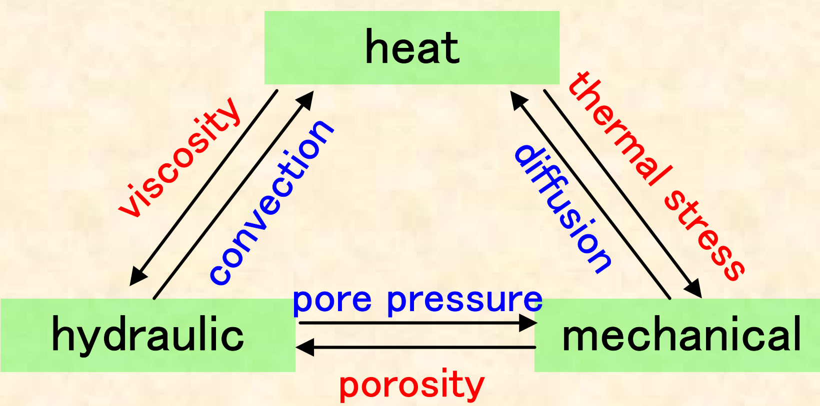

THMA coupling process

Geologic repository

Geologic repository of HLRW is usually executed at the place below 300m in stable geologic environment.

One of the most important factors in geological disposal of HLRW, is to understand the thermo-hydraulic-mechanical-air (THMA) behavior of natural barrier or host rock

I. Thermal elastoplastic model for saturated/unsaturated geomaterials

State parameters of unsaturated geomaterials

- **State variables:**
  1. **Skeleton stress**
  2. **Degree of saturation**
  3. **Void ratio**
- **Smooth transition between saturated and unsaturated state**
- **Easy to incorporate with other physical states, such as density, structure, and anisotropy**
- **Simple framework with a small number of parameters with definite physical meaning**

Compared with BBM

Basic Barcelona model: BBM

1. **Net stress**
2. **Suction**
3. **Void ratio**

$$\sigma''_{ij} = \sigma^t_{ij} - U\delta_{ij}$$

$$U = S_r u_w + (1 - S_r) u_a$$

U : mean pore pressure

s : suction

S_r : degree of saturation

σ^n_{ij} : net stress

σ''_{ij} : skeleton stress

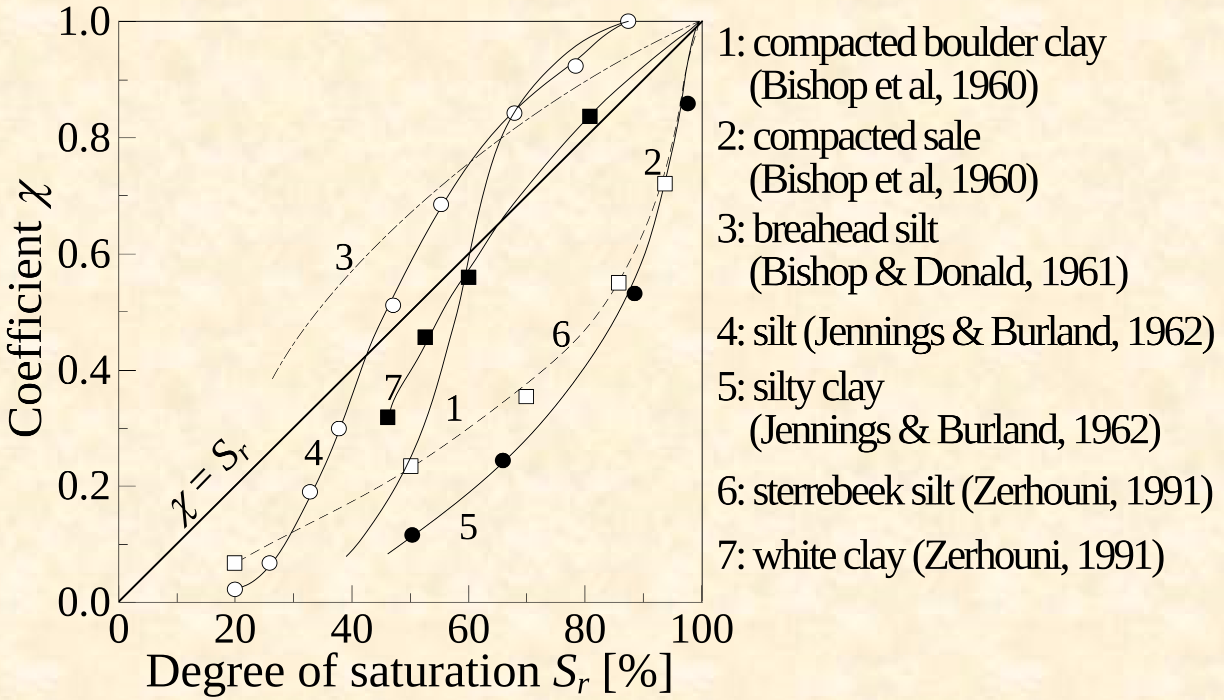

⇒Bishop's effective stress（1959）:

$$\sigma'' = \sigma - u_a + \chi(u_a - u_w) = \sigma^{net} + \chi s$$

$$\sigma''_{ij} = \sigma^t_{ij} - u_a\delta_{ij} + S_r(u_a - u_w)\delta_{ij} = \sigma^n_{ij} + S_r s\delta_{ij}$$

$$\sigma^n_{ij} = \sigma^t_{ij} - u_a\delta_{ij} \qquad s = u_a - u_w$$

$S_r = \chi$

Skeleton stress tensor here after:

$$\sigma_{ij} = \sigma''_{ij}$$

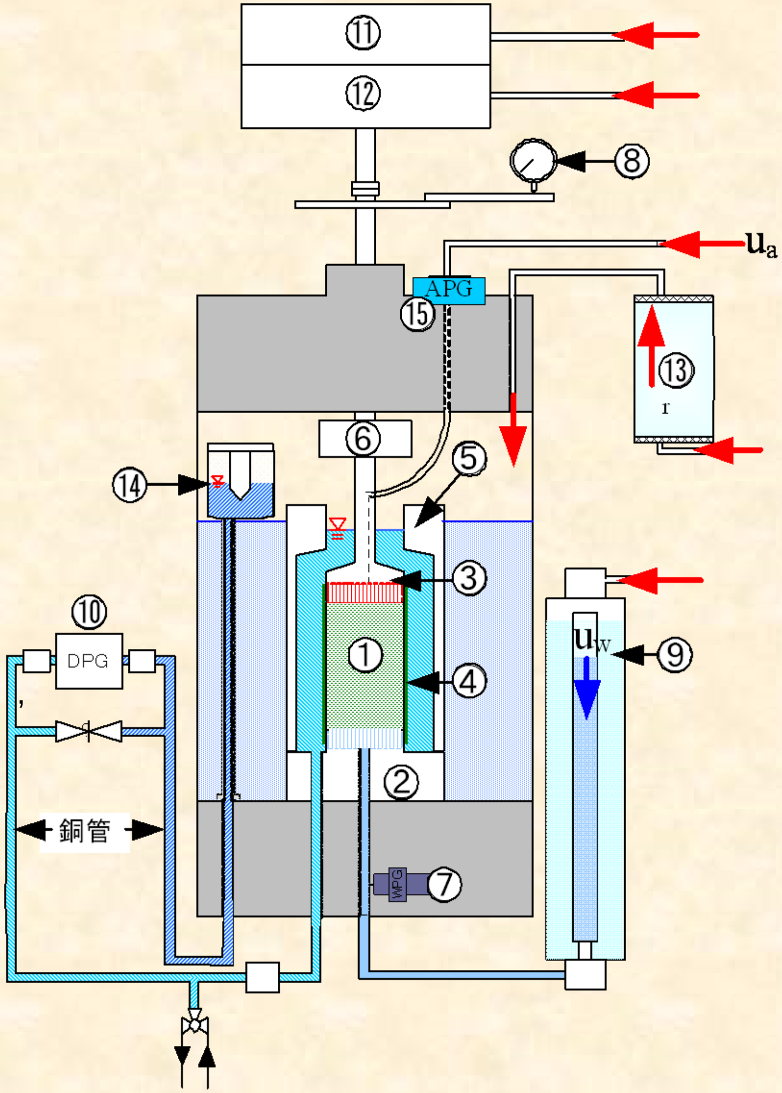

① Sample
② Pedestal
③ Load cap
④ Membrane
⑤ Inner cell
⑥ Load cell
⑦ Pore water pressure meter
⑧ Axial displacement transducer
⑨ Dual-tube bullet
⑩ Pressure difference meter for volumetric stain
⑪ Axial actuator (Up)
⑫ Axial actuator (Down)
⑬ Air supplying tank
⑭ Reference water level for inner cell
⑮ Air pressure meter

Triaxial compression device for unsaturated/saturated sample with double-cell type volume meter

(Axial translation method)

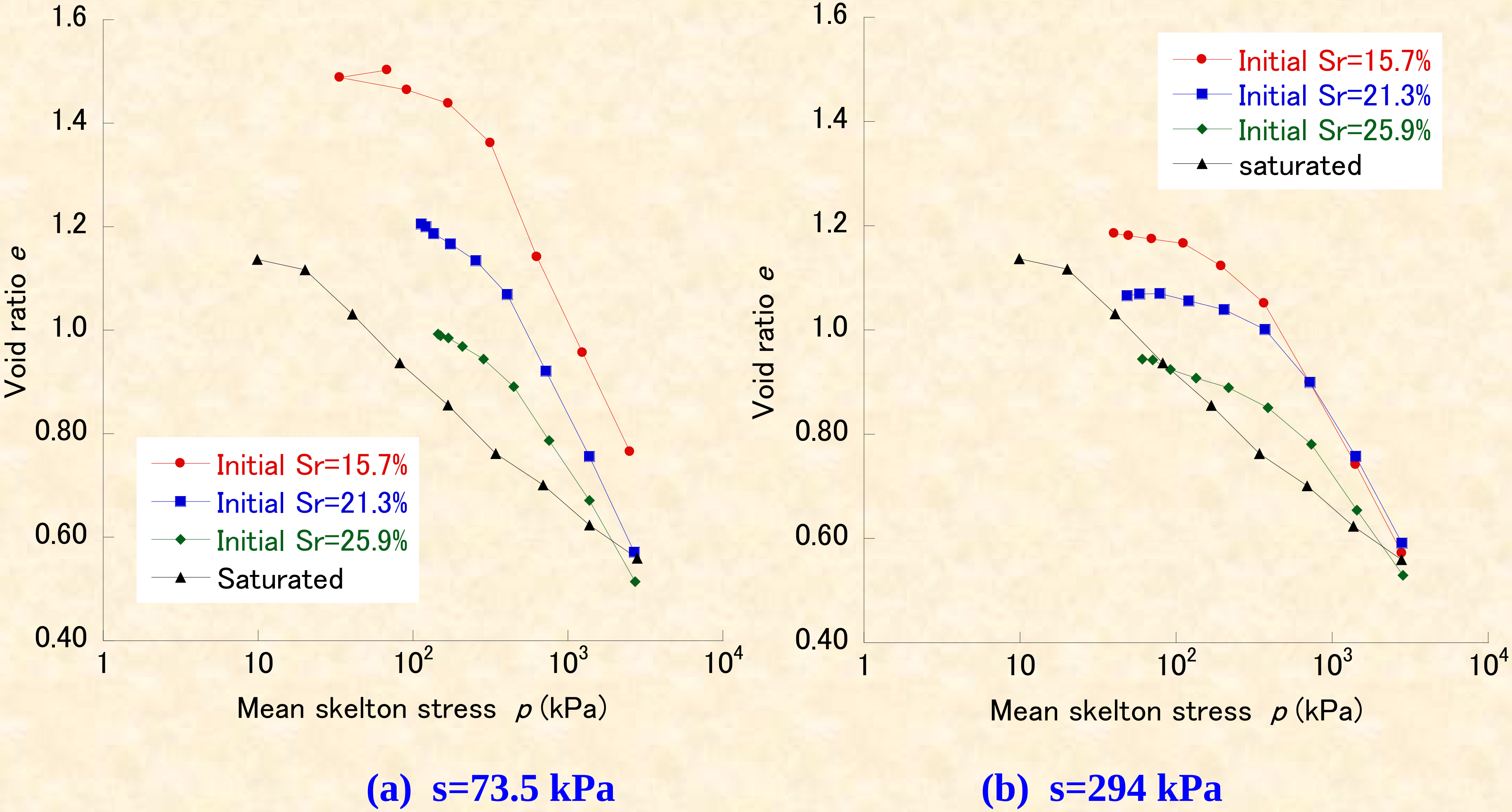

Influence of degree of saturation on e-ln *p* relation (Results of oedometer test for unsaturated soils extracted from the work by Honda, 2000)

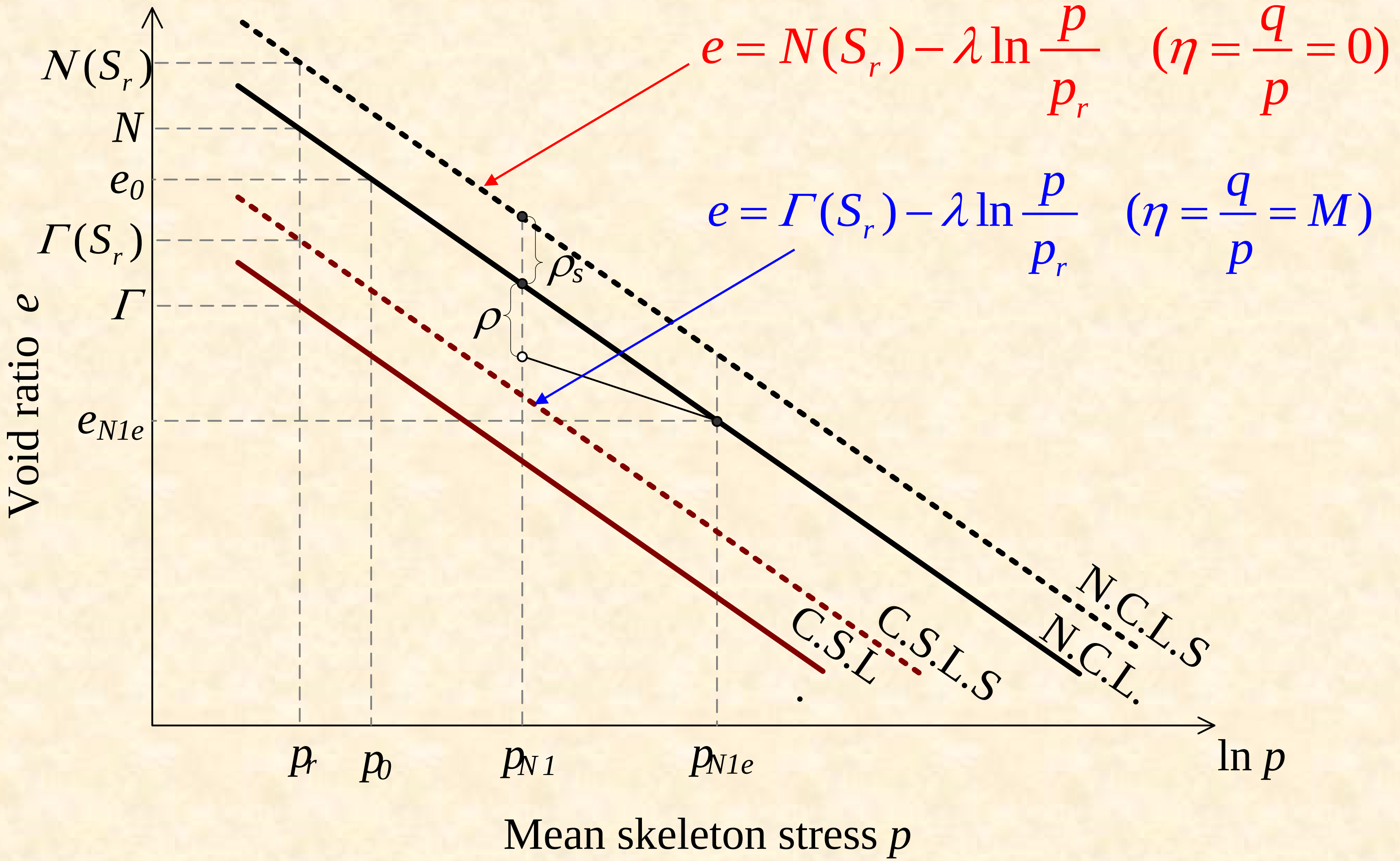

e-ln*p* relation considering moving up of *N.C.L.* and *C.S.L.* due to instauration

$$e = \chi(\eta, S_r) - \lambda \ln \frac{p}{p_r} \Rightarrow e = N(S_r) - \frac{N(S_r) - \Gamma(S_r)}{\ln 2} \ln \frac{M^2 + \eta^2}{M^2} - \lambda \ln \frac{p}{p_r}$$

$$f = \ln \frac{p}{p_0} + \frac{N(S_r) - \Gamma(S_r)}{C_p(1+e_0)\ln 2} \ln \frac{M^2 + \eta^2}{M^2} - \frac{\rho_s}{1+e_0}\frac{1}{C_p} + \frac{\rho_e}{1+e_0}\frac{1}{C_p} - \varepsilon_v^p \frac{1}{C_p} = 0$$

$$d\varepsilon_v^p = \Lambda \left.\frac{\partial f}{\partial p}\right|_{\eta=M} = 0 \quad \Rightarrow \quad N(S_r) - \Gamma(S_r) = (\lambda - \kappa)\ln 2$$

Hardening parameter

$$f = \ln \frac{p}{p_0} + \ln \frac{M^2 + \eta^2}{M^2} - \frac{\rho_s}{1+e_0}\frac{1}{C_p} + \frac{\rho_e}{1+e_0}\frac{1}{C_p} - \varepsilon_v^p \frac{1}{C_p} = 0$$

Associated flow rule: $$d\varepsilon_{ij}^p = \Lambda \frac{\partial f}{\partial \sigma_{ij}}$$

Evolution of density: $$d\left(\frac{\rho_e}{1+e_0}\right) = -\Lambda\frac{\rho^{\beta}}{p}, \quad \rho = a\rho_e + b\rho_s$$

Evolution of saturation : $$d\rho_s = -QdS_r \qquad Q = \frac{N_r - N}{S_r^s - S_r^r}$$

$$d\sigma_{ij} = (E_{ijkl} - E_{ijkl}^{p})d\varepsilon_{ij} - AE_{ijkl}\frac{\partial f}{\partial \sigma_{kl}}$$

$$E_{ijkl}^{p} = E_{ijqr}E_{mnkl}\frac{\partial f}{\partial \sigma_{mn}}\frac{\partial f}{\partial \sigma_{qr}}/D \qquad A = \frac{1}{C_p}\frac{Q}{1+e_0}dS_r\frac{1}{D}$$

$$D = \frac{h_p}{C_p} + \frac{\partial f}{\partial \sigma_{mn}}E_{mnkl}\frac{\partial f}{\partial \sigma_{kl}} \qquad h_p = \frac{\partial f}{\partial \sigma_{mm}} + \frac{\rho^{\beta}}{\sigma_{mm}}$$

Thermal effect described with the concept of equivalent stress（Zhang & Zhang, 2009）

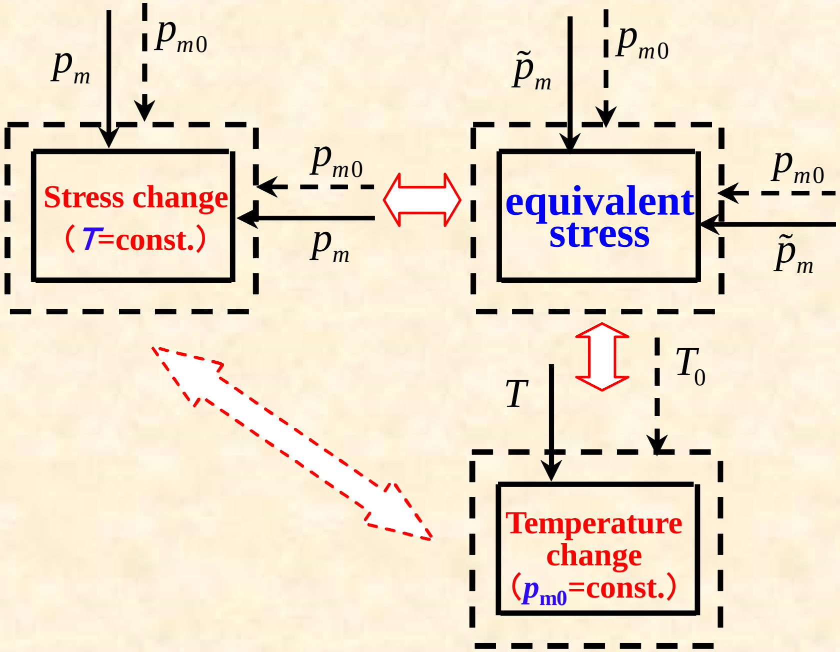

Change of temperature may also cause elastic and plastic strain

On condition that elastic strain caused by change of temperature obeys Hooke's theory, **equivalent stress is then defined as;**

$$\tilde{p}_m = p_{m0} + K\varepsilon_v^{eT} = p_{m0} + 3K\alpha_T (T - T_0)$$

$$\tilde{\rho}_e = (\lambda - \kappa)\ln[(\tilde{p}_{N1} \times \mathrm{OCR}) / p_{N1}]$$

Concept of equivalent stress is used to consider the influence of temperature and is expressed as,

Only one parameter, thermal expansion coefficient , α_T , is added to the constitutive model!

New void ratio difference, considering the influence of temperature, is given.

p_{m0}: real stress
K: bulk modulus
α^s: thermal expansion coefficient
T: current temperature
T_0: reference temperature (15°C)

Elastoplastic model for saturated/unsaturated geomaterials

$$f = \ln\frac{p}{p_0} + \ln\frac{M^2+\eta^2}{M^2} - \boxed{\frac{\rho_s}{1+e_0}\frac{1}{C_p}} + \boxed{\frac{\tilde{\rho}_e}{1+e_0}\frac{1}{C_p}} - \varepsilon_v^p\frac{1}{C_p} = 0$$

Saturation term ***Overconsolidation term***

Compared with Cam-clay model for saturated soils, only *saturation* is added

Associate flow rule: $d\varepsilon_{ij}^p = \Lambda\frac{\partial f}{\partial \sigma_{ij}}$

$$\begin{cases} \tilde{\rho}_e = (\lambda-\kappa)\ln[(\boxed{\tilde{p}_{N0}}\times \mathrm{OCR})/p_{N0}] \\ d\left(\frac{\tilde{\rho}_e}{1+e_0}\right) = -\Lambda\frac{\rho^\beta}{\boxed{\tilde{p}}}, \quad \rho = a\rho_e + b\rho_s \end{cases}$$

Equivalent stress

(i) Evolution of $\tilde{\rho}_e$ is dependent on: *Saturation* , *Overconsolidation* *and temperature*

$$\left\{\begin{array}{l} N(S_r) = N + \frac{N_r - N}{S_r^s - S_r^r}(S_r^s - S_r); \quad N_r = N(S_r^r) \\ \rho_s = N(S_r) - N = Q(S_r^s - S_r); \quad Q = \frac{N_r - N}{S_r^s - S_r^r} \\ d\rho_s = -QdS_r \end{array}\right\}$$

S_r^r **and** S_r^s**: residual saturation 100% saturation**

(ii) Evolution of ρ_s is dependent on: *Saturation*

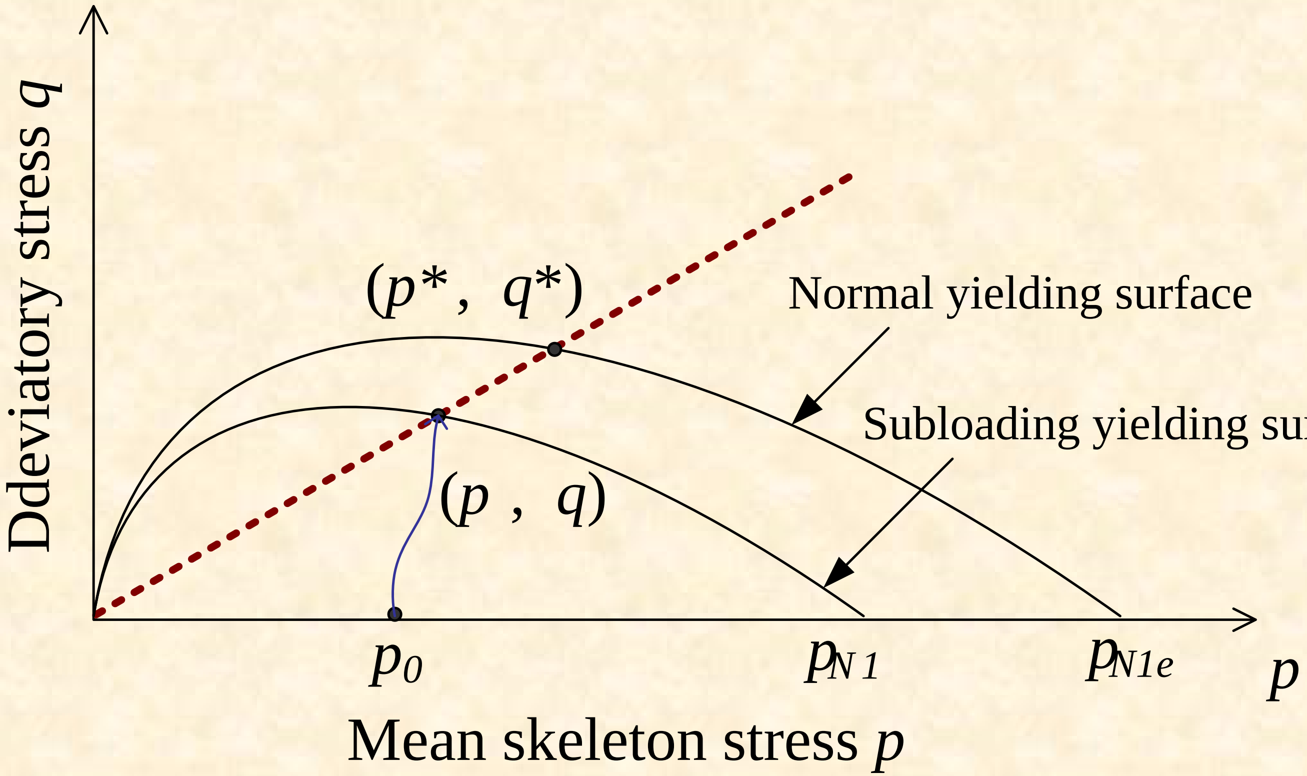

Extension of subloading concept (Hashiguchi and Ueno, 1977) to unsaturated soil in skeleton stress space

Moisture characteristic curve (MCC)

Skeleton curve

(1) Initial drying curve

$$S_r = S_r^{s0} - \frac{2}{\pi}(S_r^{s0} - S_r^r)\tan^{-1}((e^{c_1 s} - 1)/e^{c_1 s_d})$$

(2) Main drying curve

$$S_r = S_r^s - \frac{2}{\pi}(S_r^s - S_r^r)\tan^{-1}((e^{c_1 s} - 1)/e^{c_1 s_d})$$

(3) Main wetting curve

$$S_r = S_r^s - \frac{2}{\pi}(S_r^s - S_r^r)\tan^{-1}((e^{c_2 s} - 1)/e^{c_2 s_w})$$

Scanning curve

Tangential stiffness of suction-saturation relation

$$dS_r = k_s^{-1} ds \qquad k_s^{-1} = k_{s0}^{-1} + k_{s1}^{-1}$$

$$k_{s1} = k_{s1}^s(1 + c_3 \frac{1-r}{r}) \qquad r = \begin{cases} \delta_2/\delta & ds > 0 \\ \delta_1/\delta & ds \le 0 \end{cases}$$

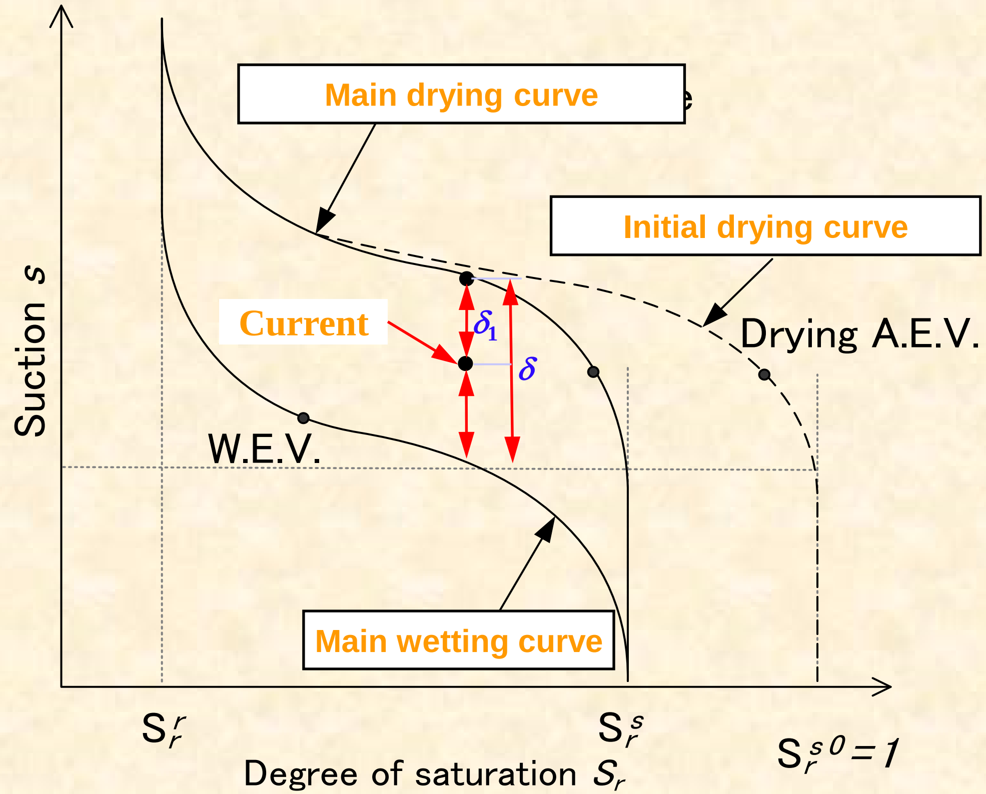

MCC

Parameters:

S_d: drying AEV; S_w: wetting AEV

S_r^r: residual S_r; S_r^s; saturated S_r

c_1 c_2 c_3: scanning parameters

k_{s0} *gradient at r =0*

Parameters involved in constitutive model

Compression index λ	0.050
Swelling index κ	0.010
Critical state parameter M	1.0
Void ratio N (p'=98 kPa on $N.C.L.$)	1.14
Poisson's ratio v	0.30
Parameter of overconsolidation a	5.00
Parameter of suction b	5.50
Parameter of overconsolidation β	1.0
Void ratio N_r (p'=98 kPa on $N.C.L.S.$)	1.28

Parameters involved in MCC

Saturated degrees of saturation S_r^s	0.82
Residual degrees of saturation S_r^r	0.64
Parameter corresponding to drying AEV (kPa) S_d	550
Parameter corresponding to wetting AEV (kPa) S_w	320
Initial stiffness of scanning curve (kPa) k_{sp}^e	200000
Parameter of shape function c_1	0.008
Parameter of shape function c_2	0.013
Parameter of shape function c_3	10.0

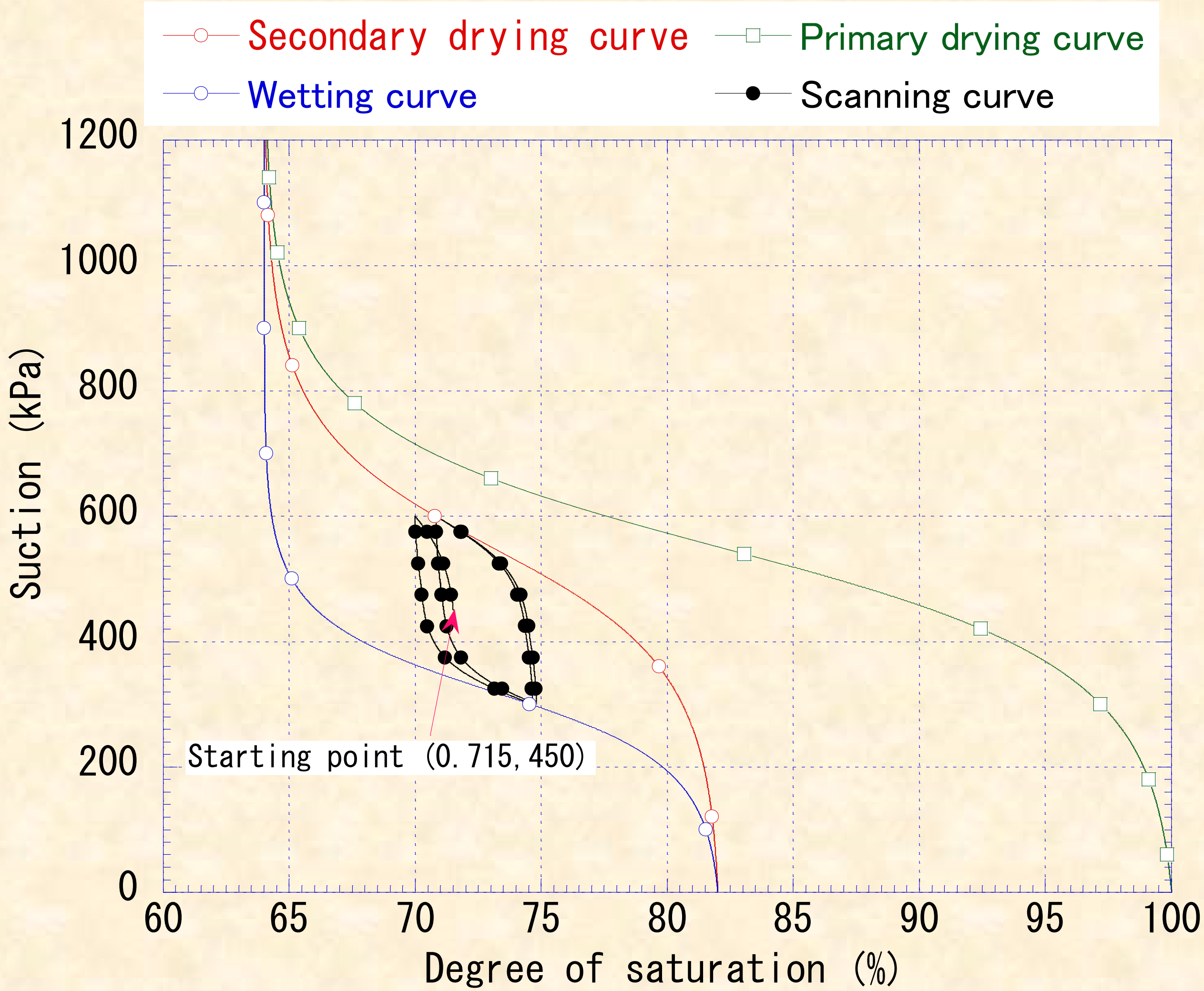

Simulated moisture characteristics curve of unsaturated fictional silt

Verification of proposed model

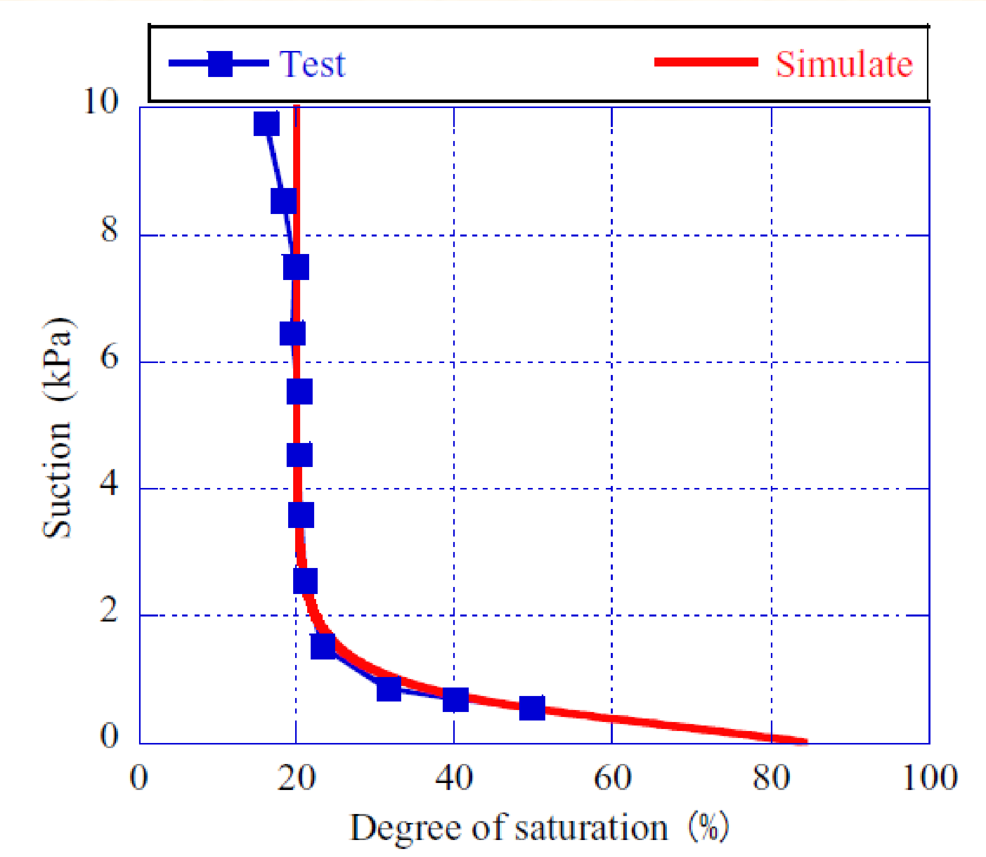

Test and simulated moisture characteristics curve of unsaturated rockfill (test data from the work by Kohgo et al, 2007)

Verification of proposed model

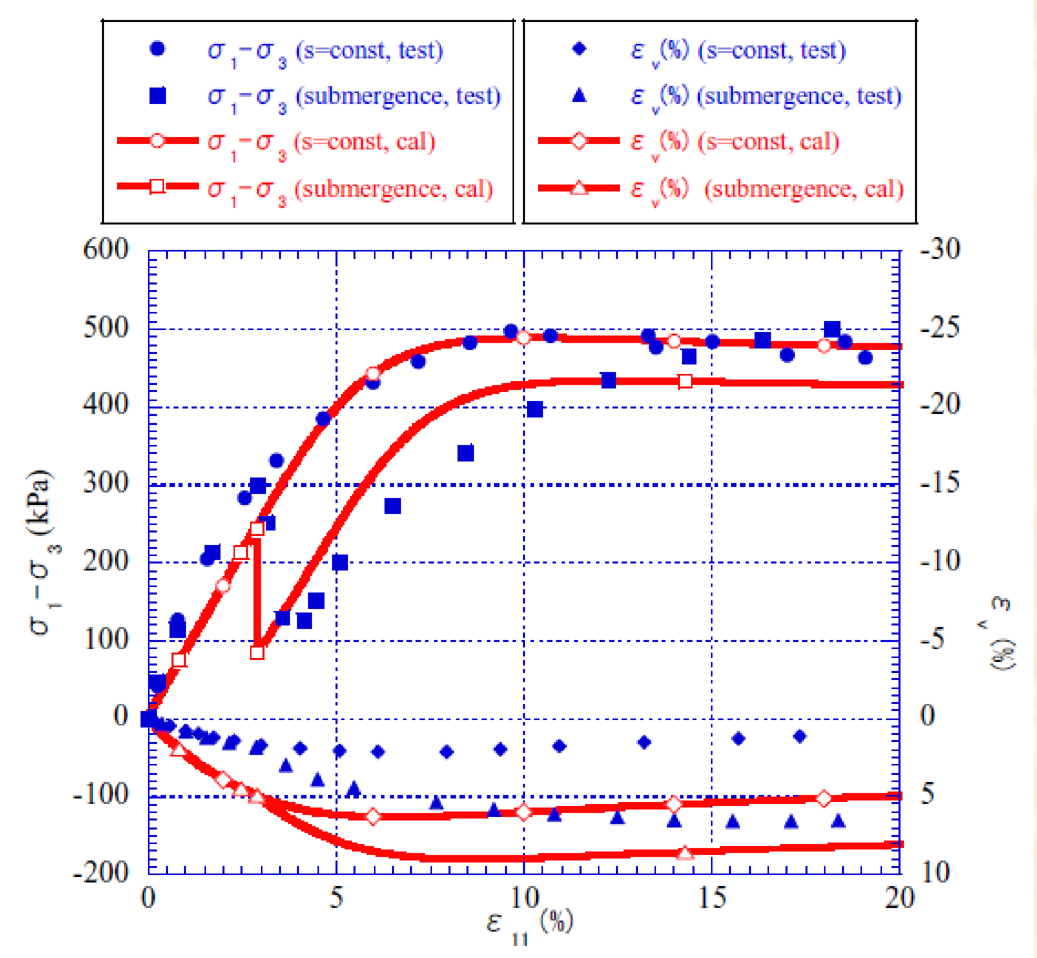

(a) Stress, strain and dilatancy relation (σ_3=100kPa)

Verification of the model by drained and exhausted triaxial compression tests for a rockfill with submergence process (test data from the work by Kohgo et al, 2007)

Verification of proposed model

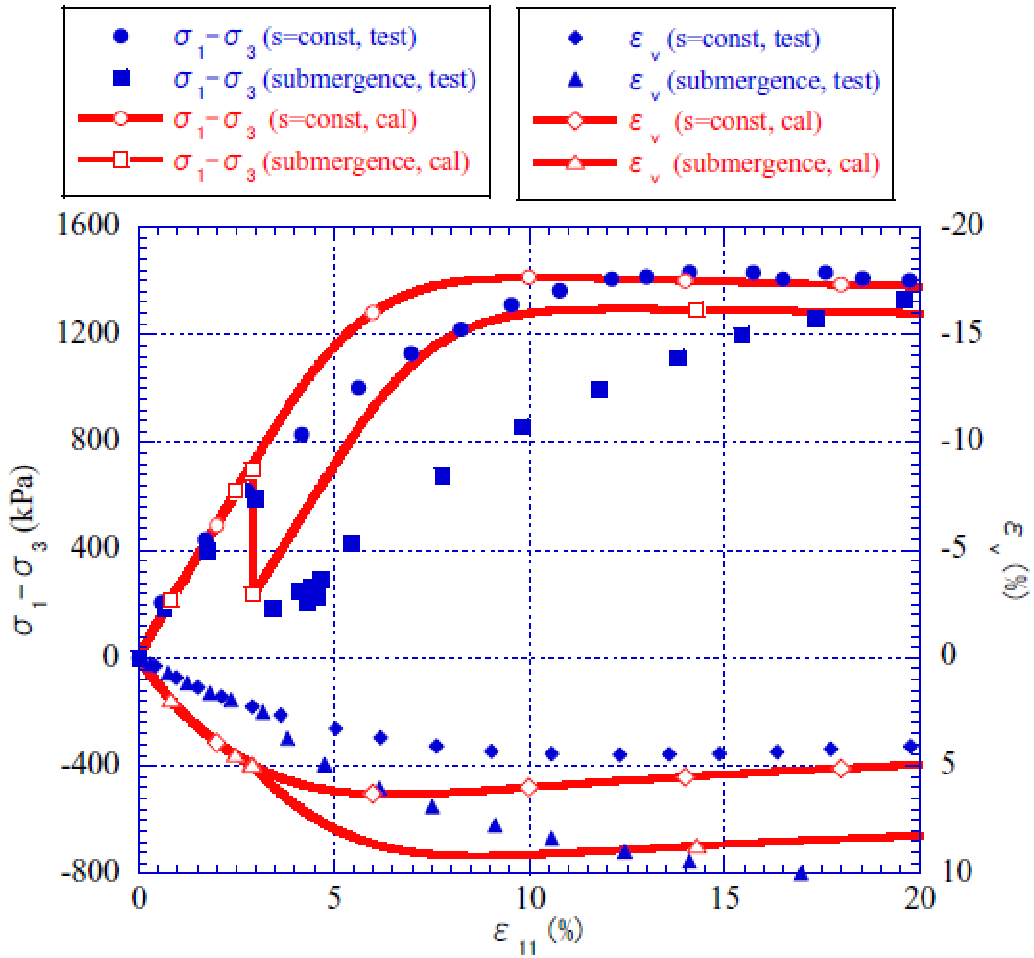

(b) Stress, strain and dilatancy relation (σ_3=300kPa)

Verification of the model by drained and exhausted triaxial compression tests for a rockfill with submergence process (test data from the work by Kohgo et al, 2007)

Verification of proposed model

1. Consolidation tests

2. Triaxial compression tests under different temperature .

(Test data from Uchaipichat and Khalili , 2009)

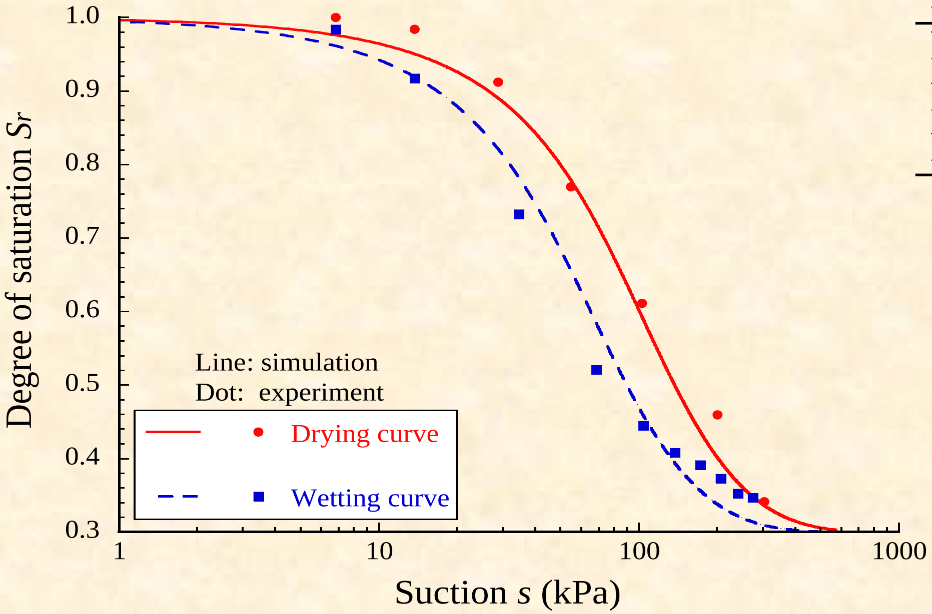

MCC

Parameters of silt in MCC

Saturated degrees of saturation S_r^s	1.00
Residual degrees of saturation S_r^r	0.30
Parameter corresponding to drying AEV (kPa) S_d	18.0
Parameter corresponding to wetting AEV (kPa) S_w	5.0
Initial stiffness of scanning curve (kPa) k_{sp}^e	90.0
Parameter of shape function c_1	0.009
Parameter of shape function c_2	0.013
Parameter of shape function c_3	3.0

Material parameters of silt

Compression index λ	0.09
Swelling index κ	0.006
Critical state parameter **M**	2.45
Void ratio N (p'=98 kPa on *N.C.L.*)	0.638
Poisson's ratio ν	0.30
Parameter of overconsolidation a	60.00
Parameter of suction b	0.00
Parameter of overconsolidation β	2.0
Void ratio N_r (p'=98 kPa on *N.C.L.S.*)	0.665

Verification of proposed model (Test data from Uchaipichat and Khalili , 2009)

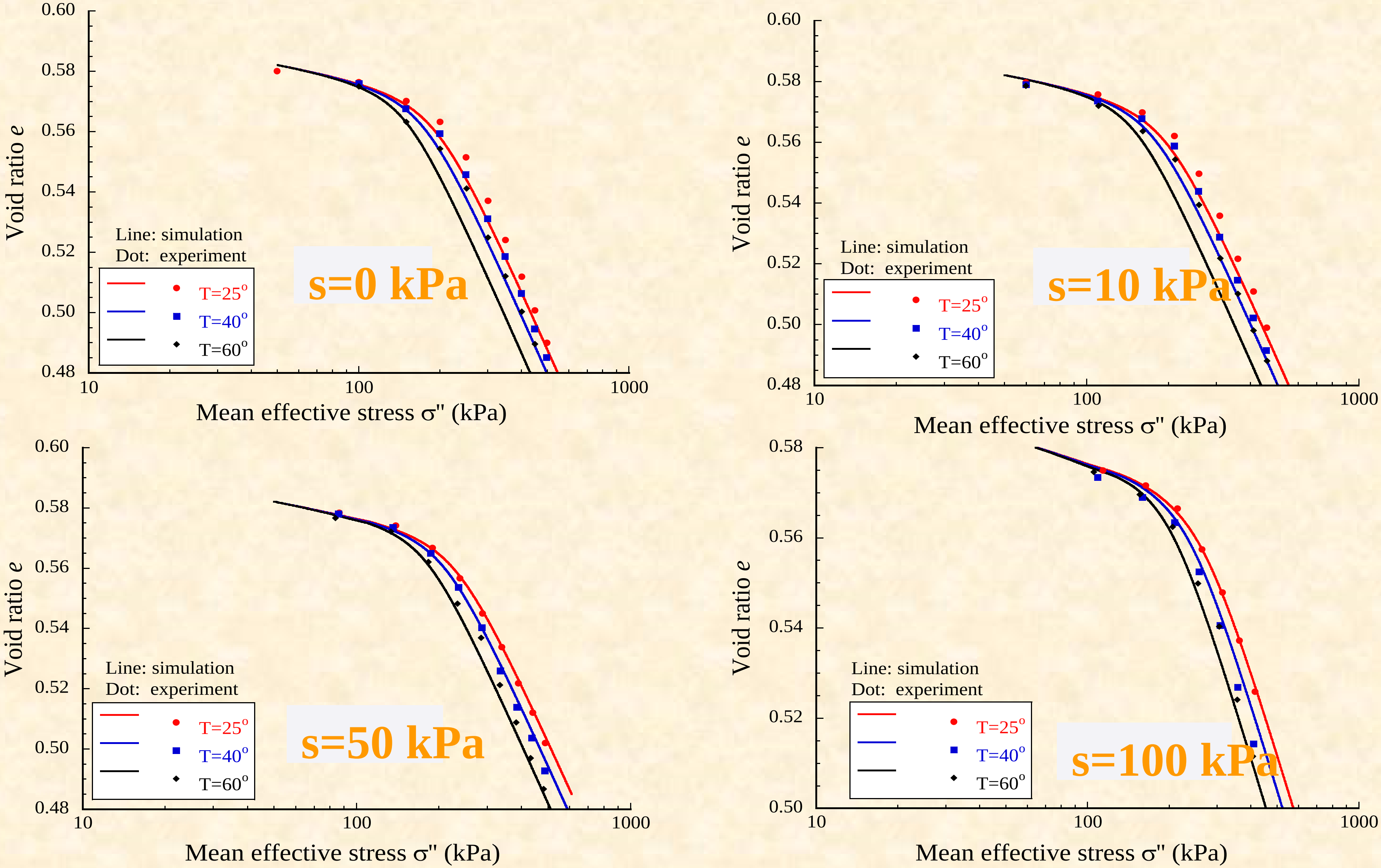

Consolidation tests under different temperature

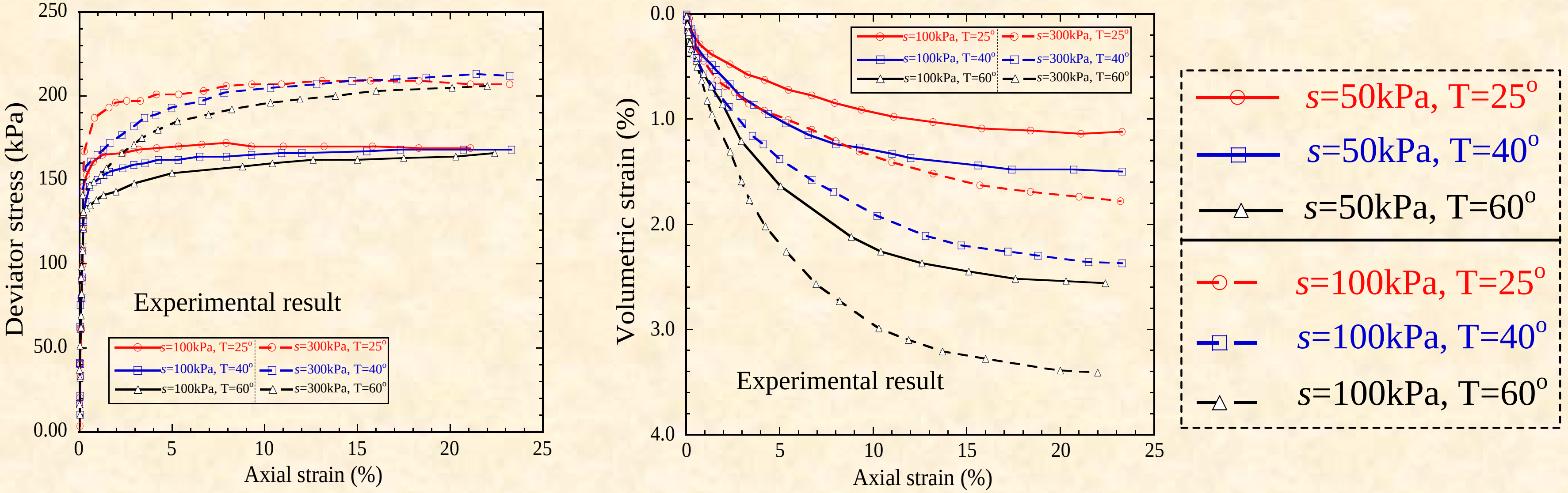

(a) experimental results (Uchaipichat and Khalili, 2009)

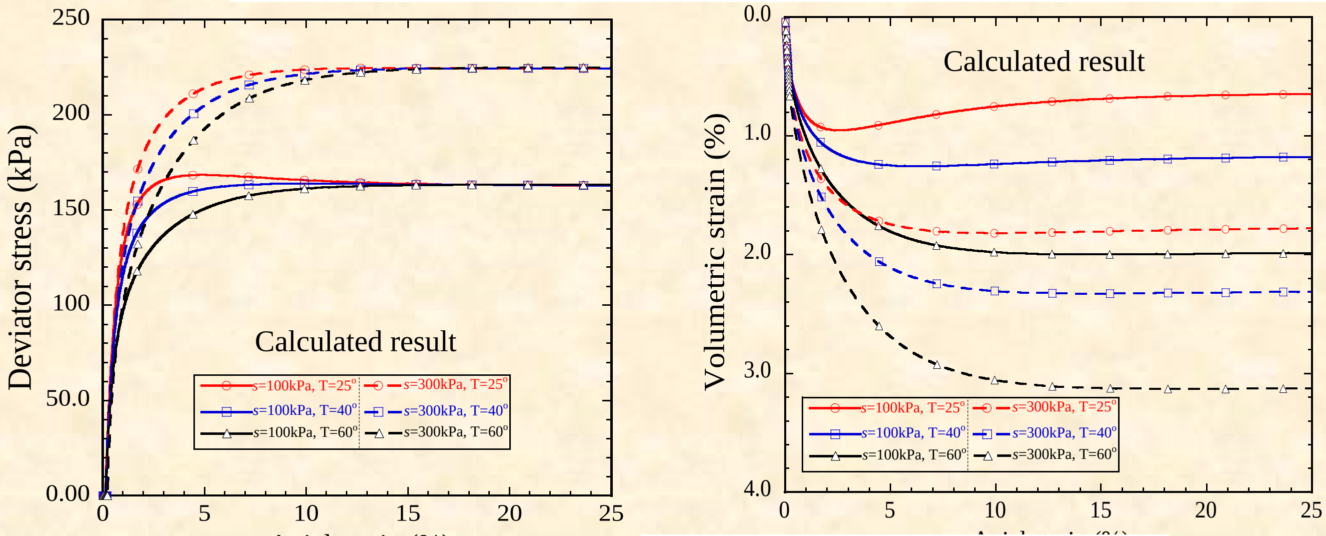

(b) calculated results

Conventional triaxial compression tests under different constant suction and temperature conditions (initial mean net stress= 50 kPa)

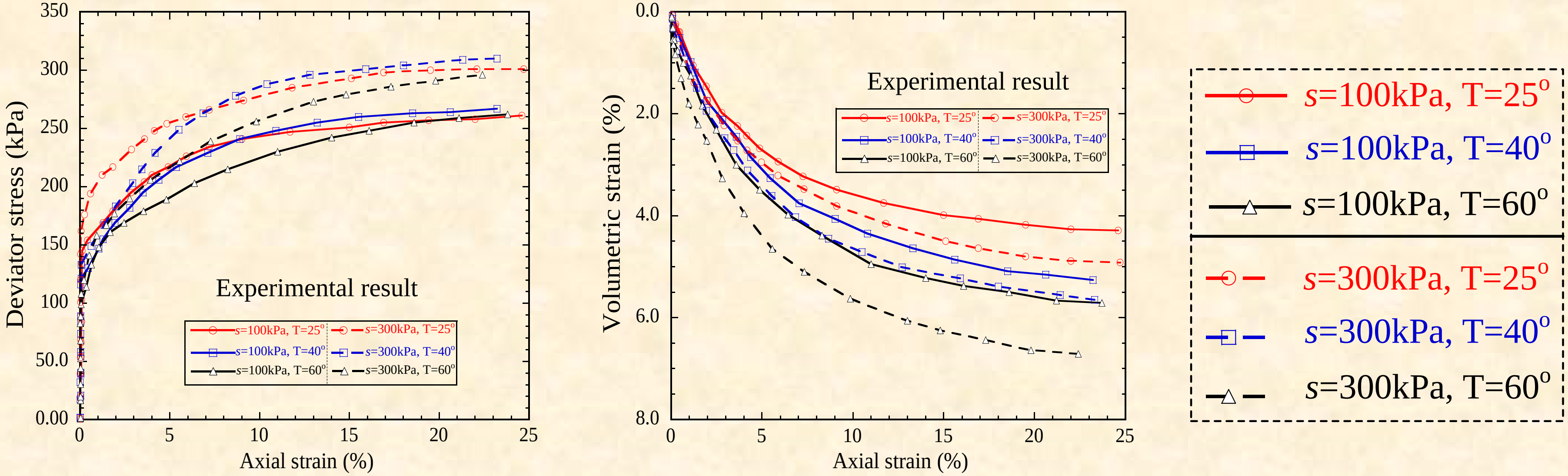

(a) experimental results (Uchaipichat and Khalili, 2009)

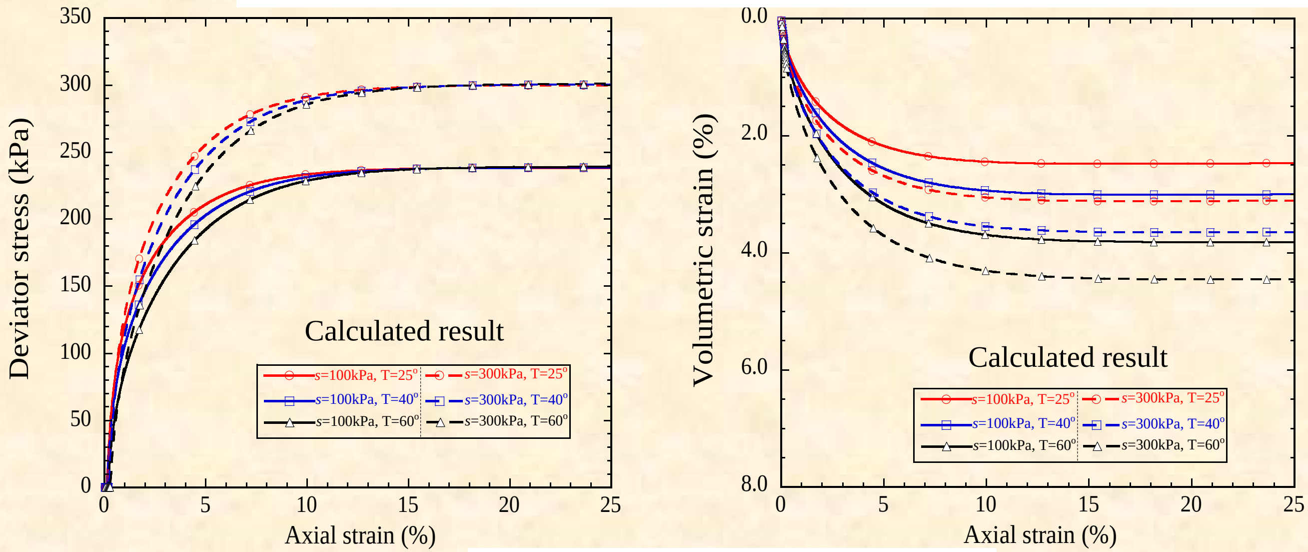

(b) calculated results

Conventional triaxial compression tests under different constant suction and temperature conditions (initial mean net stress= 100 kPa)

Triaxial compression test results
Soft sedimentary rock (saturated state)

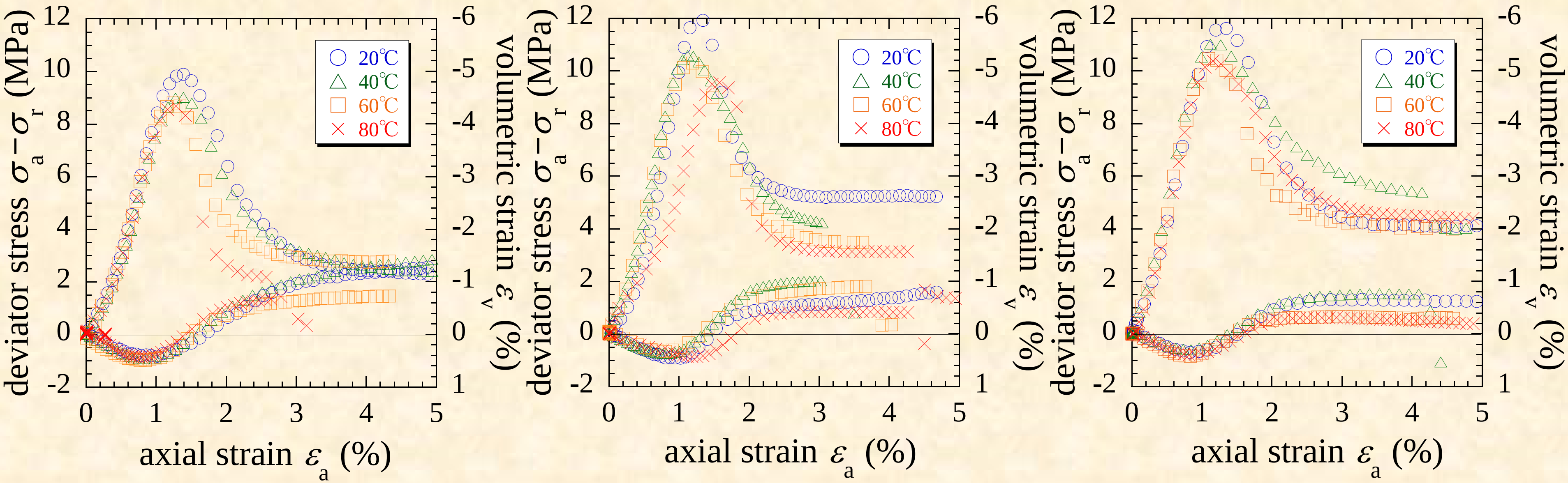

σ_3=0.49MPa σ_3=0.98MPa σ_3=1.47MPa

Stress-strain-dilatancy relation

(Test data from Zhang, Nishimura and Kageyama, 2013 & 2014)

Verification of proposed model

soft sedimentary rock (saturated state, σ_3=0.49MPa)

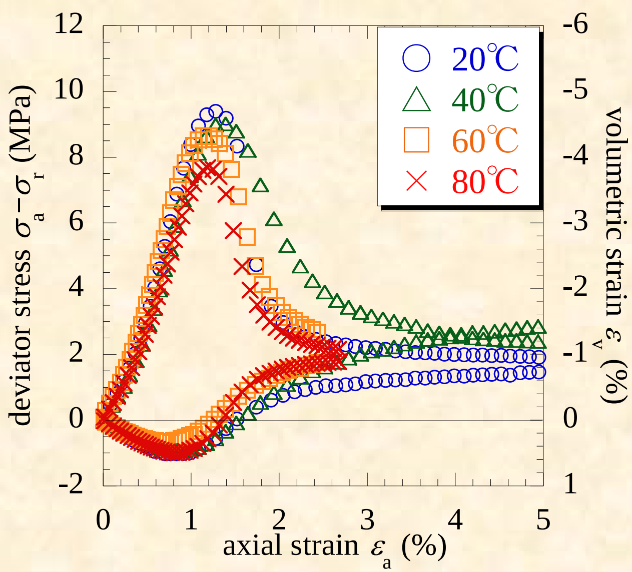

Tests

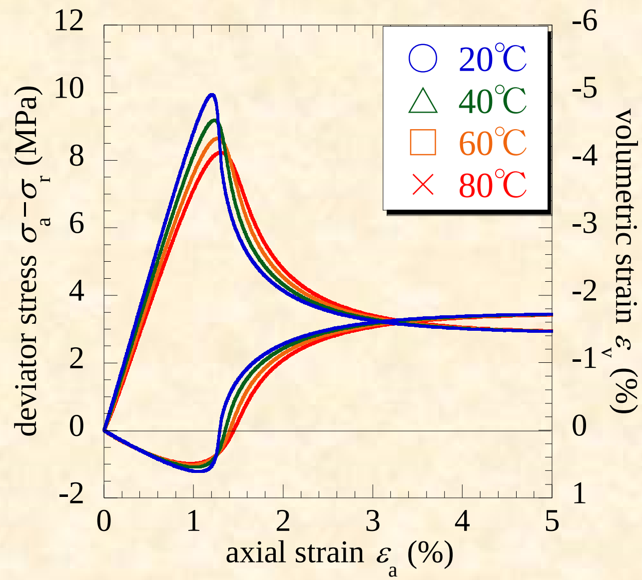

Simulation

(Test data from Zhang, Nishimura and Kageyama, 2013 & 2014)

A simple finite deformation scheme for MCC

There is a basic and intrinsic relationship among the state variables, void ratio *e*, degree of saturation S_r and gravimetric water content *w* ,

$$w = \frac{S_r e}{G_s} \qquad G_s dw = edS_r + S_r de$$

Which means that even if *dw*=0 (constant water content), if void ratio *e* changed, degree of saturation will also change!

Simulated behavior of soil at the process of drying-isotropic loading to full saturation-suction reduction

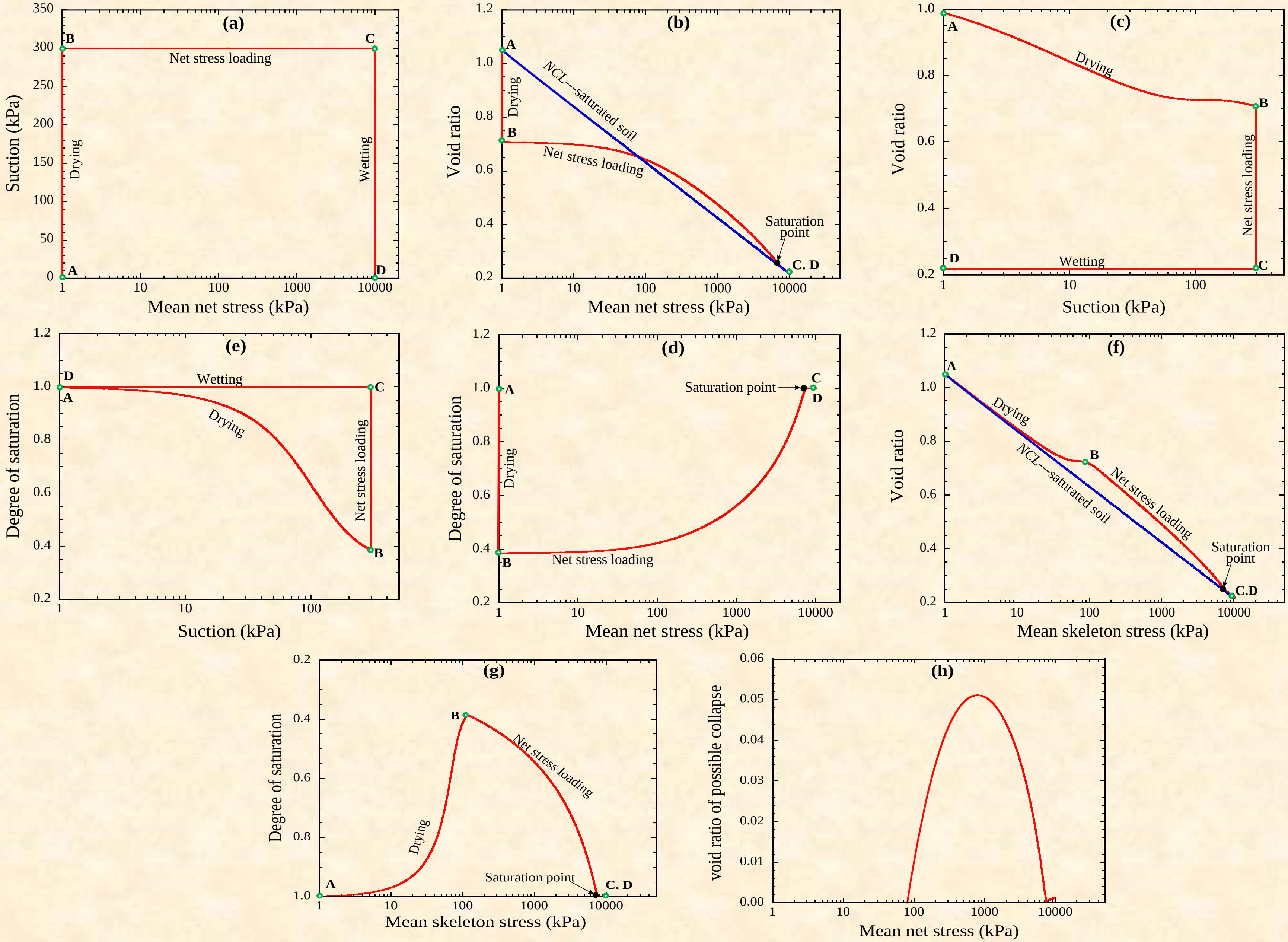

Simulated behavior of soil at the process of drying-isotropic loading-wetting collapse

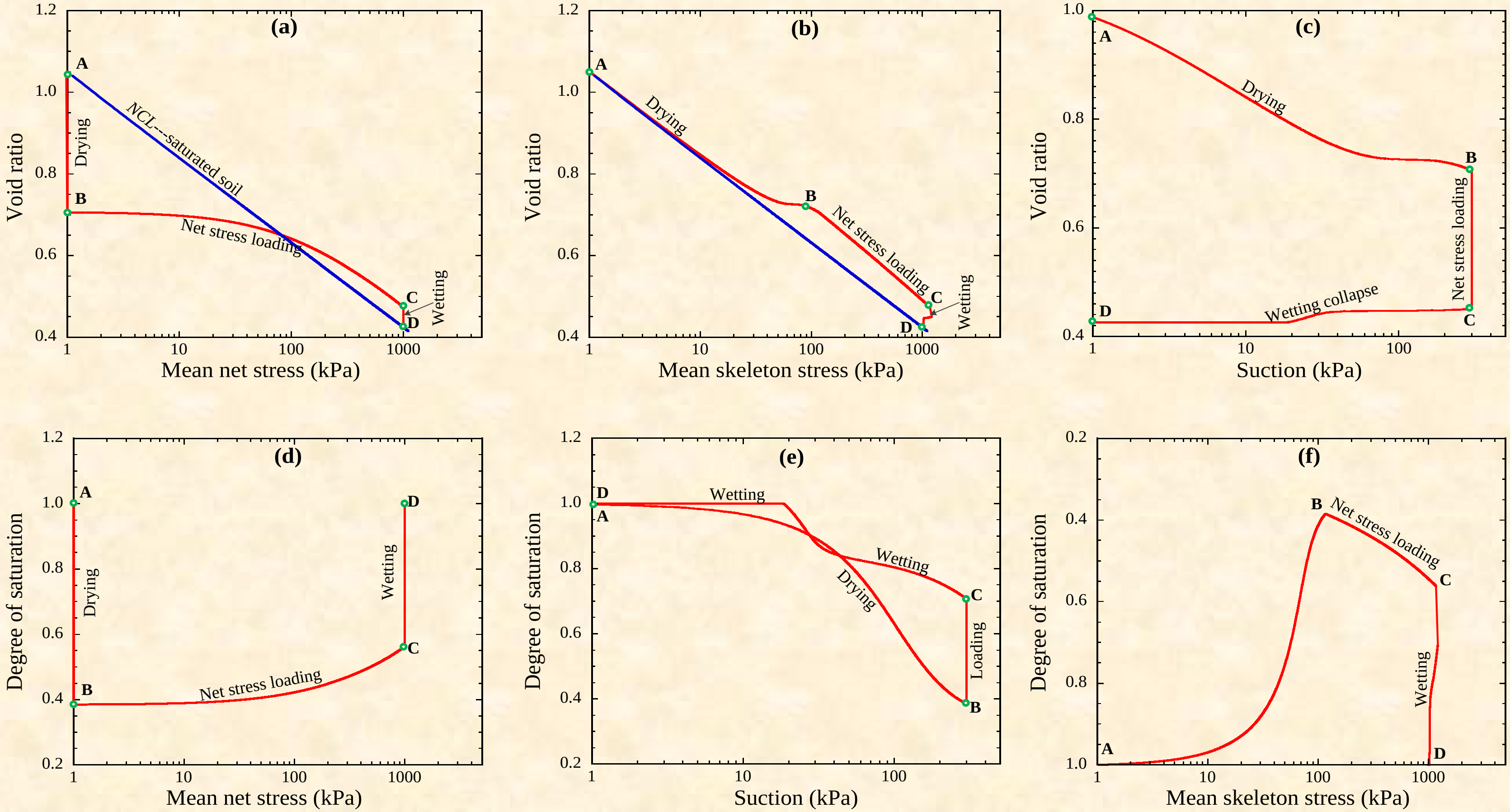

II. Field equations for THMA analysis

Soil-water-air coupling

Conservative equations for all phases

$$\frac{\partial \bar{\rho}^s}{\partial t} + \frac{\partial(\bar{\rho}^s \dot{u}_i^s)}{\partial x_i} = 0 \qquad \frac{\partial \bar{\rho}^a}{\partial t} + \frac{\partial(\bar{\rho}^a \dot{u}_i^a)}{\partial x_i} = 0 \qquad \frac{\partial \bar{\rho}^w}{\partial t} + \frac{\partial(\bar{\rho}^w \dot{u}_i^w)}{\partial x_i} = 0$$

Field equations

1. Equilibrium equation

Static loading

$$\frac{\partial \sigma_{ij}}{\partial x_j} + \rho b_i = 0$$

2. Continuum equations (solid + liquid)

$$\frac{\dot{\varepsilon}_{ii}^s}{n} - \frac{k^w}{\gamma^w}\frac{\partial^2 p^w}{\partial x_i \partial x_i} - \frac{1}{K^w}\dot{p}^w + \frac{\dot{S}_r}{S_r} = 0$$

3. Continuum equations (solid + air)

$$\frac{\dot{\varepsilon}_{ii}^s}{n} - \frac{k^a}{\gamma^a}\frac{\partial^2 p^a}{\partial x_i \partial x_i} - \frac{1}{K^a}\dot{p}^a - \frac{\dot{S}_r}{1-S_r} = 0$$

+ Neglecting energy from plastic deformation

4. Energy conservation equation

$$\rho c \frac{\partial T}{\partial t} + nS_r(\rho c)^w v_i^w \frac{\partial T}{\partial x_i} + n(1-S_r)(\rho c)^a v_i^a \frac{\partial T}{\partial x_i} = k_t \frac{\partial^2 T}{\partial x_i \partial x_i} + Q$$

Discretization in space and time domain

Boundary condition

1. Stress
2. Displacement
3. Water head
4. Air pressure
5. Temperature

Initial condition

1. Stress
2. Saturation
3. Water head
4. Air pressure
5. Temperature

Discretization of governing equations

2D isoparametric element

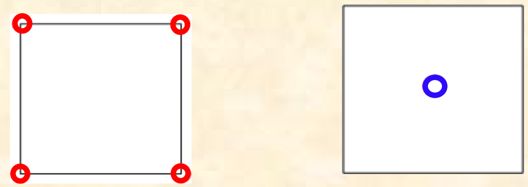

Displacement, temperature: **4 node**
Pressures of Water and air: center of gravity

Equilibrium equation

$$[K]\Delta\vec{u}_{N|t+\Delta t} + \vec{I}^{\,w}_{Sat}\, p^{w}_{dE|t+\Delta t} + \vec{I}^{\,a}_{Sat}\, p^{a}_{dE|t+\Delta t} = \Delta\vec{F}_{|t+\Delta t} + \vec{F}_{T}\,\Delta\vec{T}_{N|t+\Delta t} + \vec{I}^{\,w}_{Sat}\, p^{w}_{dE|t} + \vec{I}^{\,a}_{Sat}\, p^{a}_{dE|t}$$

Continuum equations（solid + liquid）

$$S_{r|t}\vec{K}_{v}^{T}\cdot\Delta\vec{u}_{N|t+\Delta t} - \left[\bar{\alpha} + \bar{A} + F_{sr}\right] p^{w}_{dE|t+\Delta t} + F_{sr}\, p^{a}_{dE|t+\Delta t} + \sum_{i=1}^{m}\bar{\alpha}_{i}\, p^{w}_{idE|t+\Delta t}$$

$$= -[\bar{A} + F_{sr}]\, p^{w}_{dE|t} + F_{sr}\, p^{a}_{dE|t} + \left[\bar{K}_{WT}\right]\Delta\vec{T}_{N|t+\Delta t}$$

Continuum equations（solid + air）

$$(1 - S_{r|t})\vec{K}_{v}^{T}\cdot\Delta\vec{u}_{N|t+\Delta t} + F_{sr}\, p^{w}_{dE|t+\Delta t} - \left[\bar{\beta} + \bar{B} + F_{sr}\right] p^{a}_{dE|t+\Delta t} + \sum_{i=1}^{m}\bar{\beta}_{i}\, p^{a}_{idE|t+\Delta t}$$

$$= F_{sr}\, p^{w}_{dE|t} - [\bar{B} + F_{sr}]\, p^{a}_{dE|t} + \left[\bar{K}_{AT}\right]\Delta\vec{T}_{N|t+\Delta t}$$

Discretization of governing equations

Energy conservation equation

Discretization in space (Galerkin)

$$\left[C^t\right]\left\{\dot{T}_{N|t}\right\}+\left[K^t\right]\left\{T_{N|t}\right\}=\left[f^t\right]$$

$$\left[C^t\right]=\int_V \overline{\rho c}\left[N\right]^T\left[N\right]dV$$

$$\left[f^t\right]=\int_V\left[N\right]^T EdV-\int_S q\left[N\right]^T dS$$

$$\left[K^t\right]=\int_V \bar{k}_t\frac{\partial\left[N\right]^T}{\partial x_i}\frac{\partial\left[N\right]}{\partial x_i}dV+\int_V nS_r(\rho c)^w\boldsymbol{v}_i^w\left[N\right]^T\frac{\partial\left[N\right]}{\partial x_i}dV$$

$$+\int_V n(1-\mathrm{S}_r)(\rho c)^a v_i^a\left[N\right]^T\frac{\partial\left[N\right]}{\partial x_i}dV$$

+

Discretization in time (Newmark *β*)

$$\left\{T_{N|t+\Delta t}\right\}=\left\{T_{N|t}\right\}+\Delta t\left\{\dot{T}_{N|t}\right\}+\beta\Delta t\left(\left\{\dot{T}_{N|t+\Delta t}\right\}-\left\{\dot{T}_{N|t}\right\}\right)$$

$$\left(\left[C^t\right]+\beta\Delta t\left[K^t\right]\right)\left\{\dot{T}_{N|t+\Delta t}\right\}=\left\{F^t\right\}-\left[K^t\right]\left(\left\{T_{N|t}\right\}+(1-\beta)\Delta t\left\{\dot{T}_{N|t}\right\}\right)$$

Discretization of governing equations

Overall stiffness matrix

$$\begin{bmatrix} [K] & \gamma^w \vec{H}^w_{Sat} & \vec{H}^a_{Sat} \\ S_r \vec{K}^T_v & -\gamma^w\left[\bar{\alpha}+\bar{A}+F_{sr}\right] & F_{sr} \\ (1-S_r)\vec{K}^T_v & \gamma^w F_{sr} & -[\bar{\beta}+\bar{B}+F_{sr}] \end{bmatrix} \begin{Bmatrix} \Delta\vec{u}_{N|t+\Delta t} \\ h^w_{dE|t+\Delta t} \\ p^a_{|dEt+\Delta t} \end{Bmatrix} + \begin{Bmatrix} 0 \\ \sum_{i=1}^{m} \bar{\alpha}_i \gamma^w h^w_{idE|t+\Delta t} \\ \sum_{i=1}^{m} \bar{\beta}_i p^a_{idE|t+\Delta t} \end{Bmatrix}$$

$$= \begin{bmatrix} \Delta\vec{F}_{|t+\Delta t} + \vec{F}_T \Delta\vec{T}_{N|t+\Delta t} + \gamma^w \vec{H}^w_{Sat} h^w_{dE|t} + \vec{H}^a_{Sat} p^a_{dE|t} \\ -(\bar{A}+F_{sr})\gamma^w h^w_{dE|t} \quad + F_{sr} p^a_{dE|t} + \left[\bar{K}_{WT}\right]\Delta\vec{T}_{N|t+\Delta t} \\ F_{sr}\gamma^w h^w_{dE|t} - (\bar{B}+F_{sr}) p^a_{dE|t} + \left[\bar{K}_{AT}\right]\Delta\vec{T}_{N|t+\Delta t} \end{bmatrix}$$

$$\left(\left[C^t\right]+\beta\Delta t\left[K^t\right]\right)\dot{\vec{T}}_{N|t+\Delta t} = \left[f^t\right]-\left[K^t\right]\left(\vec{T}_{N|t} + (1-\beta)\Delta t\dot{\vec{T}}_{N|t}\right)$$

Displacement, water head, air pressure and temperature as unknown variables

III. Slope failure in unsaturated Sirasu ground

THMA coupling analysis in FE-FD scheme (Temperature=Const.)

Triaxial compression test of silty clay under undrained and unvented condition (Test data from Oka et al., 2011)

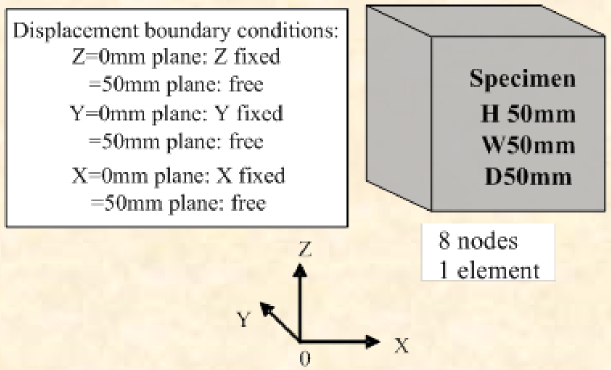

One element mesh and boundary conditions

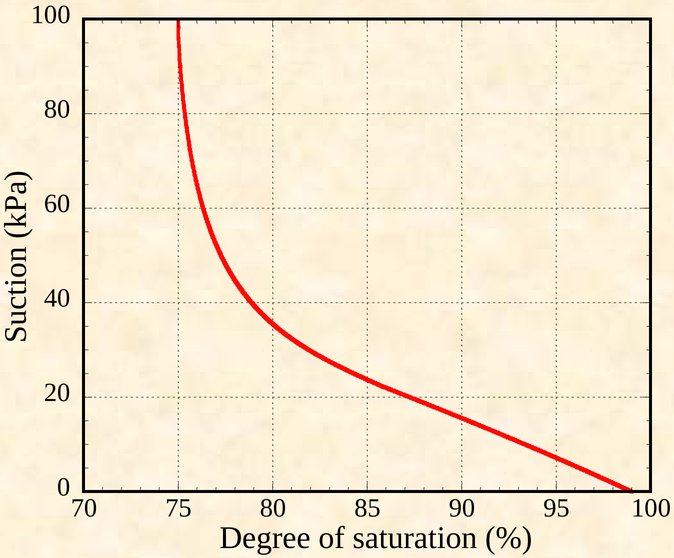

MCC

σ_{30}= 450kPa
p_{a0}= 250kPa
S_0 =10kPa, 30kPa, 50kPa, 100kPa
$\dot{\varepsilon}_0$= 0.5%/min
Temp. = 20^{o}C

Parameters of MCC of silty clay

Saturated degrees of saturation S_r^s	0.99
Residual degrees of saturation S_r^r	0.10
Parameter corresponding to drying AEV (kPa) S_d	220.2
Parameter corresponding to wetting AEV (kPa) S_w	5.10
Initial stiffness of scanning curve (kPa) k_{sp}^e	58500
Parameter of shape function c_1	0.0108
Parameter of shape function c_2	0.010
Parameter of shape function c_3	24.0

Material parameters of silty clay

Compression index λ	0.123
Swelling index κ	0.062
Critical state parameter M	1.00
Void ratio N (p'=98 kPa on $N.C.L.$)	1.00
Poisson's ratio ν	0.30
Parameter of overconsolidation a	5.00
Parameter of suction b	0.50
Parameter of overconsolidation β	1.00
Void ratio N_r (p'=98 kPa on $N.C.L.S.$)	1.18

Comparison between test and calculation

Stress-strain relation | Air pressure | Pore water pressure

Test

Calculation

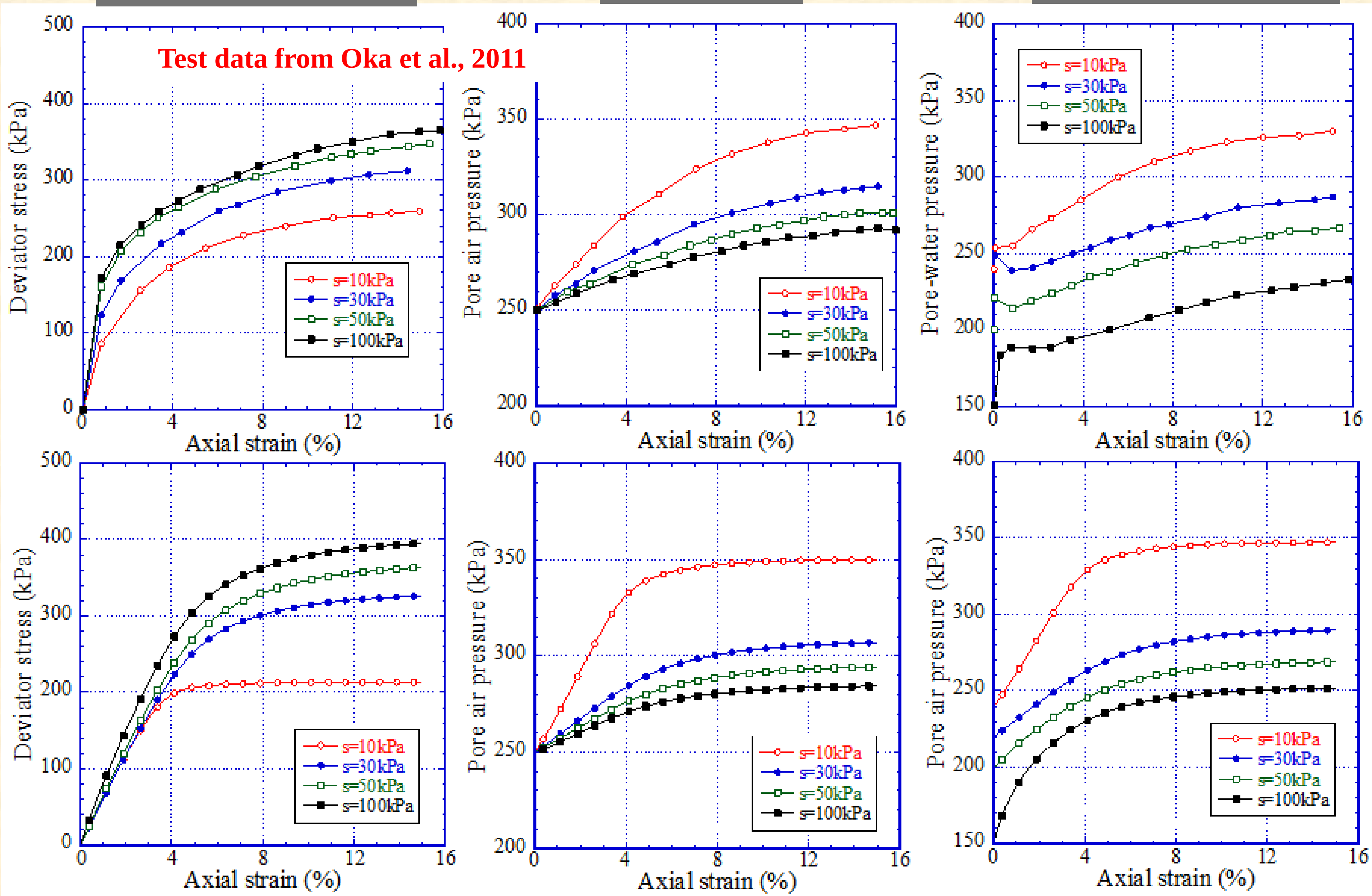

Model test (Kitamura et al., 2007)

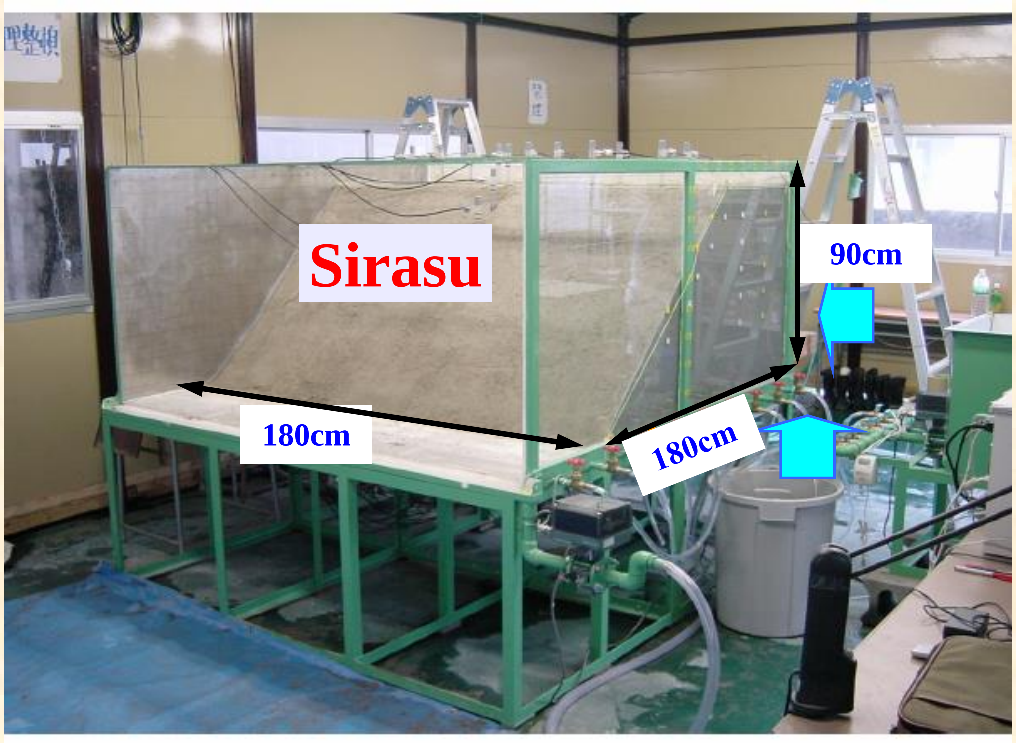

Test box

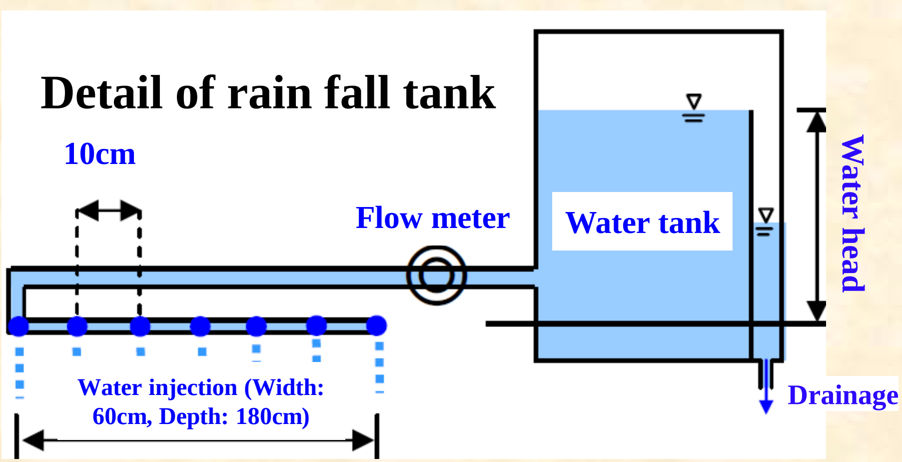

Rain falling device

Test conditions

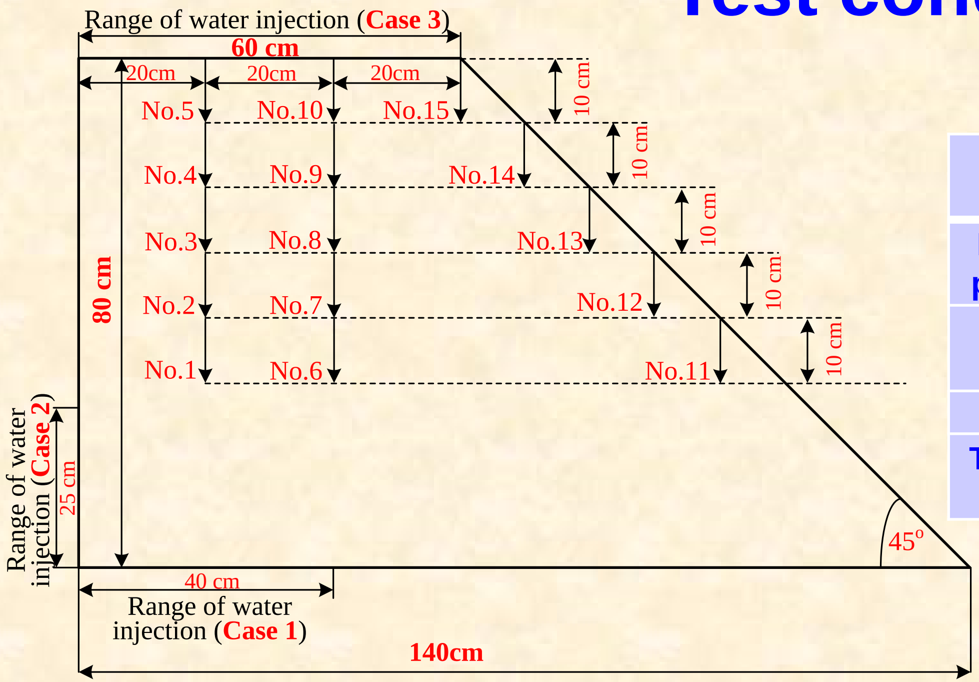

Location of tensiometers and water injection pattern

Physical properties of Sirasu

	Case1	Case2	Case3
Density of soil particle (g/cm³)	2.45	2.40	2.45
Water content in nature (%)	25.6	23.3	23.1
Void ratio	1.57	1.47	1.57
Total density of soil (g/cm³)	1.20	1.20	1.17

Drainage conditions

	Case1	Case2	Case3
Top	drained	drained	drained
Bottom	undrained	undrained	undrained
Back side	undrained	undrained	undrained
Slope face	drained	drained	drained

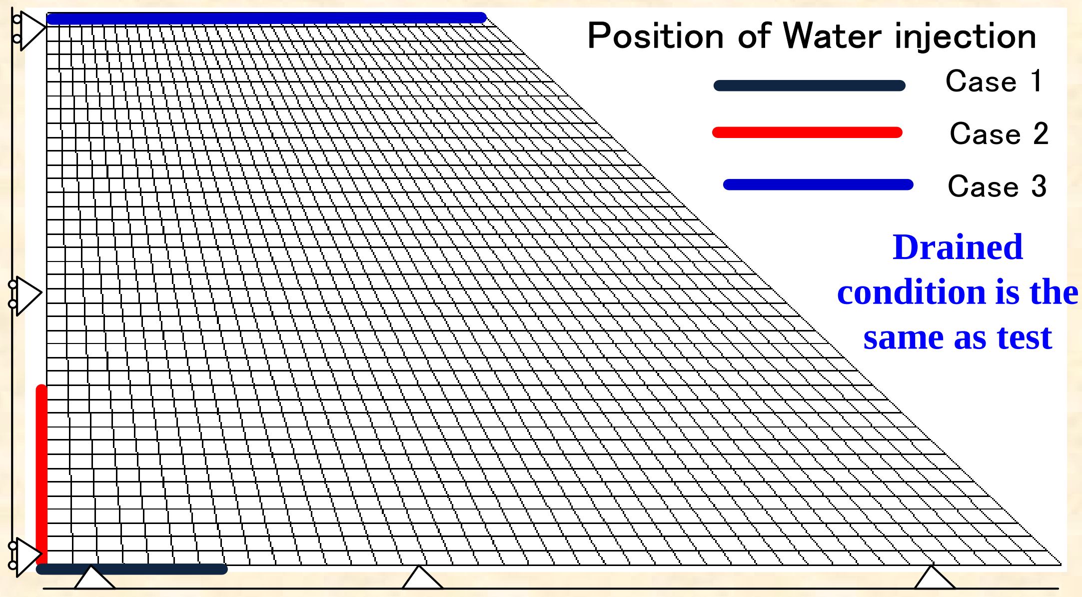

FEM mesh and loading condition

Calculation conditions

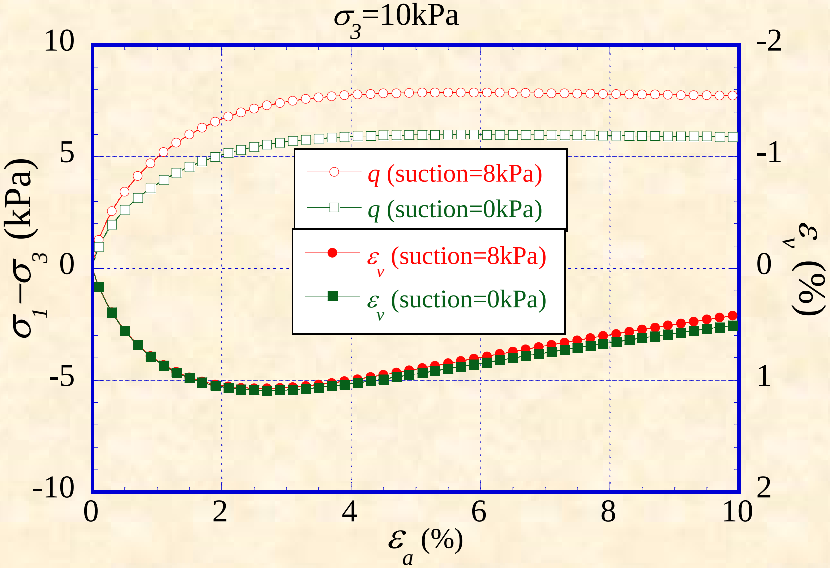

Element behavior of Sirasu

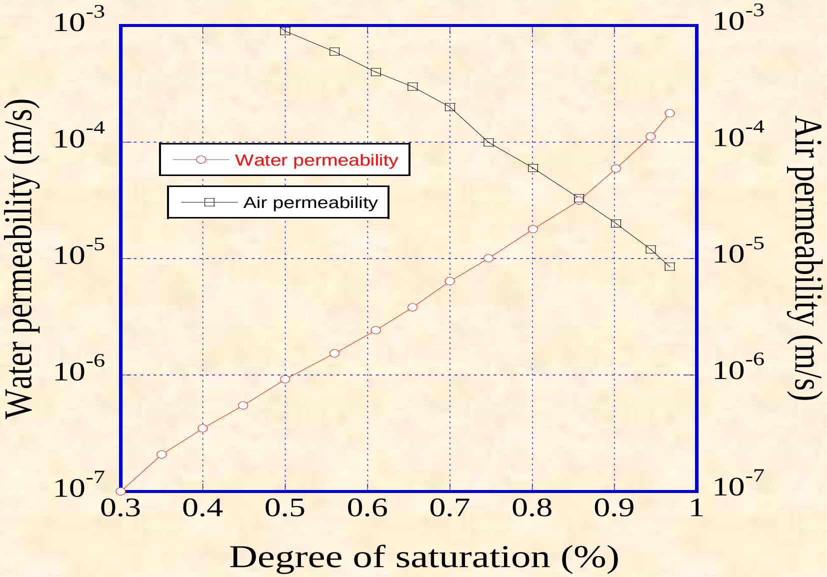

Relationship between permeability of water & air with saturation

Material parameters

Compression index λ	0.055
Swelling index κ	0.010
Critical state parameter M	1.0
Void ratio N (p'=98 kPa on *N.C.L.*)	1.55
Poisson's ratio ν	0.30
Parameter of overconsolidation a	2.00
Parameter of suction b	0.50
Parameter of overconsolidation β	1.0
Void ratio N_r (p'=98 kPa on *N.C.L.S.*)	1.57

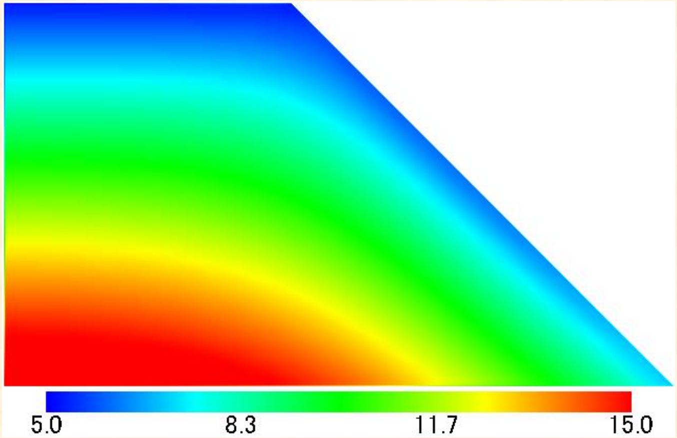

Gravitation stress field+5kPa

Soil water characteristic curve (MCC)

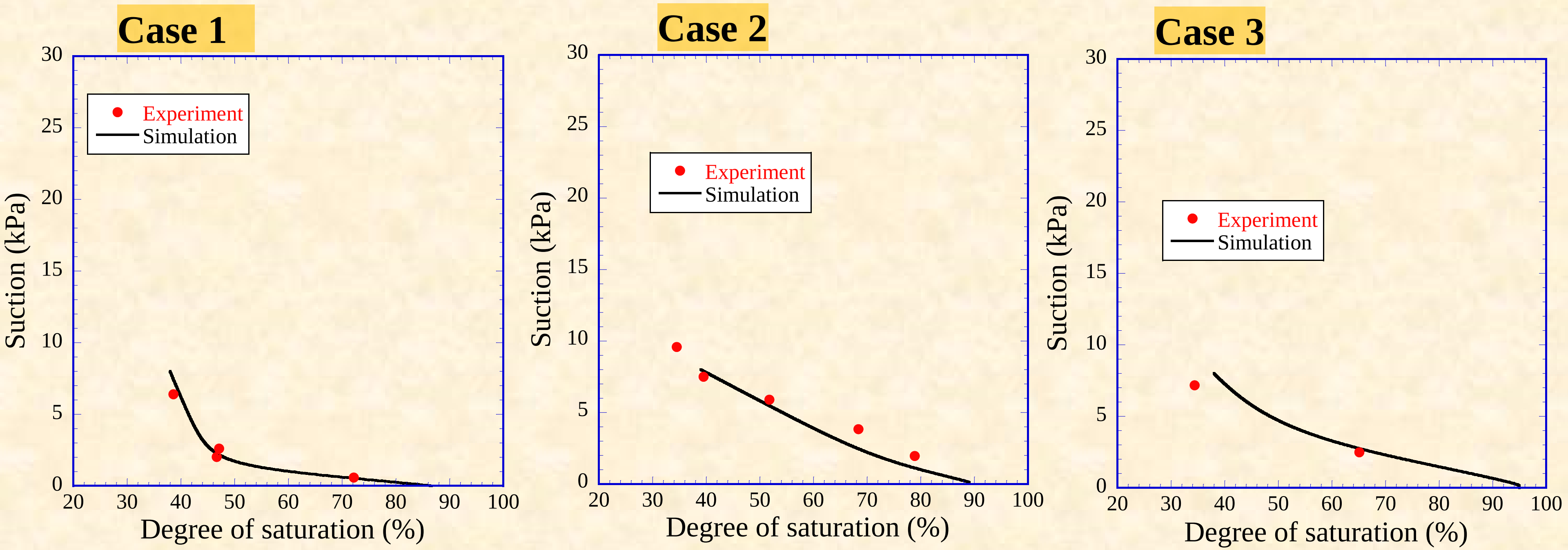

Parameters of MCC

	Case 1	Case 2	Case 3
Saturated degrees of saturation S_r^s	**0.87**	**0.89**	**0.95**
Residual degrees of saturation S_r^r	**0.20**	**0.25**	**0.20**
Parameter corresponding to drying AEV (kPa) S_d	**12.0**	**15.0**	**12.0**
Parameter corresponding to wetting AEV (kPa) S_w	**0.07**	**0.10**	**0.17**
Initial stiffness of scanning curve (kPa) k_{sp}^e	**90.0**	**20.0**	**50.0**
Parameter of shape function c_1	**0.30**	**0.30**	**0.33**
Parameter of shape function c_2	**0.60**	**0.40**	**0.18**
Parameter of shape function c_3	**30.0**	**50.0**	**5.0**

Initial condition

Suction: 8kPa

Saturation: 38%

Comparison of EPWP (Case 1)

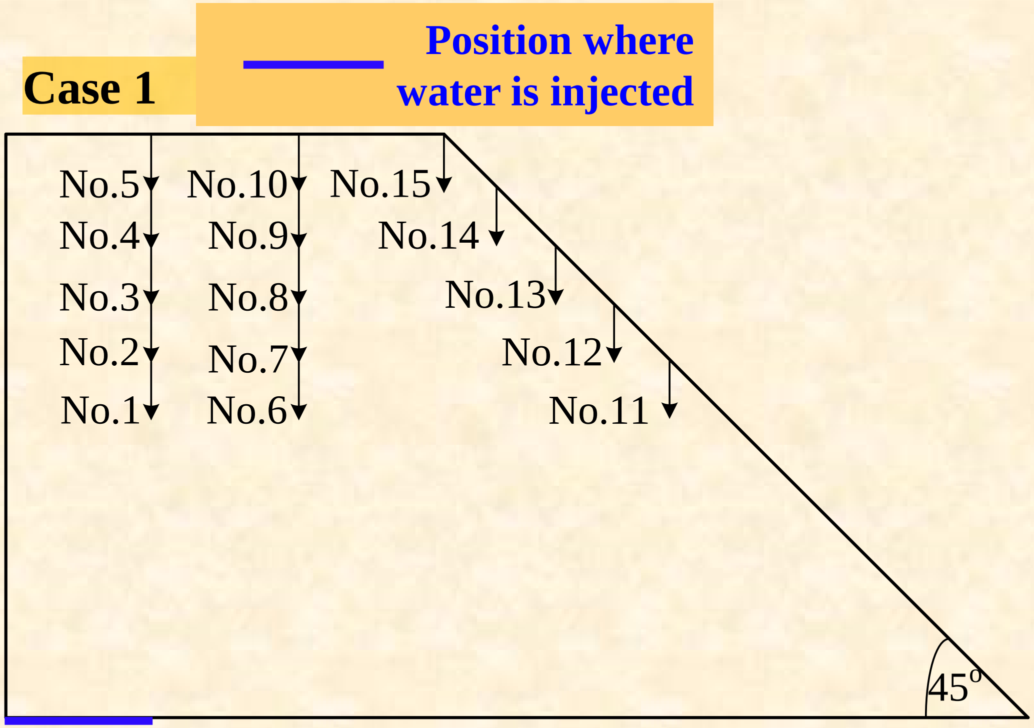

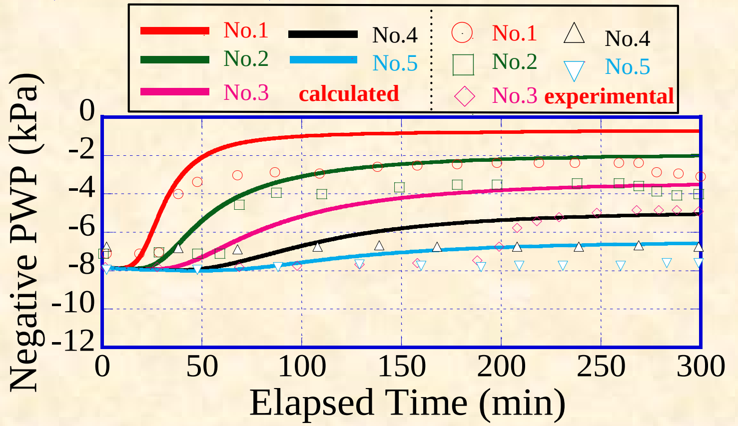

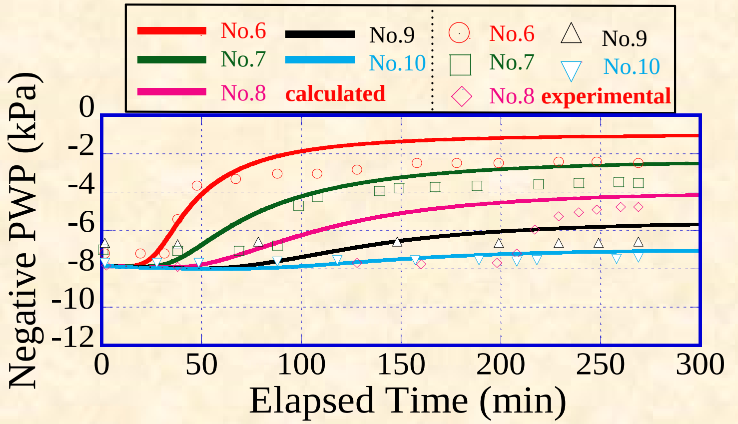

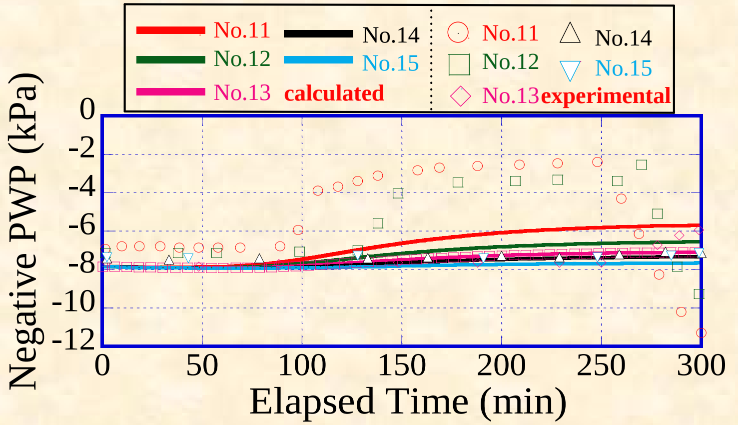

Calculation is on the whole coincident with test. The failure time is also the same in calculation and test. In slope surface, however, the lose of suction in calculation is much slower than that at test

Comparison of EPWP (Case 2)

Case 2

Position where water is injected

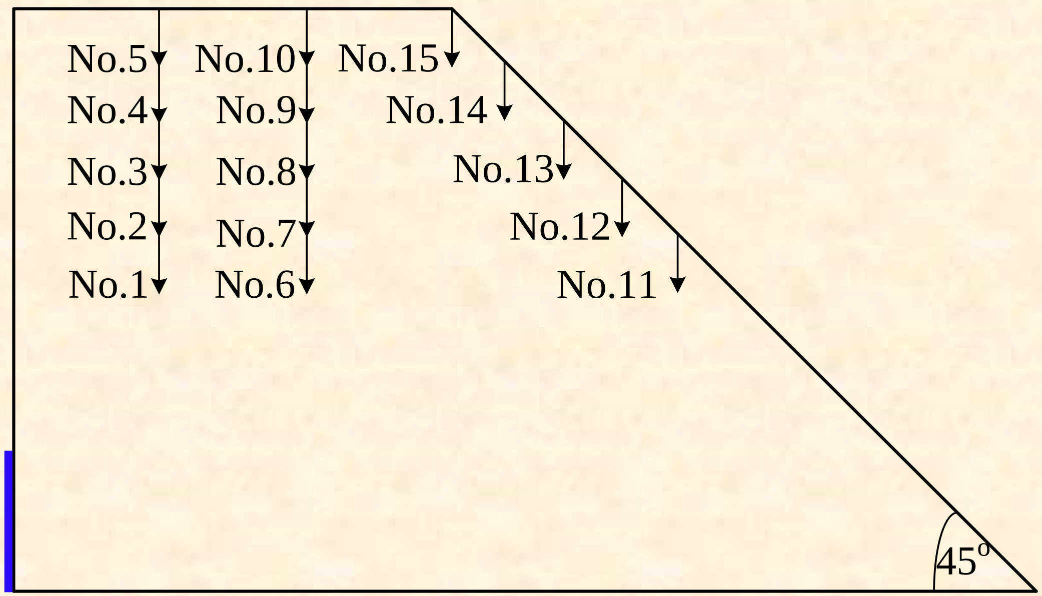

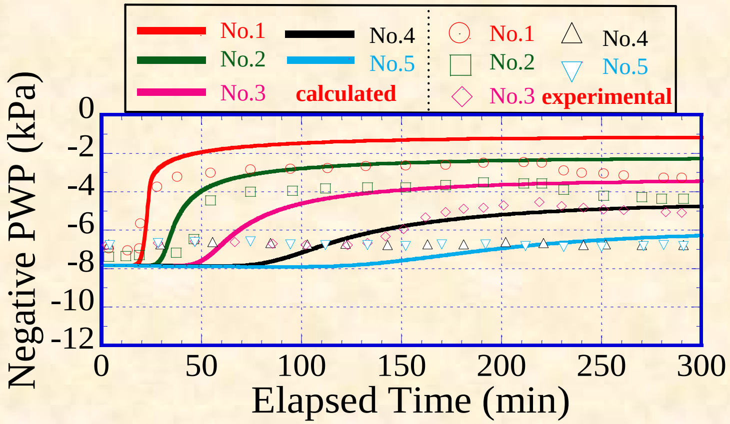

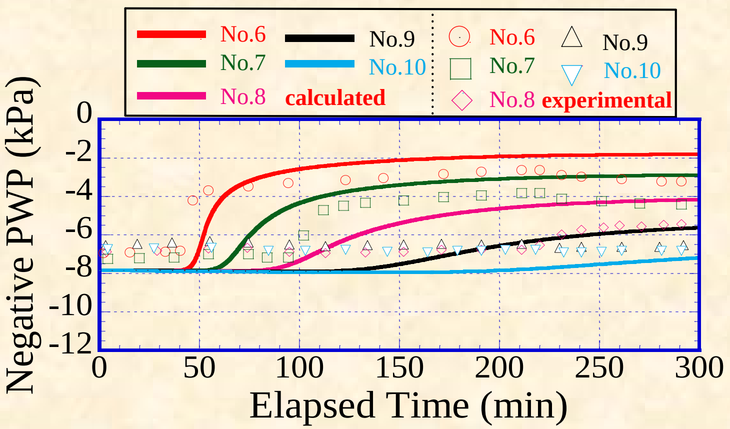

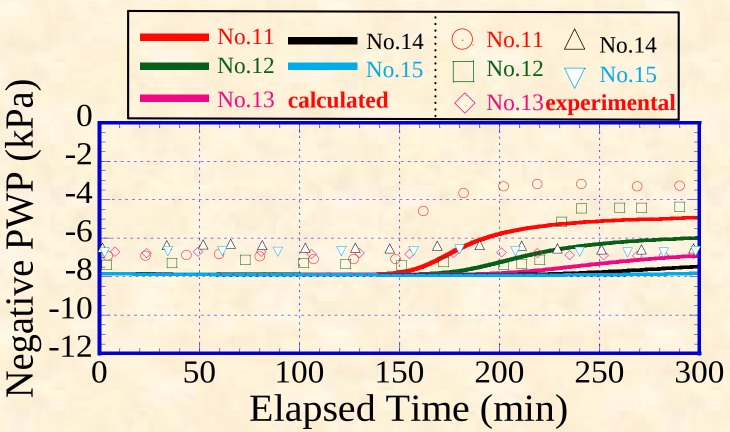

Calculation is on the whole coincident with test. In slope surface, however, the lose of suction in calculation is much slower than that at test

Comparison of EPWP (Case 3)

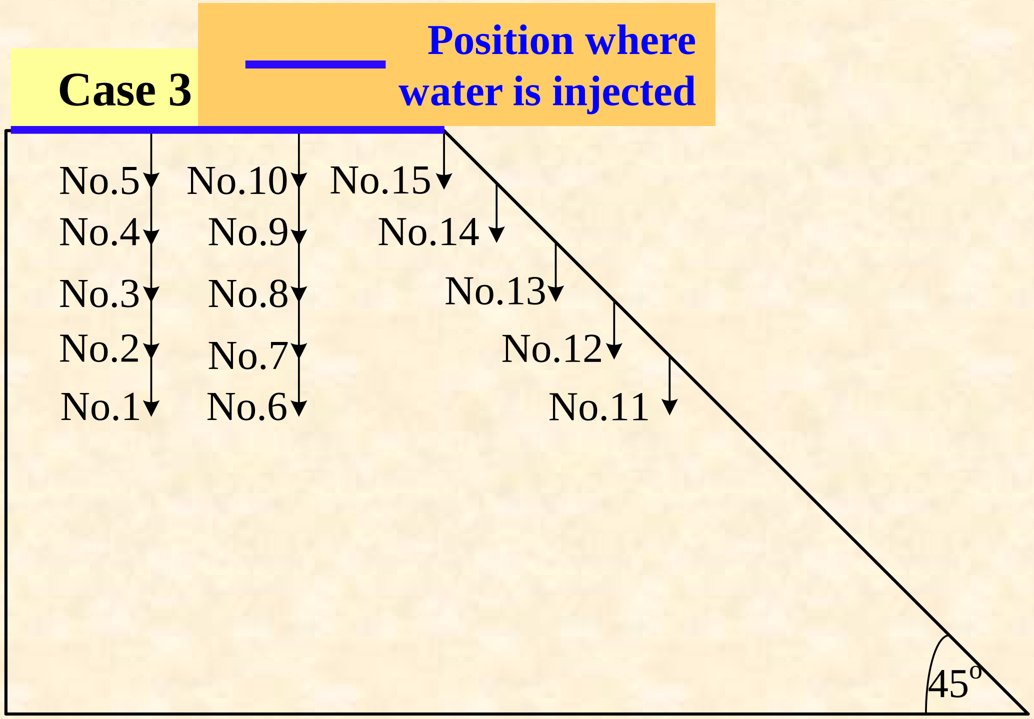

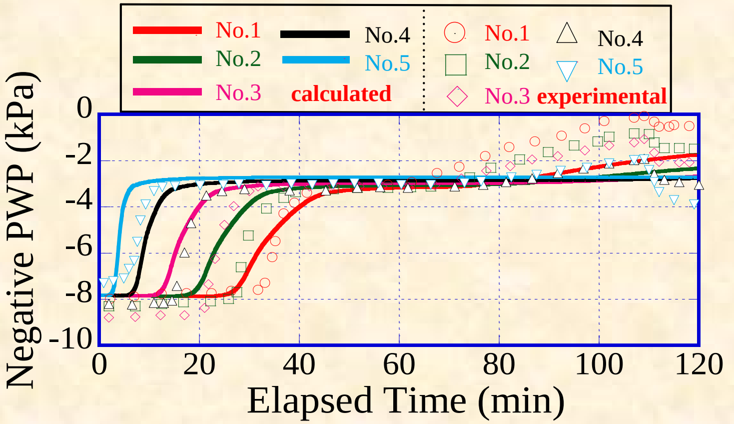

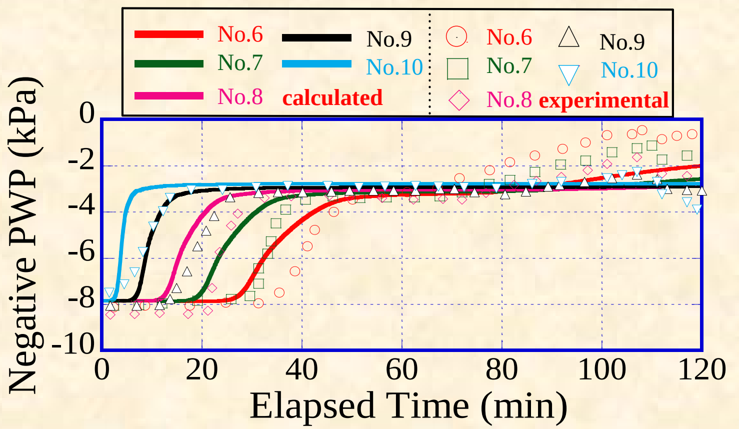

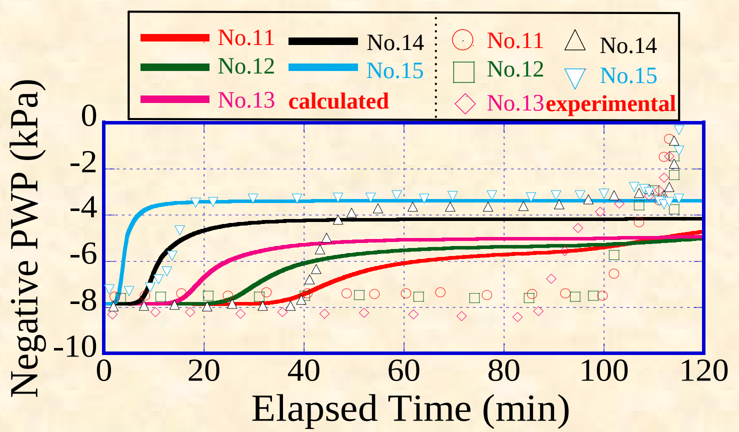

Calculation is on the whole coincident with test. The failure time is also the same in calculation and test.

Change of degree of saturation

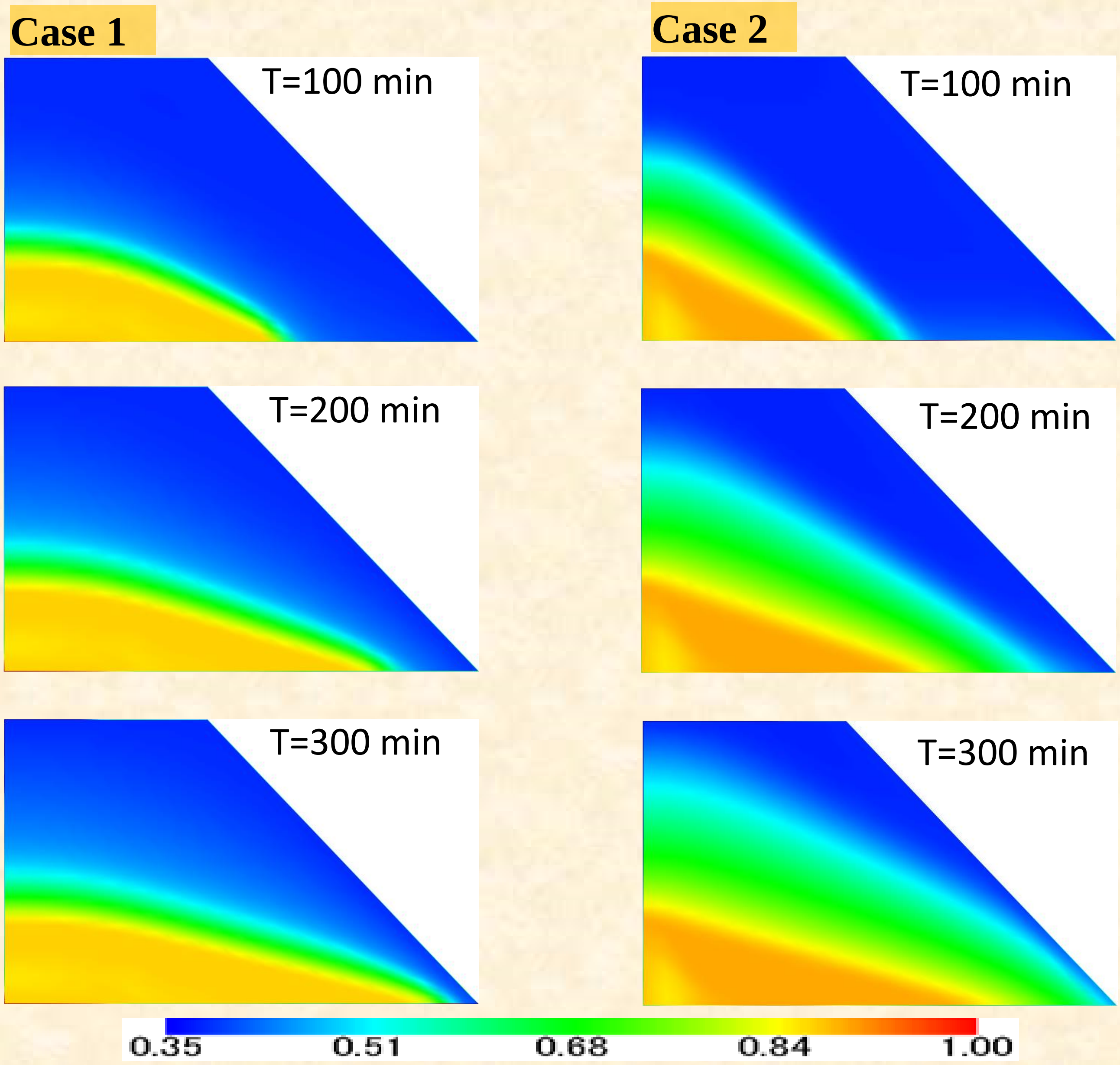

Change of degree of saturation

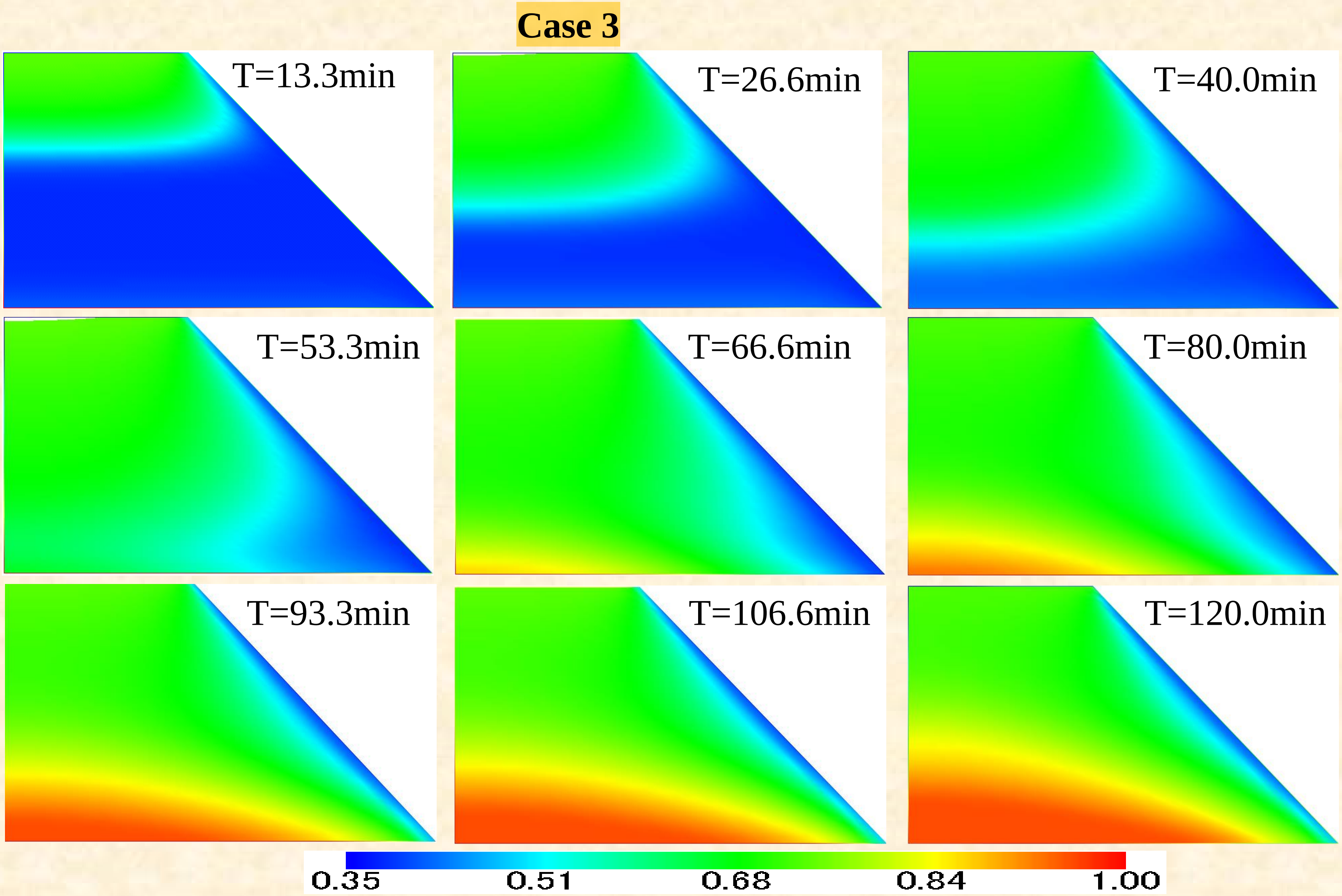

Shear strain $\sqrt{2I_2^p}$ **(**I_2^p**: 2nd invariant of deviatoric plastic strain)**

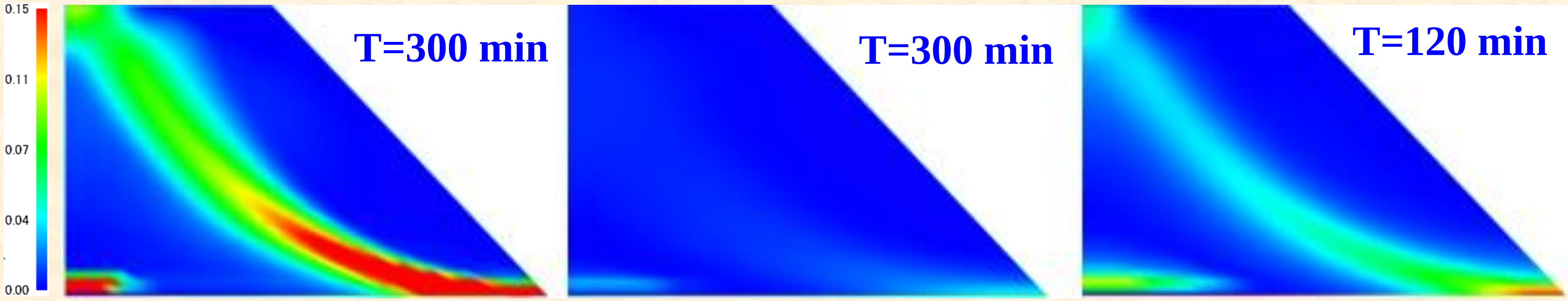

Case 1 **Case 2** **Case 3**

Distribution of deviatoric plastic strain

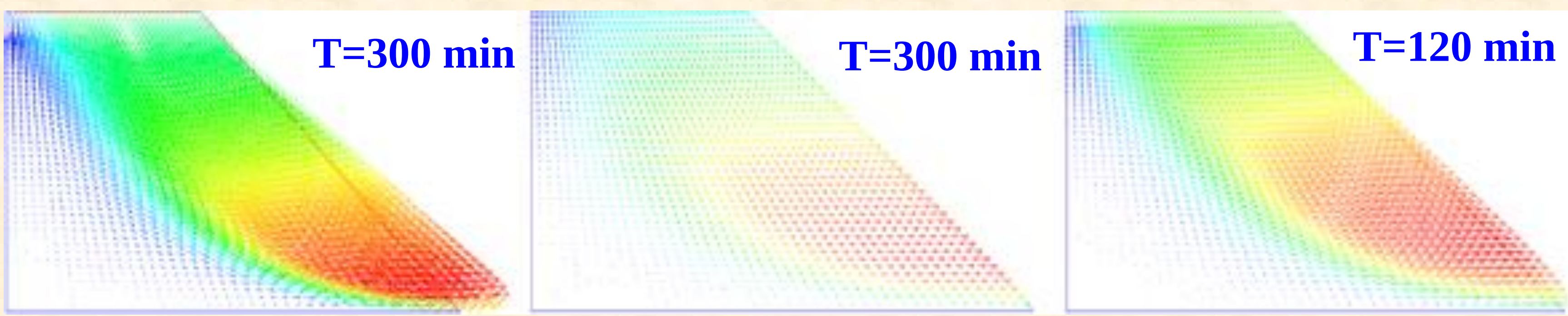

Distribution of displacement vector

The calculations are totally the same as the tests, that is, Case 1 and Case 3 are much easier to fail than Case 2

IV. THMA coupling analysis of heating test for saturated geomaterials

(p_a=constant, S_r=1.0)

Heating test for saturated rock (Gens et al.,2007)

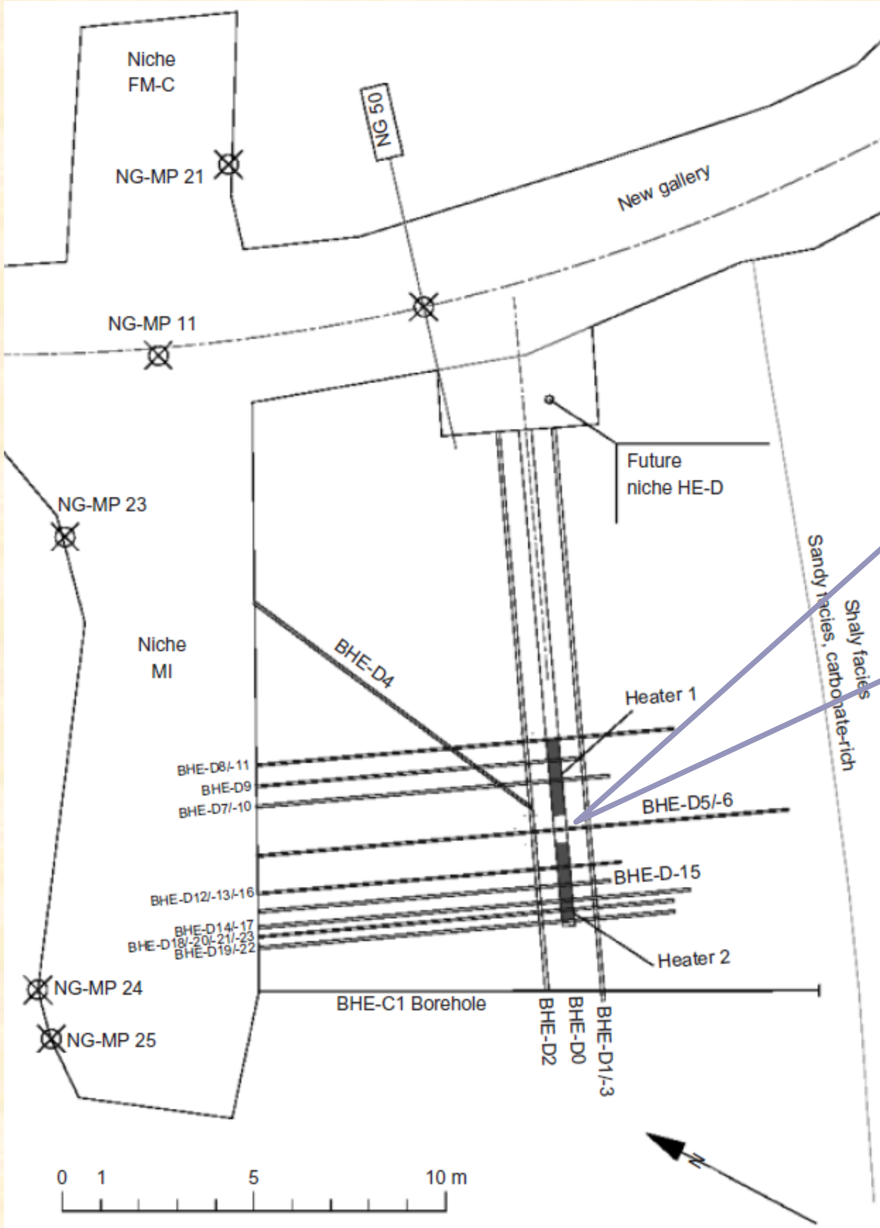

Layout of test site

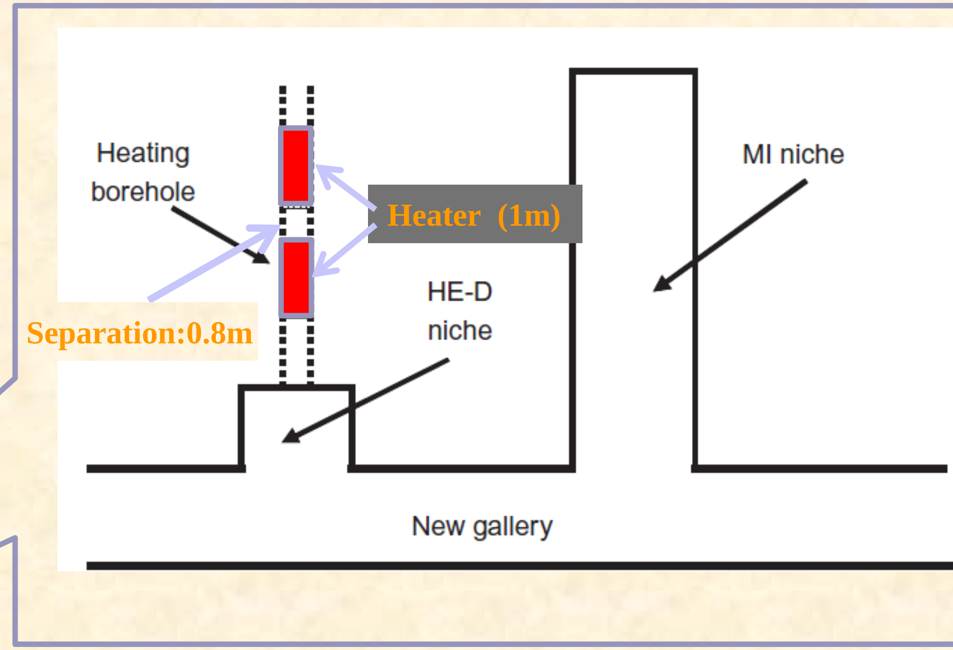

Multi stages of the heating tests

Stage	Start: day	End: day	Duration : day	Activity
1	0	90	90	Heating (325W/heater)
2	91	339	248	Heating (975W/heater)
3	340	518	180	Cooling

3D THMA analysis conditions

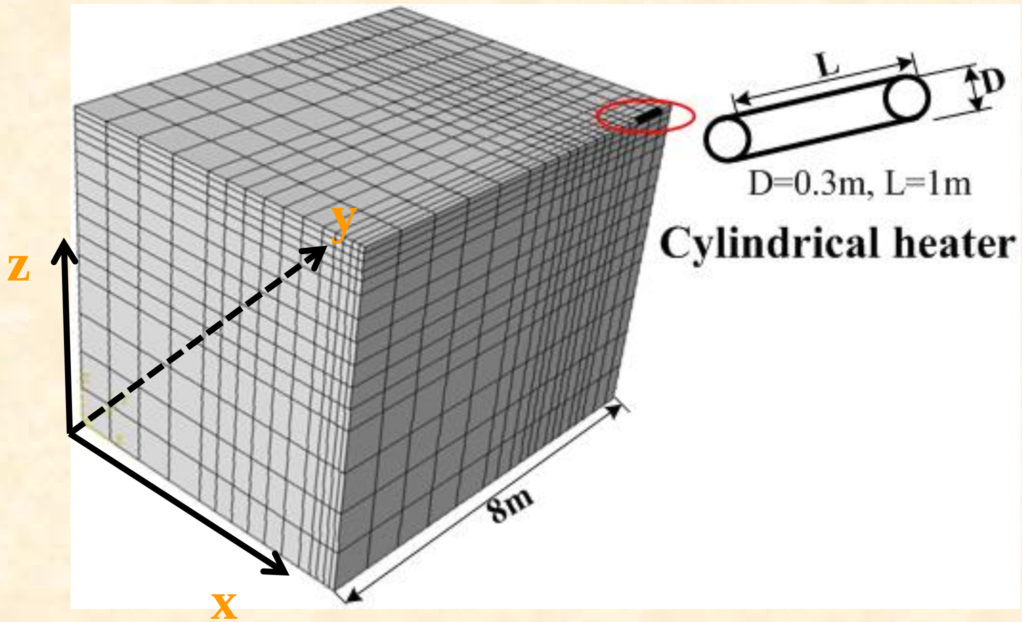

3D FEM mesh

Initial condition:

Water pressure: **1 MPa**

Mean stress: **5 MPa**

Temperature: **15°C**

Boundary conditions:

Up, back and right planes:

undrained and heat insulated

Other planes:

Drained and fixed temperature (15°C)

Material parameters and physical parameters

Material parameters

Compression index λ	0.0026
Swelling index κ	0.00064
Critical state parameter M	1.0
Void ratio N (p'=98 kPa on *N.C.L.*)	0.85
Poisson's ratio ν	0.30
Parameter of overconsolidation a	2.00
Parameter of suction b	0.50
Parameter of overconsolidation β	1.0
Void ratio N_r (p'=98 kPa on *N.C.L.S.*)	0.85

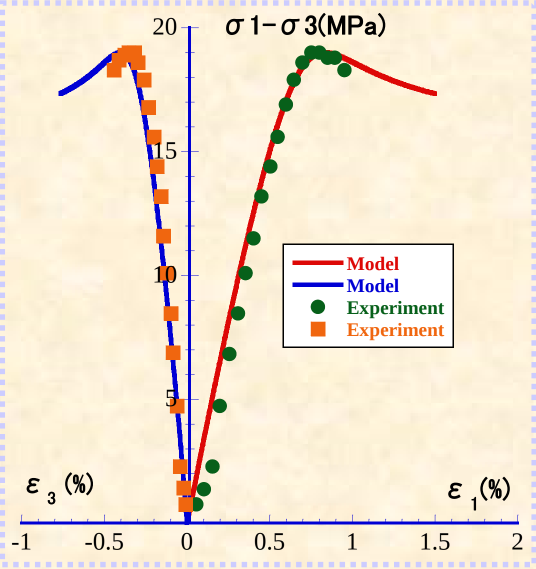

Element simulation of triaxial compression test (σ_3=8 MPa)

Physical parameters

Thermal expansion coefficient α_t(K^{-1})	8.0e-06
Thermal expansion coefficient α^w(K^{-1})	2.1e-04
Thermal conductivity k_t (kJ m^{-1} K^{-1}Min^{-1})	0.18
Specific heat C (kJ Mg^{-1} K^{-1})	840.
Heat transfer coefficient of air boundary a_c ((kJ m^{-2} K^{-1} Min^{-1})	236.
Specific heat of water C_w (kJ Mg^{-1} K^{-1})	4184.

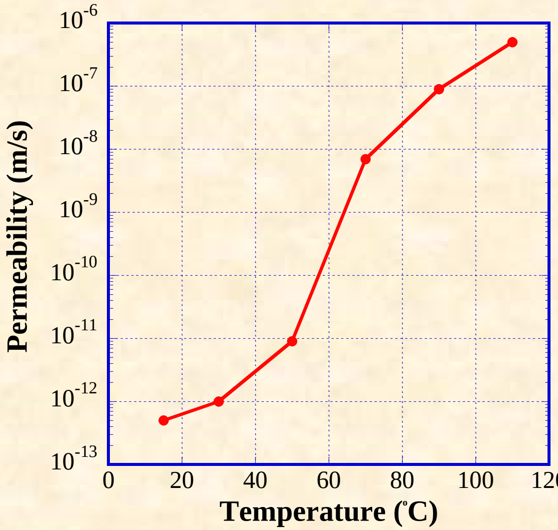

Relation between permeability and temperature

Comparison between test and calculation (temperature)

D: distant of measuring point to heater

Z: z coordinate of measuring point

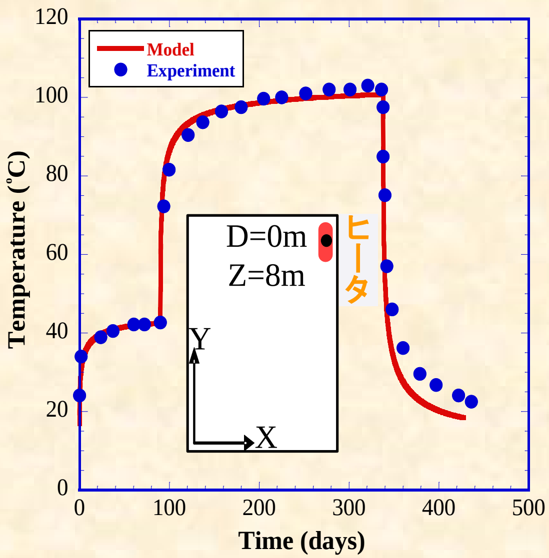

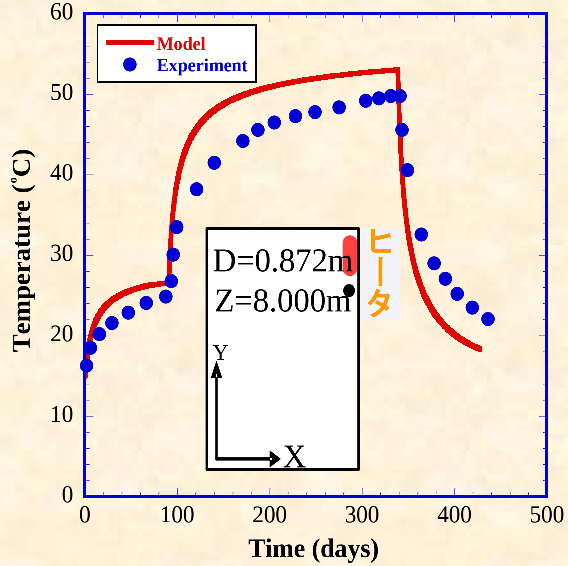

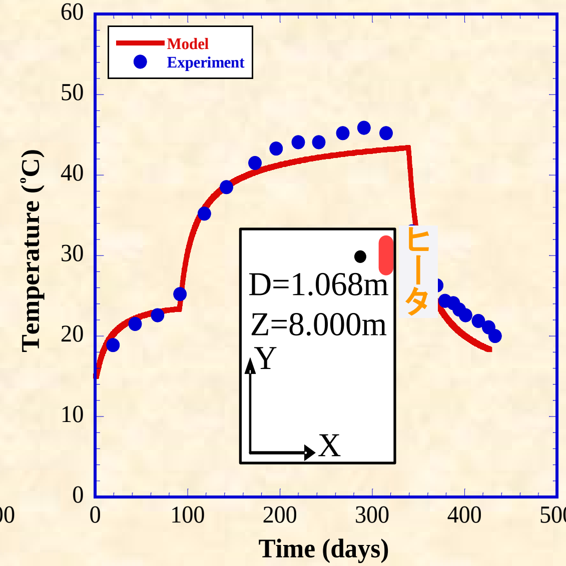

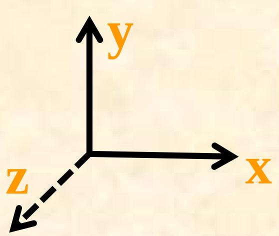

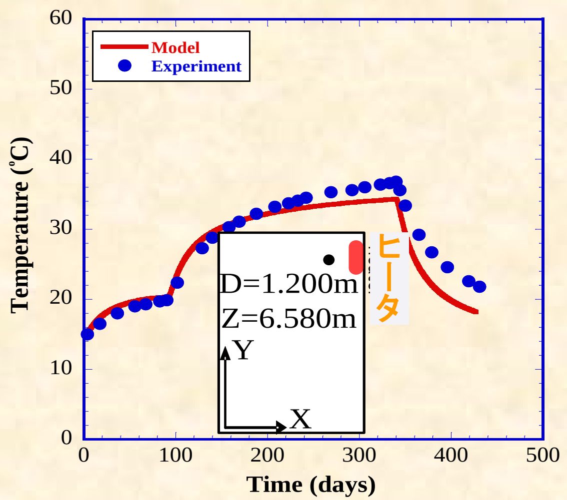

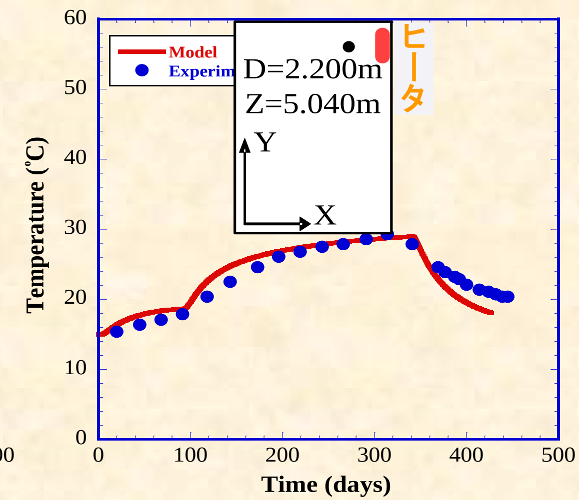

Change of temperature at different positions

Comparison between test and calculation (EPWP)

D: distant of measuring point to heater

Z: z coordinate of measuring point

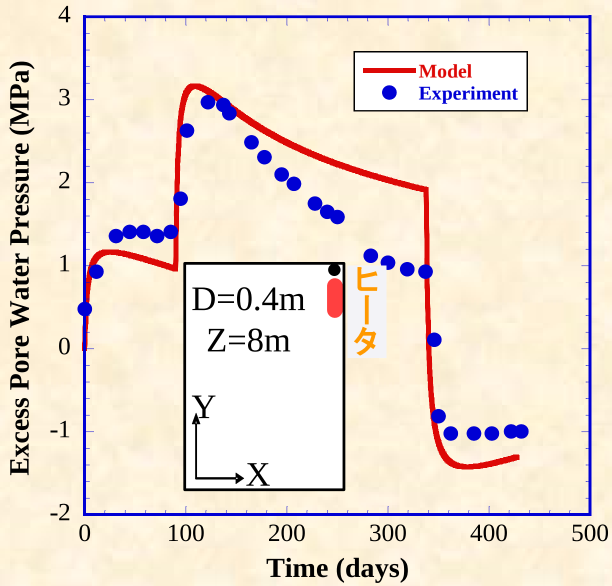

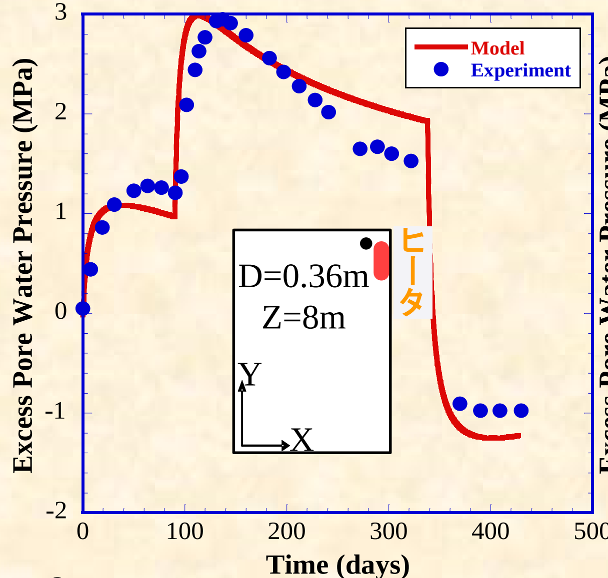

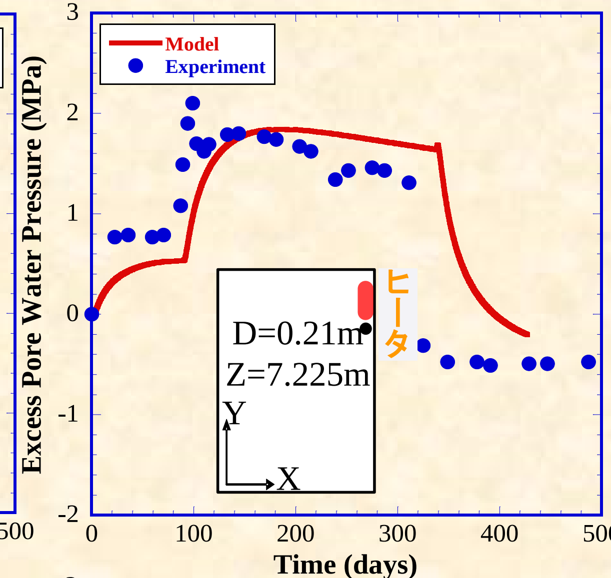

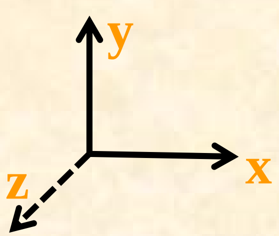

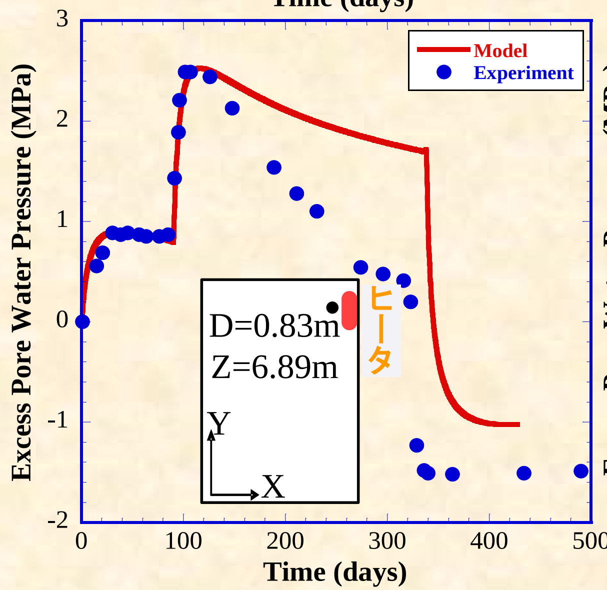

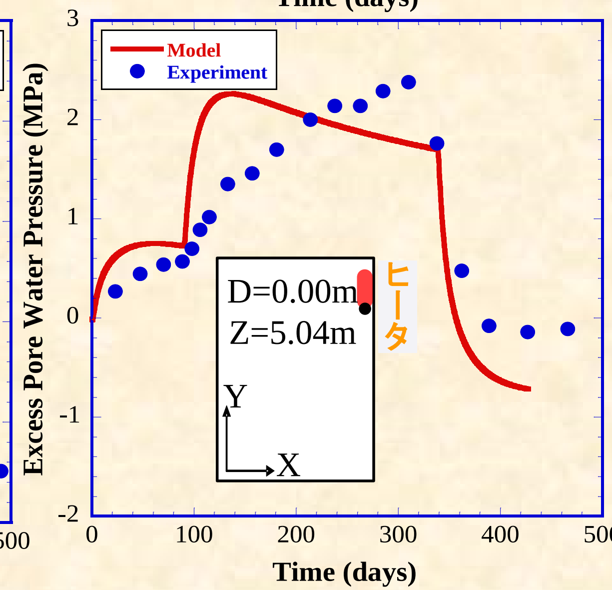

Change of EPWP at different positions

Comparison between test and calculation (Strain)

D: distant of measuring point to heater
Z: z coordinate of measuring point

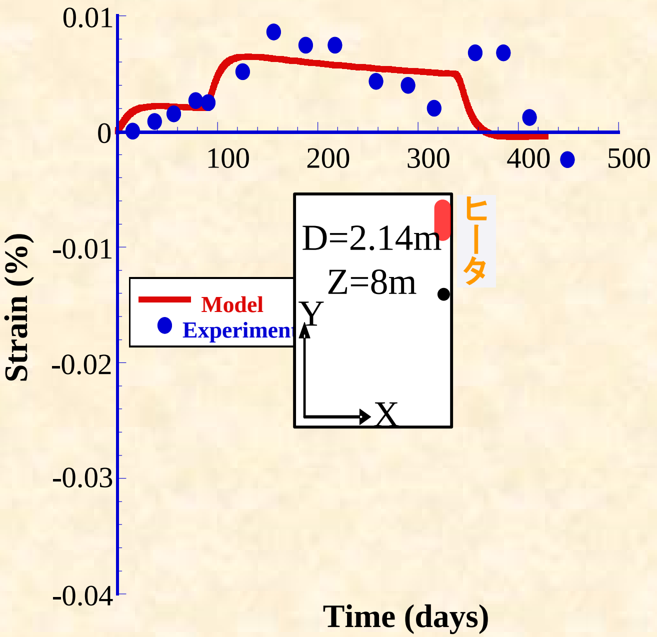

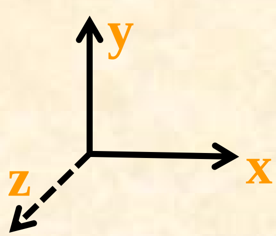

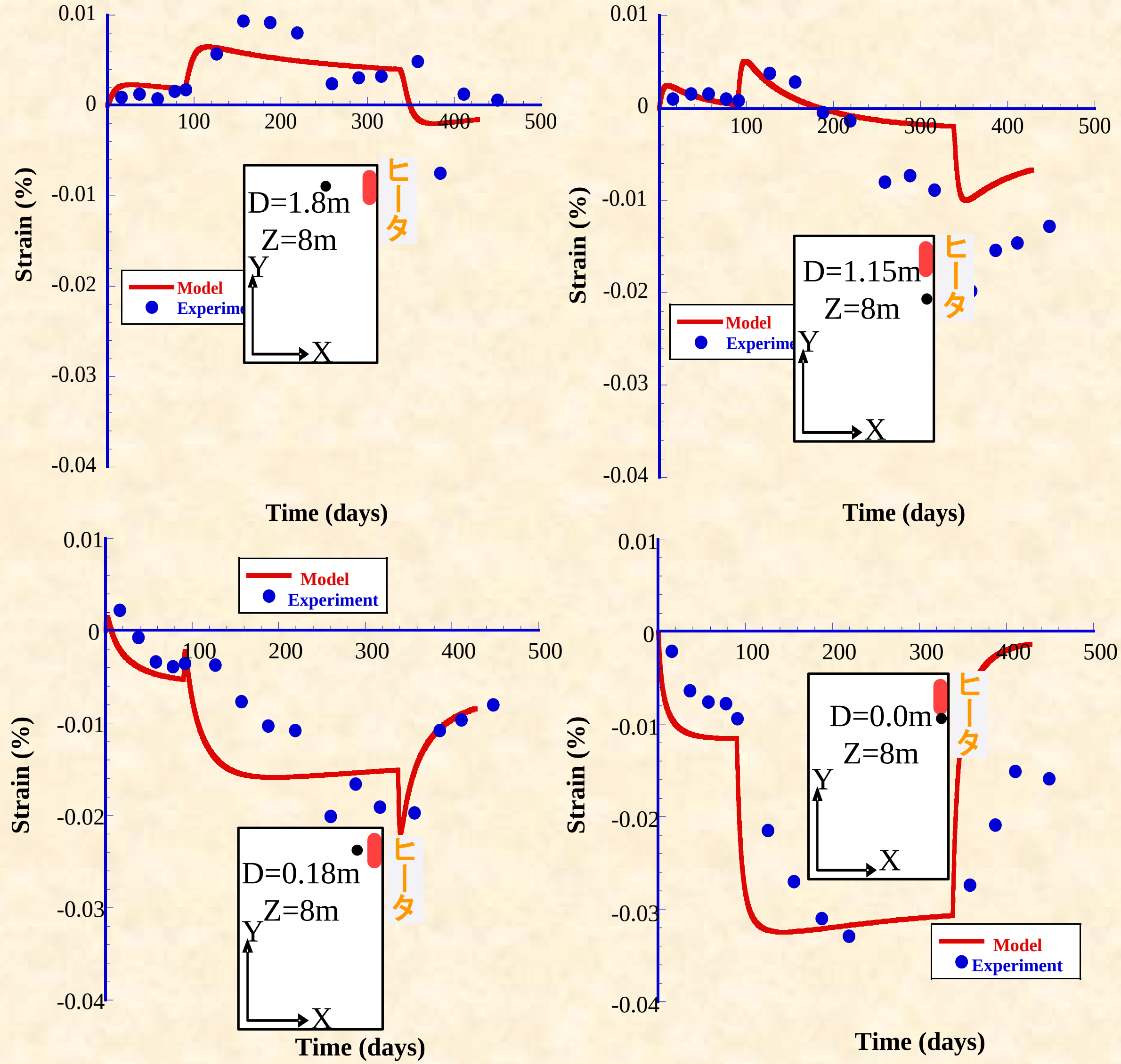

Change of Deviatory strain at different positions

Distribution of temperature (only calculation)

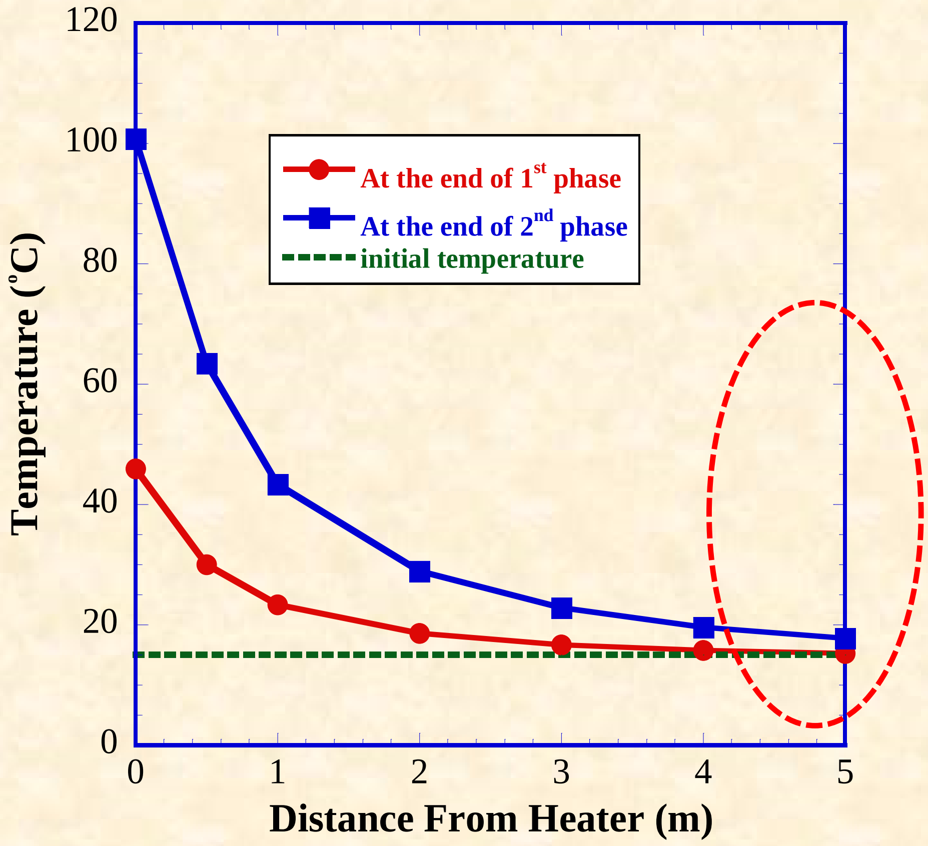

Distribution of temperature

- ✓ Temperature only changed in limited area (D<5m)
- ✓ Reason : Small thermal conductivity of rock

V. THMA coupling analysis of heating test for saturated/ unsaturated geomaterial

(p_a=0, S_r≤1.0)

Heating tests (Munoz, 2006)

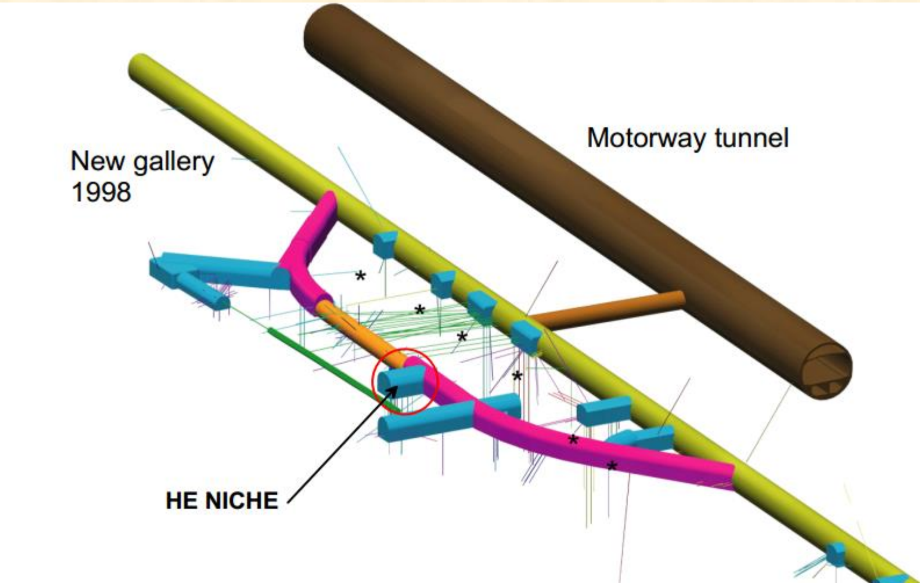

3D view of the Mont Terri Undergound Rock Laboratory

Layout of heating test

Rock

Heater
(ϕ75mm)

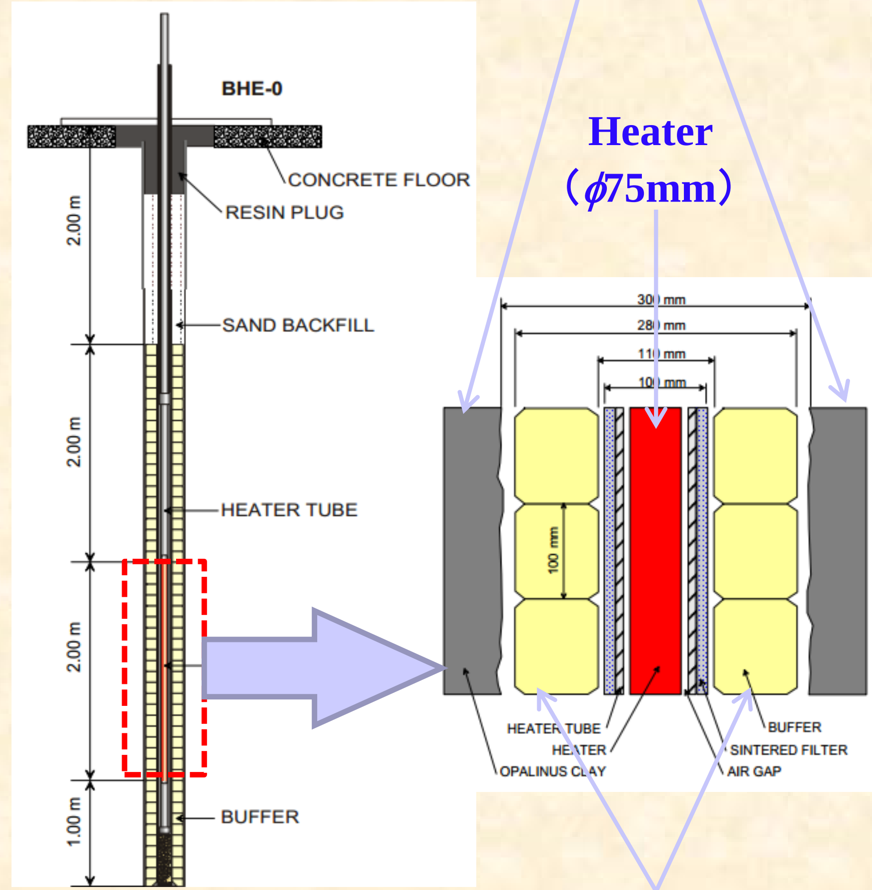

Boring hole
(ϕ 0.3m; Depth: 7m)

Bentonite buffer

Testing stages

Stage	Start (day)	End (day)	Time (day)	Action
1	0	982	982	hydration phase
2	982	1522	540	heating phase
3	1523	1800	278	Cooling phase

Analytical conditions

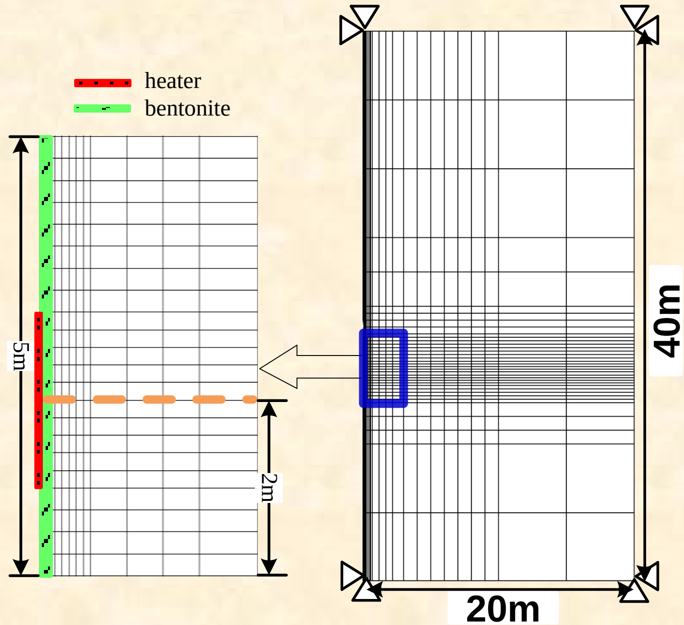

FEM mesh and boundary condition

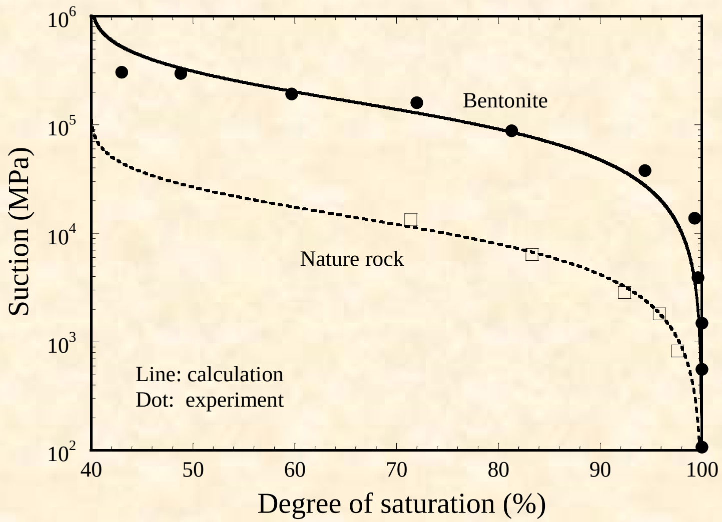

MCC

Material parameters of bentonite and rock

	Bentonite	Rock
Compression index λ	0.0050	0.0020
Swelling index κ	0.010	0.0001
Critical state parameter M	1.80	1.90
Void ratio N (p'=98 kPa on $N.C.L.$)	1.04	0.62
Poisson's ratio ν	0.30	0.30
Parameter of overconsolidation a	5.0	5.0
Parameter of suction b	0.00	0.00
Parameter of overconsolidation β	1.0	1.0
Void ratio N_r (p'=98 kPa on $N.C.L.S.$)	1.06	0.65
Thermal expansion coefficient (1/K)	1.0×10^{-5}	3.0×10^{-6}
Thermal expansion coefficient of water (1/K)	2.1×10^{-4}	
Thermal conductivity (kJ m^{-1} K^{-1}Min^{-1})	0.06	0.12
Specific heat (kJ Mg^{-1} K^{-1})	723	874
Specific heat of water (kJ Mg^{-1} K^{-1})	4184	

Parameters of MCC

	Bentonite	Rock
Saturated degrees of saturation S_r^s	1.00	1.00
Residual degrees of saturation S_r^r	0.40	0.40
Parameter corresponding to drying AEV (kPa) S_d	11000	21000
Parameter corresponding to wetting AEV (kPa) S_w	800	1000
Initial stiffness of scanning curve (kPa) k_{sp}^e	25000	90000
Parameter of shape function c_1	0.000001	0.00003
Parameter of shape function c_2	0. 000005	0.00006
Parameter of shape function c_3	30.0	50.0

Initial conditions

Unsaturated bentonite: s=136MPa; S_r=70%

Saturated soft rock: water head=40m

Result: 1st stage

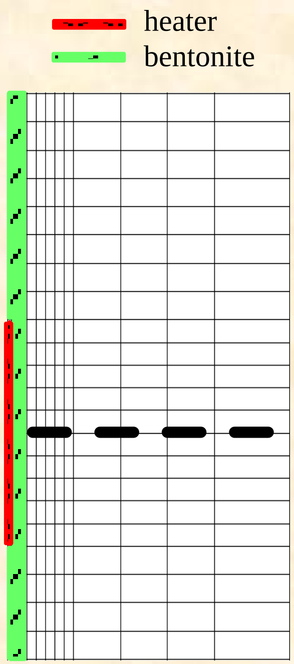

D : distance from heater

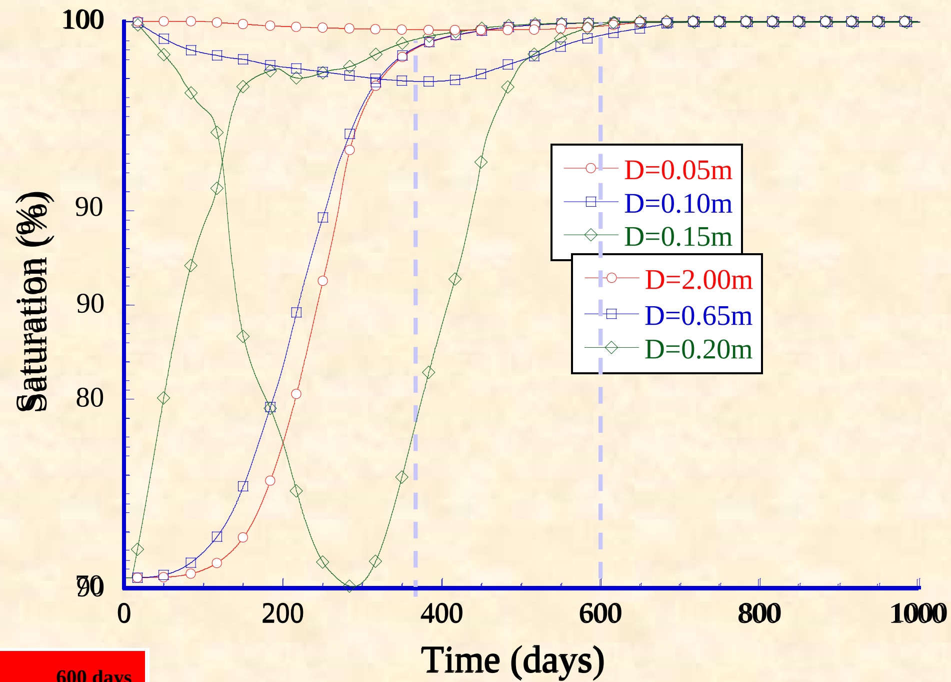

Change of saturation in bentonite and neighboring rock

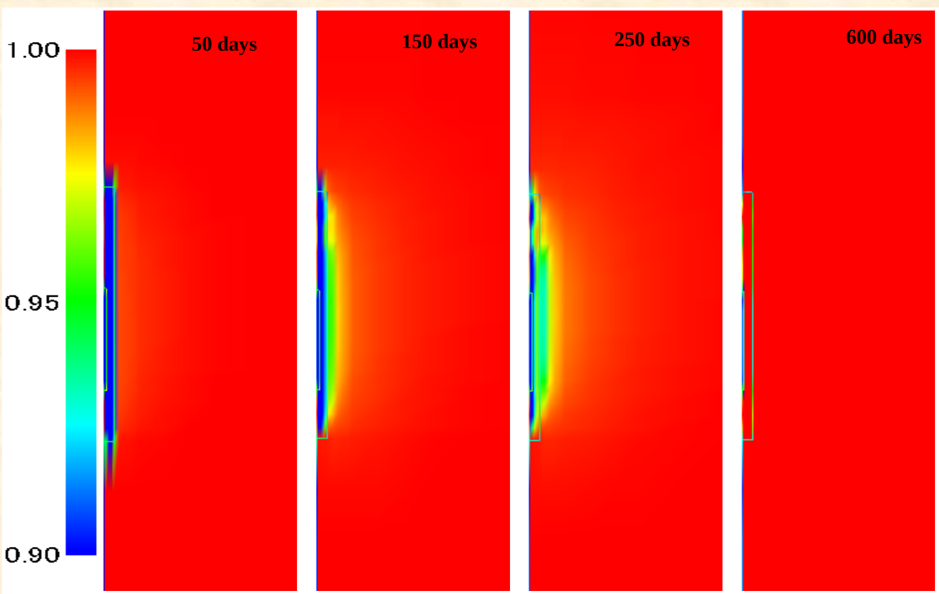

Distribution of saturation

Result: 2^{nd} and 3^{rd} stages

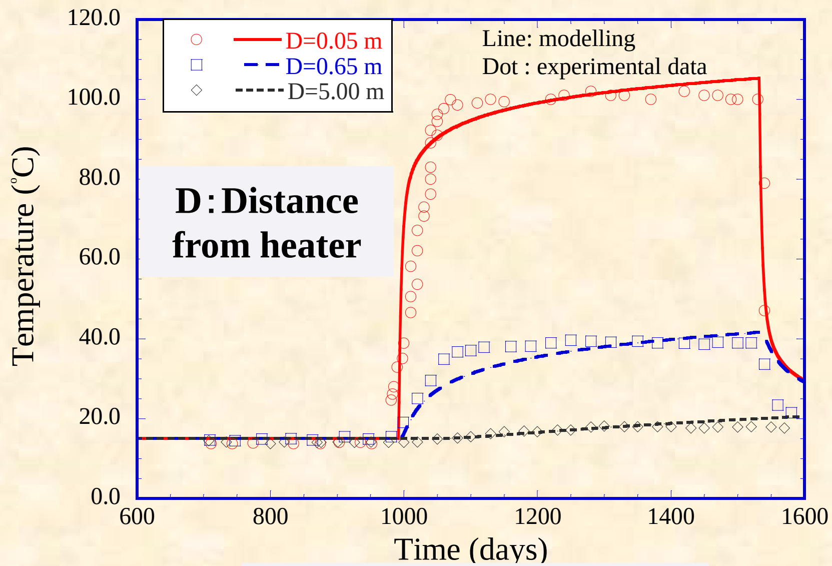

Change of temperature

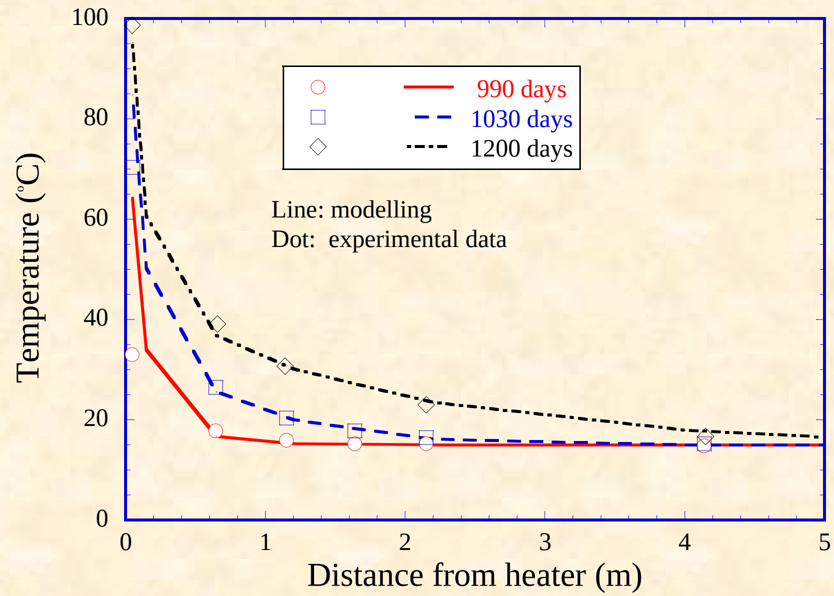

Distribution of temperature

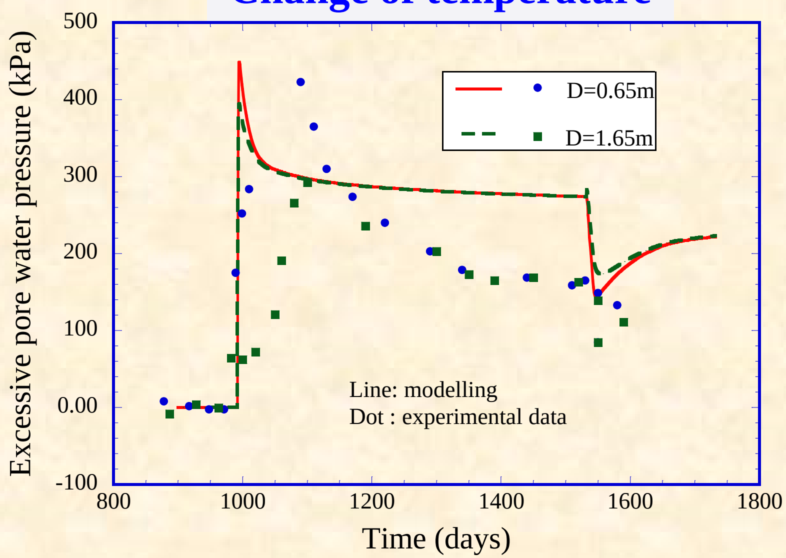

Change EPWP

- Quick change of temperature can be clearly simulated
- No prominent change of temperature at the place 5m away from the heat source
- Change of EPWP due to temperature can be clearly simulated

VI. THMA coupling analysis for geologic repository of HLRW

(p_a=0, S_r≤1.0)

THMA coupling analysis for geologic repository of HLRW

FEM mesh

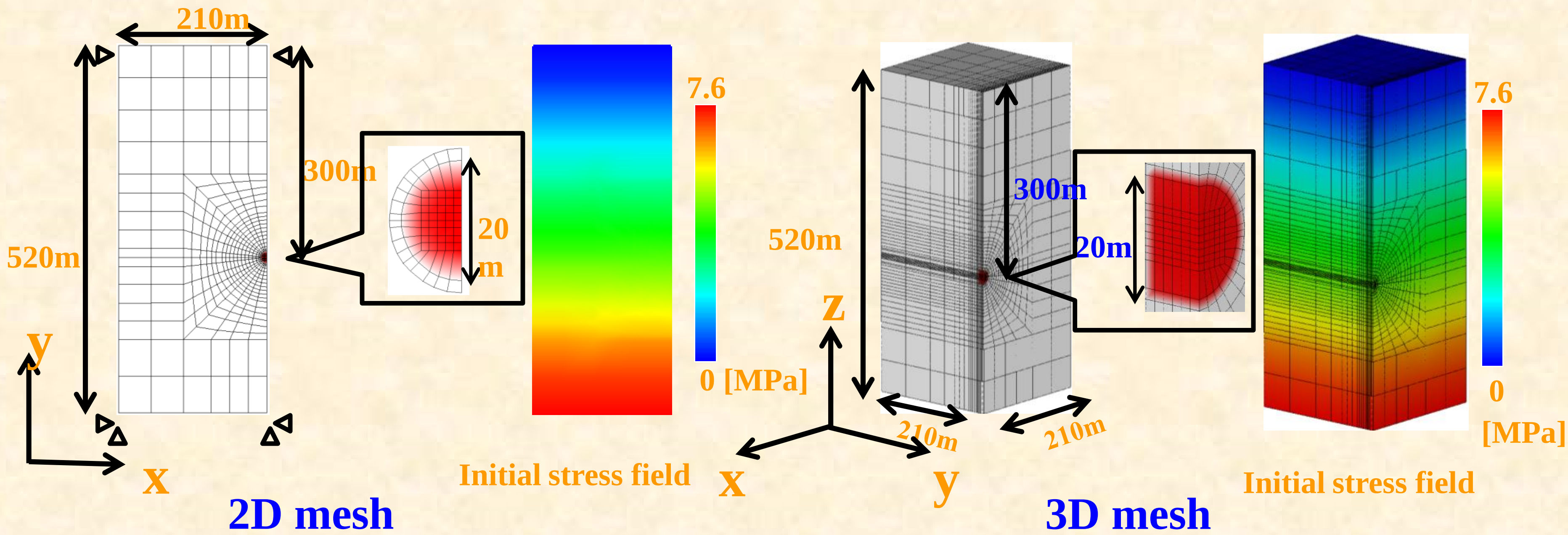

Thermal, boundary and initial conditions

- **Boundary condition**: fixed in side and bottom surfaces
- **Hydraulic condition**: only drained at top surface
- **Thermal condition**: all the surfaces far from the heating source are at constant temperature of 15°C
- **Material**: heating source is elastic
- **Initial saturation**: soft rock is saturated but heating source and bentonite are unsaturated

FEM---Setting of heat source

Heat released from nuclear waste is given as follow proposed by Thunvik and Braester (1991) :

$$Q(t)/Q_0 = \alpha_1 e^{-\alpha_2 t} + (1-\alpha_1)e^{-\alpha_3 t}$$

The initial heat Q_0 is given 28.28 kJ/m^3 /min.

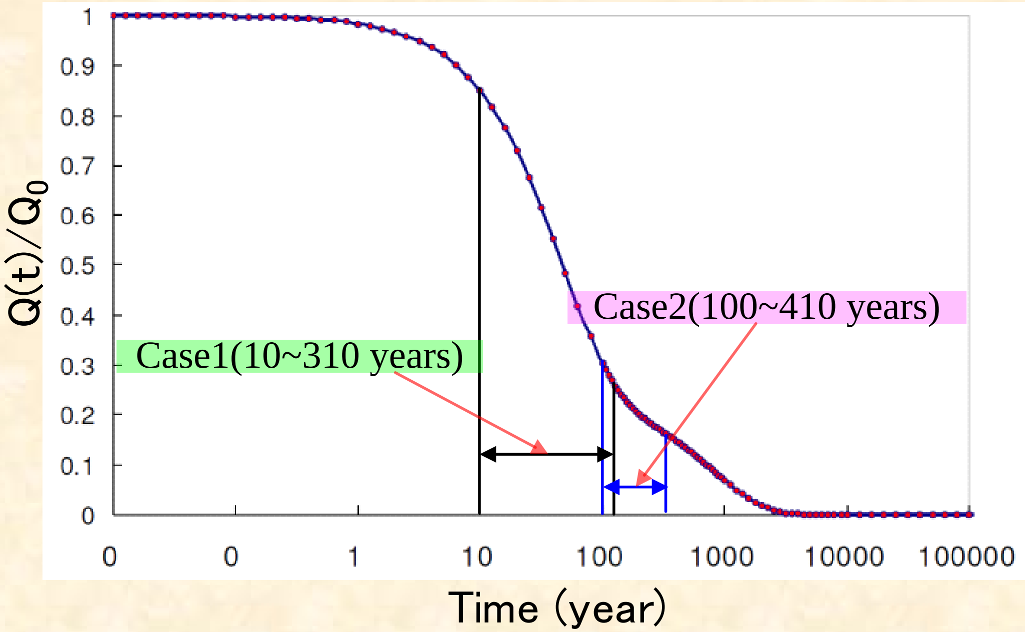

The relation of decay rate and time

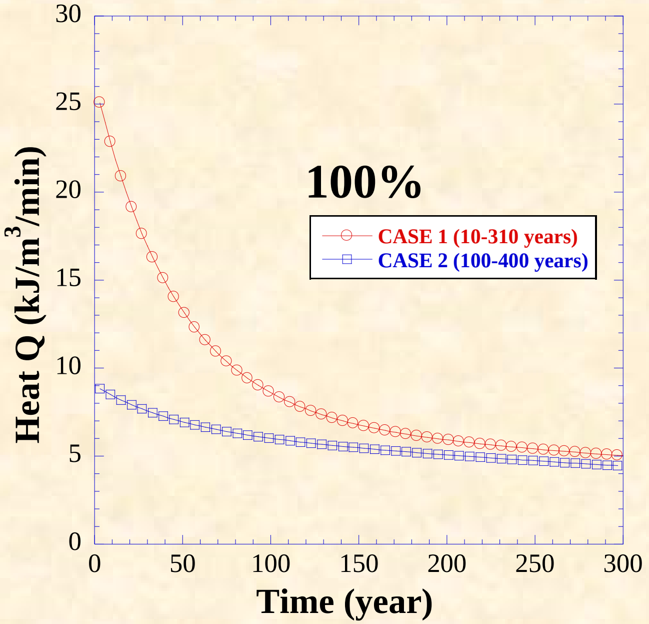

Heat emission as input in FEM

FEM---Setting of heat source

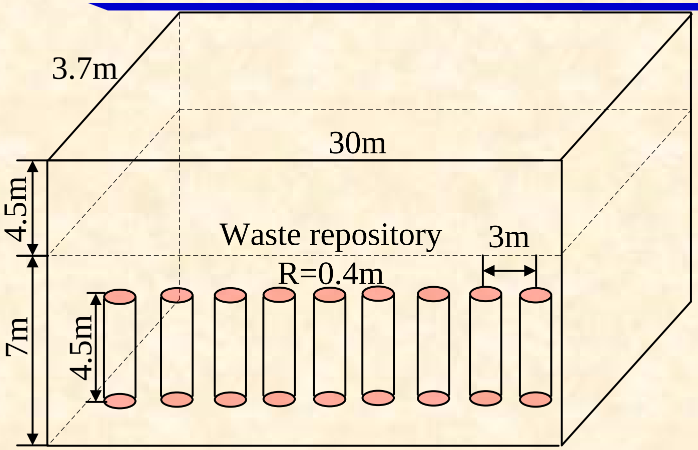

The schematic diagram of the field project

1. Volume of HLRW only occupies about 1.6% of total tunnel volume, correspondingly the heat emission as input in FEM is given 1.6%.

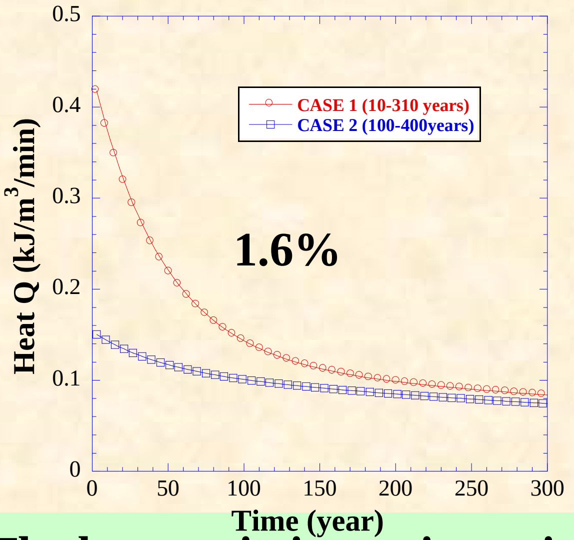

The heat emission as input in FEM

2. Heat emission decreases greatly between 10 years and 100 years from the decay rate-time relation. Two cases are considered starting from 10 years and 100 years after emplacing into repository respectively. The calculated times are 300 years in two cases.

MCC and initial condition

MCC（Munoz et al, 2006)

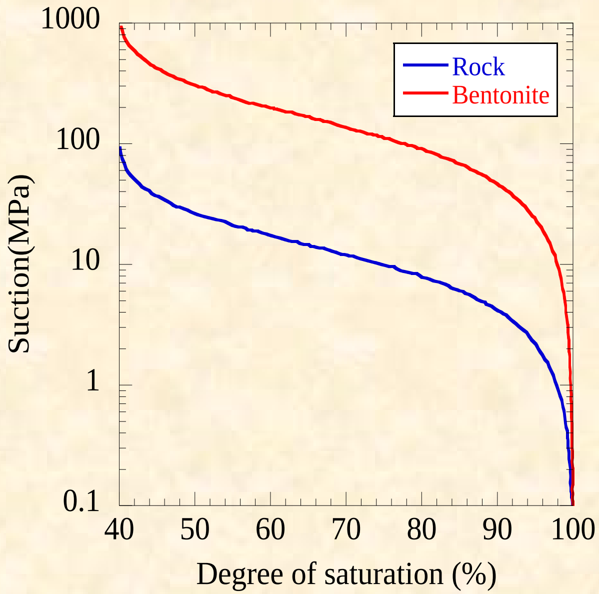

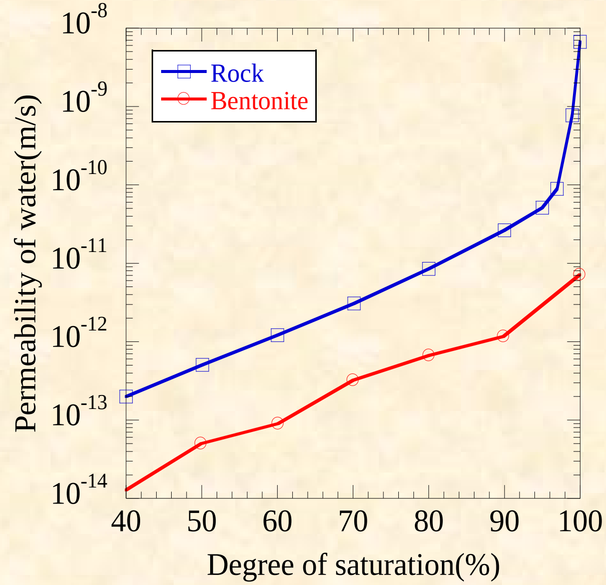

Initial condition

	Rock	Bentonite
Saturation [%]	100	86
Suction [MPa]	0	62
Total head [m]	520	-6945

Material parameters for constitutive model

	Bentonite	Rock
Parameter of overconsolidation a	5.000	2.000
Parameter of suction b	0.5	0.5
Parameter of overconsolidation β	1.00	1.10
Void ratio (*p'*=98 kPa on *N.C.L*) N	1.040	0.450
Void ratio (*p'*=98 kPa on *N.C.L.S*) Nr	1.060	0.530
Thermal expansion coefficient (1/K) α_T	-1.0×10^{-6}	-2.5×10^{-5}
Thermal conductivity (kJ m^{-1} K^{-1} Min^{-1}) K_t^S	0.060	0.200
Specific heat (kJ Mg-1 K-1) C^S	723	840
Thermal expansion coefficient of water (1/K) α_T	2.1×10^{-4}	2.1×10^{-4}

Parameters for MCC

	Bentonite	Rock
Compression index λ	0.050	0.010
Swelling index κ	0.010	0.001
Void ratio (*p'*=98 kPa on *N.C.L*) e_0	1.040	0.500
Poisson's ratio ν	0.300	0.120
Saturated degrees of saturation S_r^s	1.00	1.00
Residual degrees of saturation S_r^r	0.40	0.40
Parameter corresponding to drying AEV (kPa) S_d	11000	21000
Parameter corresponding to wetting AEV (kPa) S_w	800	1000
Initial stiffness of scanning curve (kPa) k_{sp}^e	25000	90000
Parameter of shape function c_1	0.000001	0.00003
Parameter of shape function c_2	0.000005	0.00006
Parameter of shape function c_3	30.0	50.0

Temperature change 2 (3D)

Saturated condition (without bentonite)

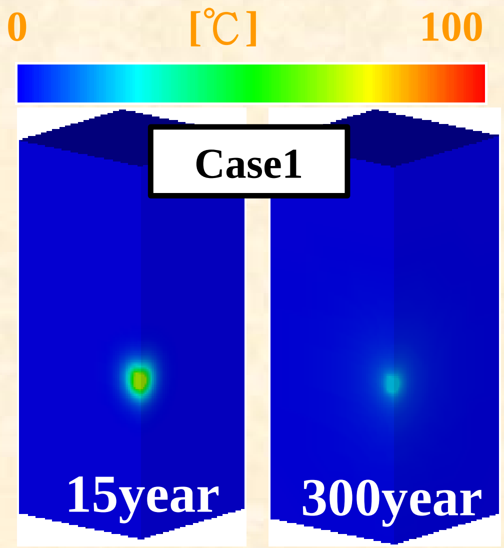

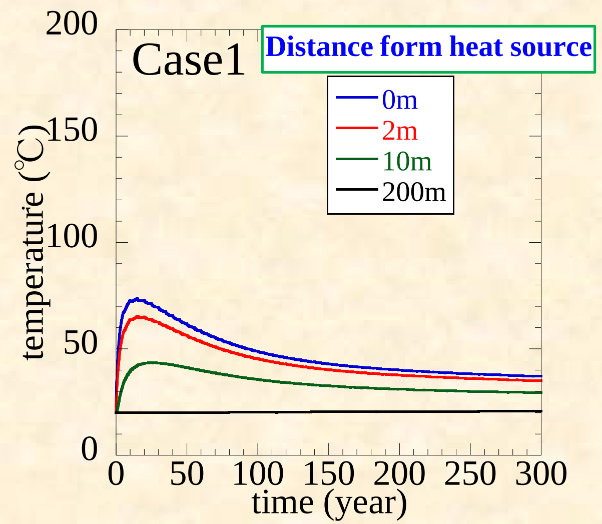

Unsaturated condition (with bentonite)

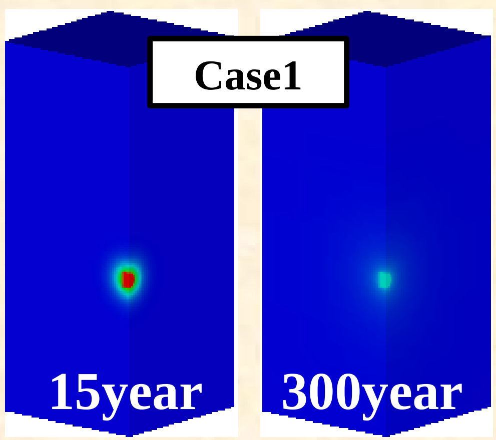

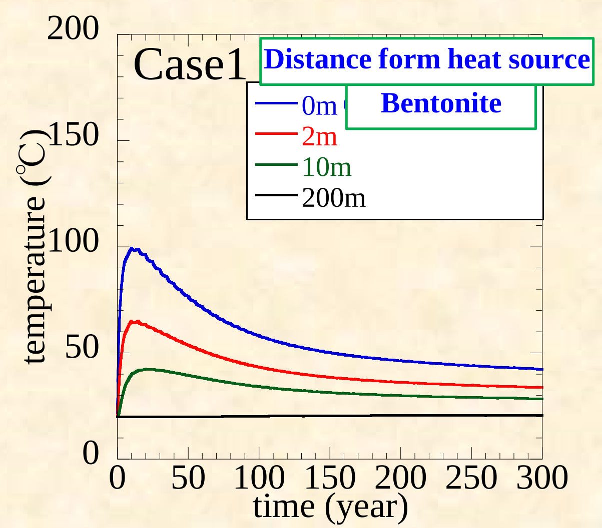

Changes of saturation and suction

2D analysis

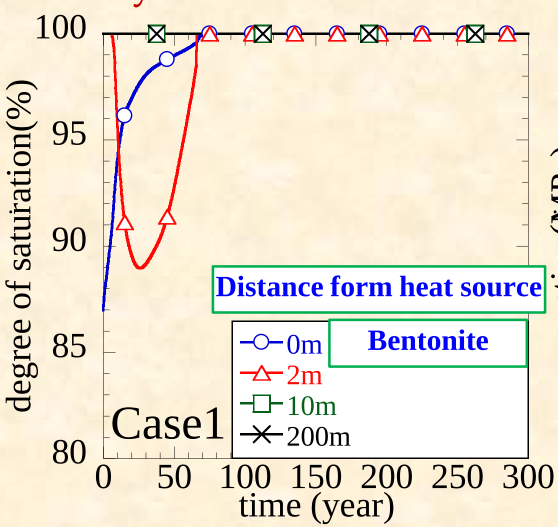

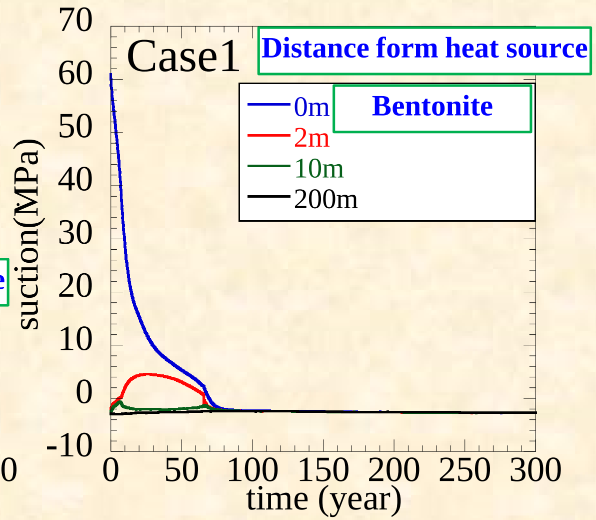

2D analysis

Bentonite → absorption

Rock → change from drainage to absorption

3D analysis

Bentonite → absorption

Rock → always saturated

3D analysis

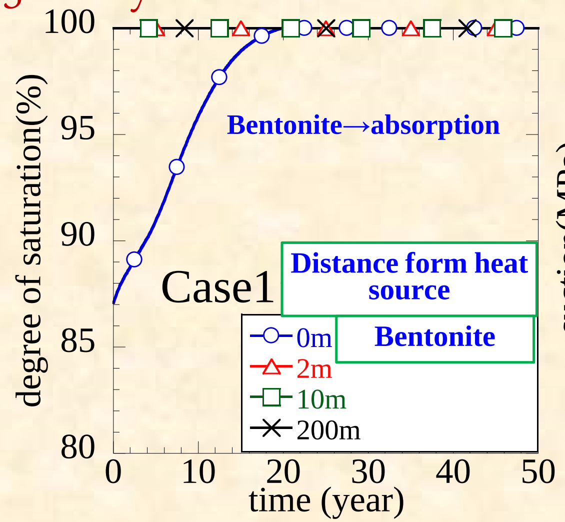

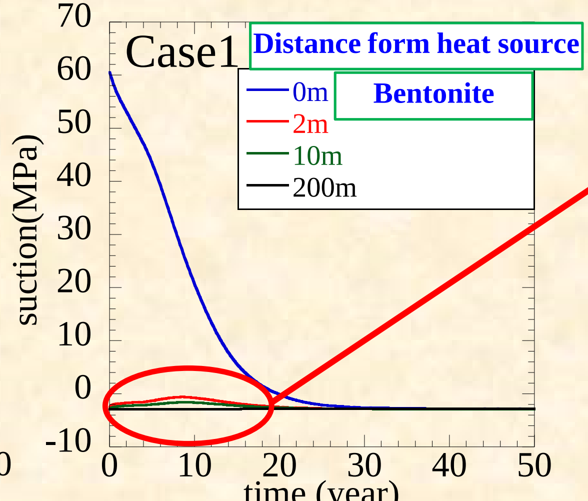

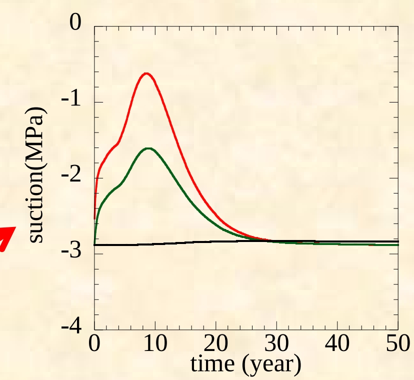

- Initial suction is -3MPa (300m beneath water level)
- Bentonite is much less in 3D than in 2D → water supplying from rock to bentonite is much less in 3D

Change of saturation

Change of suction

Changes of volumetric and deviatory strains (2D)

Saturated condition (without bentonite)

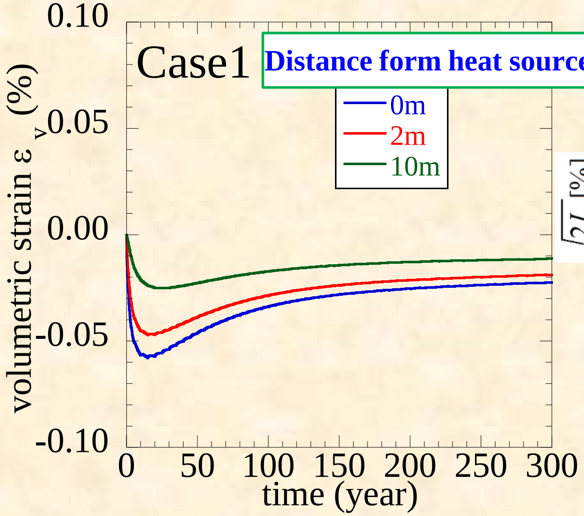

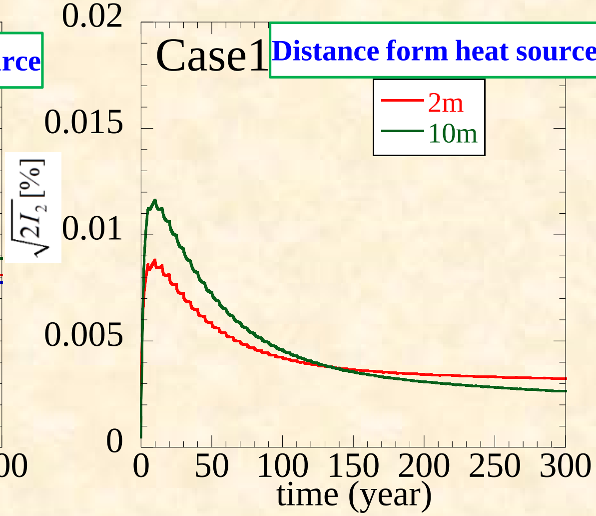

Volumetric expansion near heating source

Thermal effect is confirmed

Substantial shear strain happened in rock when bentonite is involved !

Unsaturated condition (with bentonite)

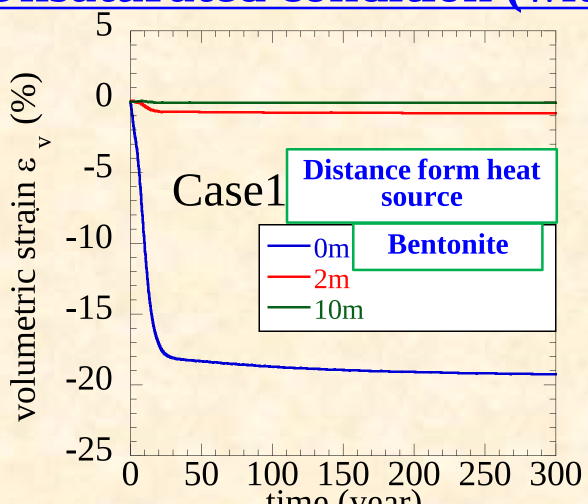

Volumetric strain

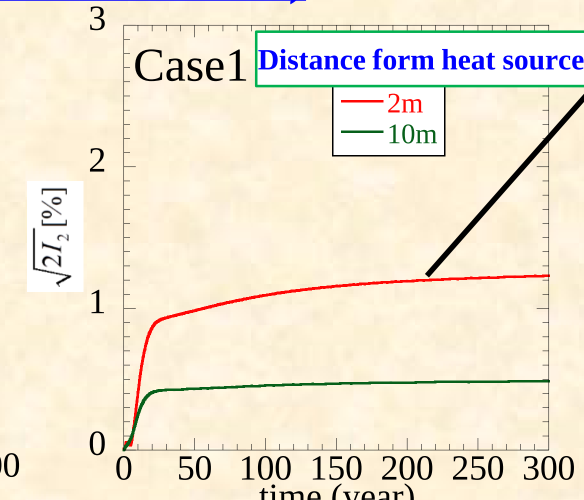

Deviatory strain

Volumetric expansion of bentonite is far larger than that of rock

mainly coursed by huge decrease of suction

Comparison of temperature between Case 1 and 2 (2D)

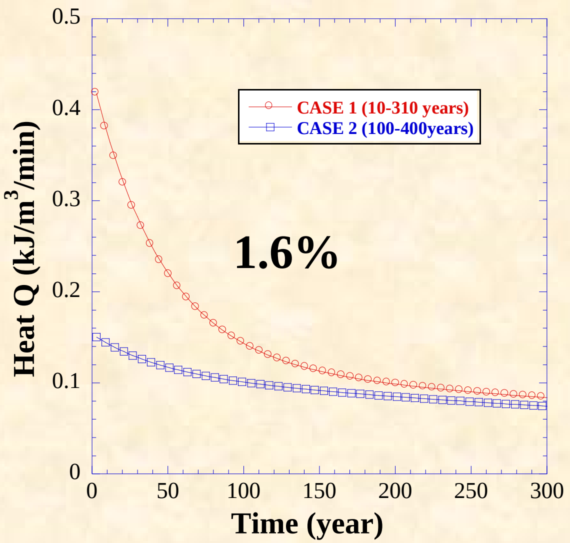

Heat emission input in FEM

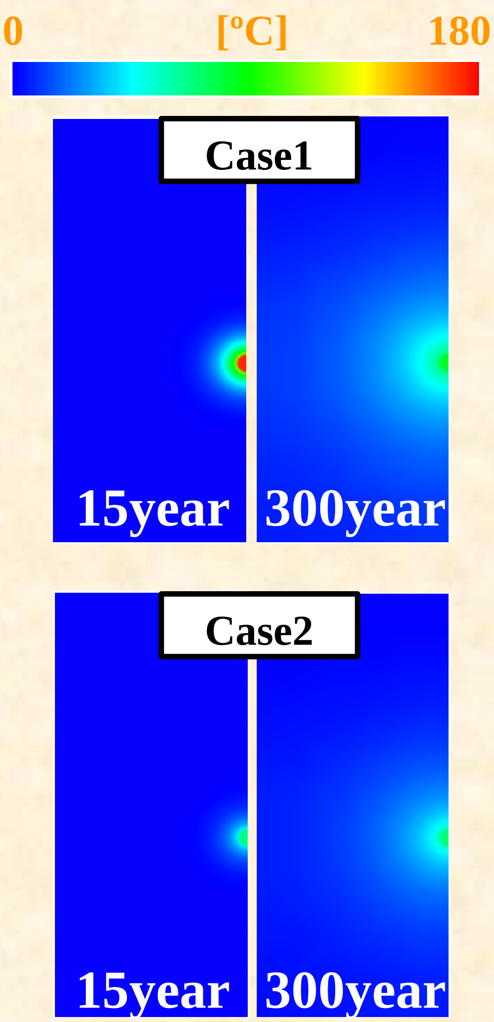

Distribution of temperature

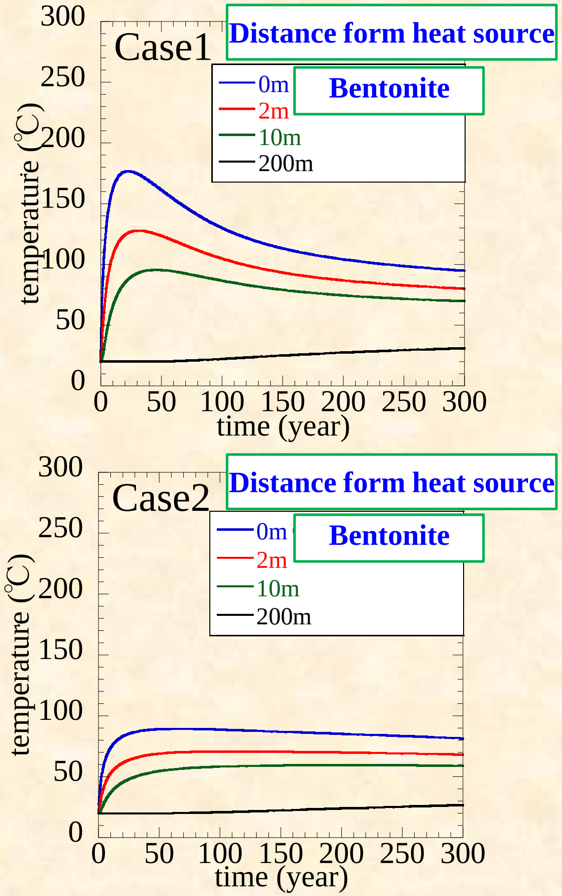

Change of temperature

Comparison of saturation between Case 1 and 2 (2D)

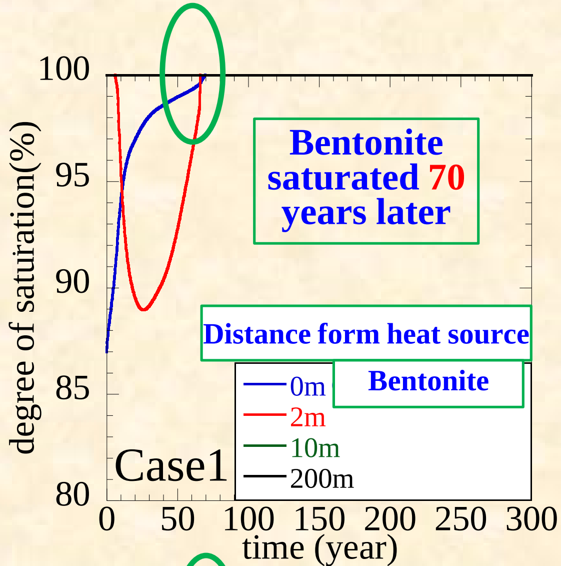

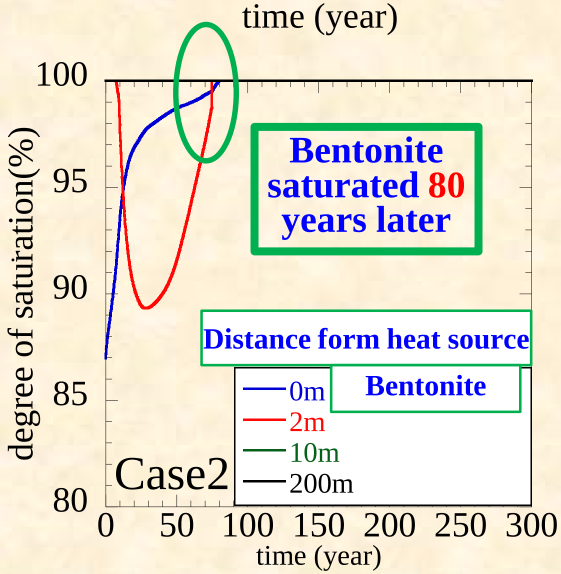

Change of saturation (2D)

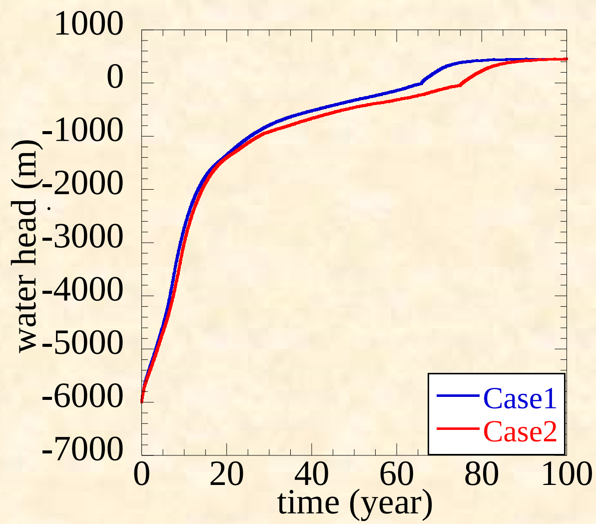

Change of total water head

Reason why saturated quickly when heating is strong

strong heating results in quick increase of excess pore water pressure

quick decrease of suction **($s=u_a-u_w$)**

Saturated quickly

Comparison of volumetric strain between Case 1 and 2 (2D)

In Case 2 (relative weak heating source), expansive of bentonite is larger, why?

Taking more time to reach saturated state → S_r developed slower → ρ_s also developed slower

$$d\rho_s = -QdS_r$$

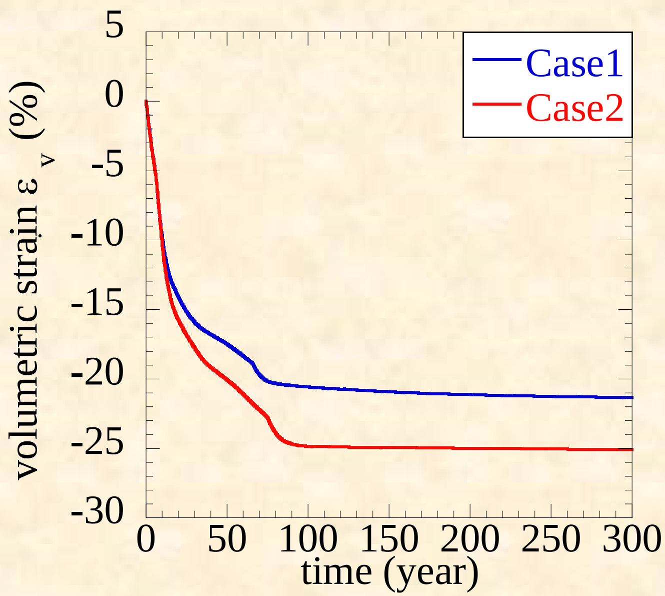

Change of volumetric strain of bentonite (2D)

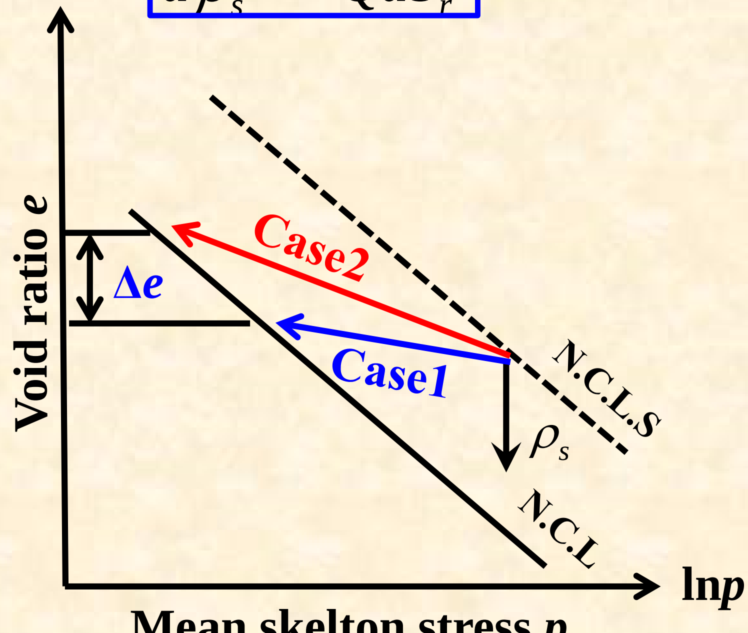

Trace in absorption process of bentonite *e-lnp*

Due to slower develop of ρ_s, extra ***Δe*** happened in Case 2

Comparison of deviatory strain between Case 1 and 2 (2D)

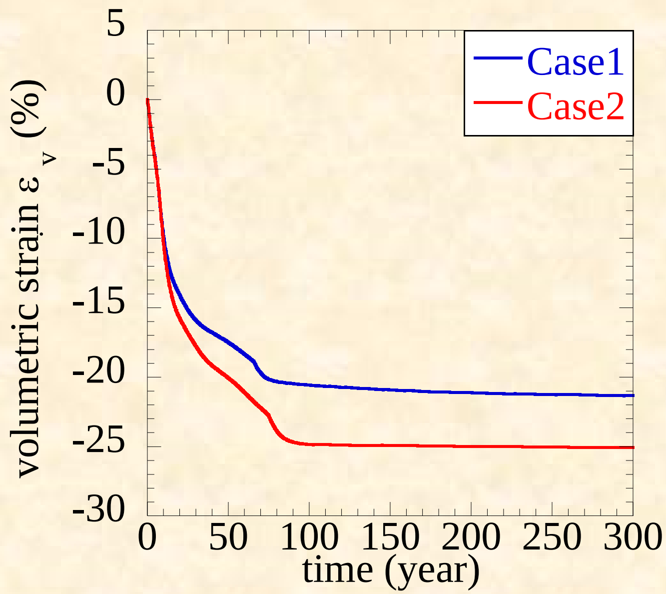

Change of volumetric strain of bentonite (2D)

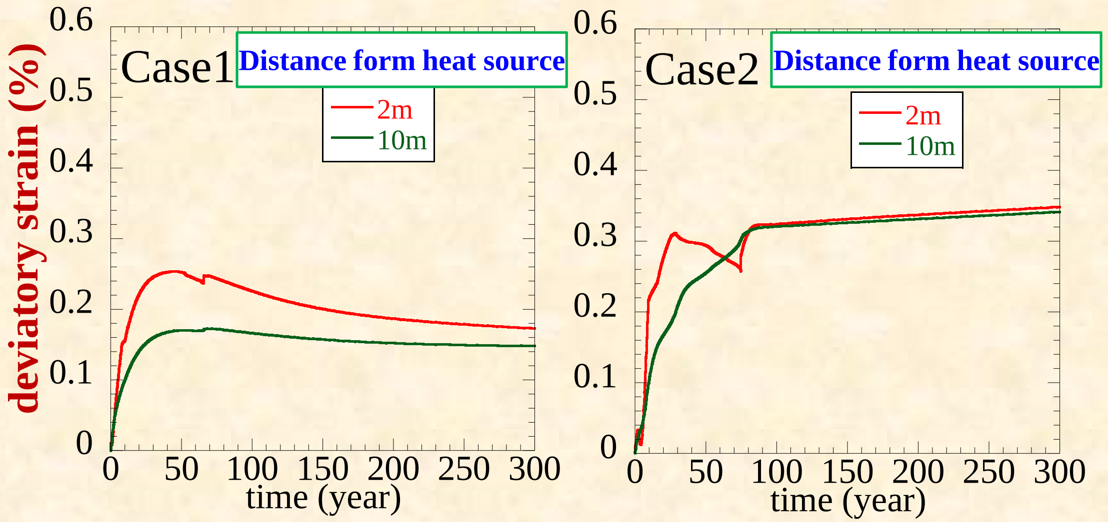

Change of deviatory strain of rock (2D)

- **Deviatory strain in surrounding rock due to huge swelling of bentonite**
- **In case 2, volumetric strain in bentonite is much larger→larger deviatory stain**

CONCLUSIONS

- A thermo-elastoplastic model for unsaturated/saturated geomaterials has been introduced based on the concept of equivalent stress and subloading surface, which can not only describe properly the thermodynamic behavior, but also overconsolidated behavior of soft sedimentary rocks.
- Verification by laboratory tests and field observation proved the validity of the proposed numerical method
- Field equations in THMA FE-FD analysis has been introduced to treat thermo-soil-water-air coupling problem. As a application, a field problem of geological repository of high-level nuclear waste is simulated in unsaturated/saturated condition.
- In 2D simulation, the calculated results shows that the temperature has a great influence on THMA coupling behavior of natural soft rock.

Thank you for your attention!